ISSN 2186-3644 Online ISSN 2186-361X

IRDR

Intractable & Rare Diseases Research

Volume 9, Number 3
August, 2020

www.irdrjournal.com

IRDR
Intractable & Rare Diseases Research

ISSN: 2186-3644
Online ISSN: 2186-361X
CODEN: IRDRA3
Issues/Year: 4
Language: English
Publisher: IACMHR Co., Ltd.

Intractable & Rare Diseases Research is one of a series of peer-reviewed journals of the International Research and Cooperation Association for Bio & Socio-Sciences Advancement (IRCA-BSSA) Group and is published quarterly by the International Advancement Center for Medicine & Health Research Co., Ltd. (IACMHR Co., Ltd.) and supported by the IRCA-BSSA.

Intractable & Rare Diseases Research devotes to publishing the latest and most significant research in intractable and rare diseases. Articles cover all aspects of intractable and rare diseases research such as molecular biology, genetics, clinical diagnosis, prevention and treatment, epidemiology, health economics, health management, medical care system, and social science in order to encourage cooperation and exchange among scientists and clinical researchers.

Intractable & Rare Diseases Research publishes Original Articles, Brief Reports, Reviews, Policy Forum articles, Case Reports, News, and Letters on all aspects of the field of intractable and rare diseases research. All contributions should seek to promote international collaboration.

IRCA-BSSA Group Journals

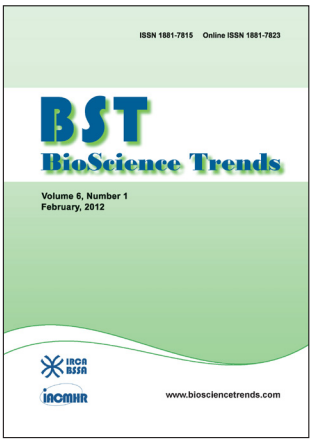

ISSN: 1881-7815
Online ISSN: 1881-7823
CODEN: BTIRCZ
Issues/Year: 6
Language: English
Publisher: IACMHR Co., Ltd.
www.biosciencetrends.com

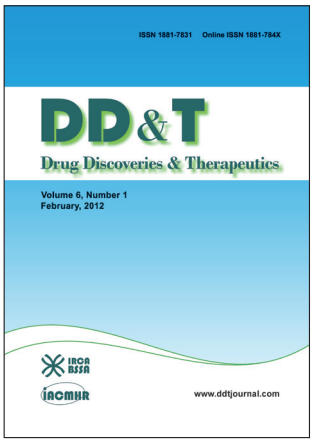

ISSN: 1881-7831
Online ISSN: 1881-784X
CODEN: DDTRBX
Issues/Year: 6
Language: English
Publisher: IACMHR Co., Ltd.
www.ddtjournal.com

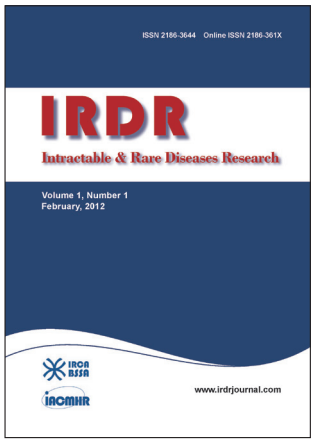

ISSN: 2186-3644
Online ISSN: 2186-361X
CODEN: IRDRA3
Issues/Year: 4
Language: English
Publisher: IACMHR Co., Ltd.
www.irdrjournal.com

Intractable & Rare Diseases Research

Editorial and Head Office

Pearl City Koishikawa 603, 2-4-5 Kasuga, Bunkyo-ku,
Tokyo 112-0003, Japan

E-mail: office@irdrjournal.com
URL: www.irdrjournal.com

Editorial Board

Original Article

Brief Report

Case Report

Communication

Original Article

DOI: 10.5582/irdr.2020.03028

Cost-effectiveness analysis of enzyme replacement therapy (ERT) for treatment of infantile-onset Pompe disease (IOPD) in the Iranian pharmaceutical market

Reza Hashempour[1], Majid Davari[2,3,*], Abolghasem Pourreza[1], Mohammadreza Alaei[4], Batoul Ahmadi[1]

[1] Department of Health Management and Economics, School of Public Health, Tehran University of Medical Science, Tehran, Iran;
[2] Department of Pharmacoeconomics and Pharmaceutical Administration, Faculty of Pharmacy, Tehran University of Medical Science, Tehran, Iran;
[3] Pharmaceutical Management & Economics Research Center, Tehran University of Medical Science, Tehran, Iran;
[4] Department of Pediatric Endocrinology, Faculty of Medicine, Shahid Beheshti University of Medical Sciences, Tehran, Iran.

SUMMARY Infantile-onset Pompe disease (IOPD) or acid maltase deficiency is a rare metabolic disorder. It is caused by a deficiency in functioning of the enzyme acid alpha-glucosidase and leads to the accumulation of glycogen in the liver, heart, muscle, and other tissues. Myozyme is an effective drug, but it imposes a heavy financial burden on societies and healthcare systems. Therefore, this study was conducted to analyze the cost-effectiveness of Myozyme compared to conventional therapy for the treatment of IOPD. PubMed, Scopus, Web of Science, and Cochrane library databases were searched on December 2018 to identify the effectiveness of Myozyme versus conventional therapy. Then, a cost-effectiveness and a cost utility study were conducted in patients suffering from IOPD. In this cost effectiveness and cost utility analysis, Markov and decision tree models were used for modeling. Model parameters were obtained from international data, and the perspective of the payer was considered. Every cycle was one year; the model was run for 22 cycles. TreeAge pro 2011 was used for analysis. Finally, one-way and probabilistic sensitivity analyses were performed. Two papers were included and 39 patients were evaluated as the treatment group in both studies. Results revealed the effectiveness of Myozyme. Results also revealed a wide range of adverse reactions. Enzyme replacement therapy (ERT) resulted in 4.21038 quality-adjusted life years (QALY) per $381,852. The incremental cost per QALY was $96,809 and the incremental cost per life years gained (LYG) was 74,429 over a 22-year time horizon. Sensitivity analysis indicated the robustness of the results. Myozyme is effective for IOPD and could increase the life expectancy of patients significantly. However, since the calculated incremental cost per QALY was 17 times higher than the GDP per capita of Iran, Myozyme is not cost effective in Iran.

Keywords Myozyme, enzyme replacement therapy, Pompe disease, cost-effectiveness, Iran

1. Introduction

Pompe disease is an inherited metabolic disorder that is also known as acid-maltase deficiency or glycogen storage disease type 2 (GSD type 2) (*1,2*). The disease is caused by a mutation in the acid alpha-glucosidase gene, which is necessary for degradation of glycogen (*3*). A deficiency of acid-maltase causes the accumulation of glycogen in the lysosomes of the heart, liver, skeletal muscle, and other tissues (*4,5*) and it has destructive effects on muscles (*6*). This stored glycogen first affects skeletal and cardiac muscles (*7*) and then causes feeding abnormalities, cardiac hypertrophy, weakness, respiratory insufficiency, hypotonia, and eventually death (*8*). The incidence of this orphan disease is 1 in 40,000 live births (*9*).

There are two forms of Pompe disease, infantile-onset Pompe disease (IOPD), and late-onset Pompe disease (LOPD) (*10*). IOPD is more severe and appears in the first months of life (*11*). The early symptoms are cardiomegaly, muscle weakness, hepatomegaly, hypotonia, and death in the first year of life (*11*). LOPD (*i.e.* juvenile- and adult-onset) can occur as early as the age of 1 year to as late as the sixth decade of life (*3,11,12*). The age of the onset of symptoms depends on the severity of the deficiency in acid-maltase. The

more severe the deficiency, the faster the symptoms appear (*13*).

Enzyme replacement therapy (ERT) with human acid alpha-glucosidase (Myozyme) has been available since 2006 for both IOPD and LOPD (*14*). Studies have indicated that Myozyme can improve the survival rate, respiratory efficiency, and cardiac and motor function (*13*). However the improvements depend entirely on the age and onset of drug therapy (*8*); the sooner the treatment is started, the outcomes are better. Nonetheless, there are two main problems with Myozyme. First it requires high dosages and it has a low level of effectiveness (*15*). Second, the cost of Myozyme is substantial and imposes a substantial burden on healthcare systems and societies. Two studies have conducted economic evaluations in developed countries (*12,16*) but no study has economically evaluated ERT in a developing country like Iran. Therefore, the aim of this study was to perform a cost-utility analysis of Myozyme versus conventional therapy to treat IOPD in Iran.

2. Materials and Methods

This study was approved by the Tehran University of Medical Sciences ethics committee (approval No. IR.TUMS.SPH.REC.1396.2902).

2.1. Study design

A cost-utility analysis was conducted for ERT in patients with classic IOPD. Currently, ERT is the only treatment available for patients with IOPD. There is no medical comparator for treatment of IOPD and thus conventional therapy was considered as a comparator of Myozyme in this study. Conventional therapy consists of ventilatory care, nutrition, and care in the pediatric intensive care unit (PICU). Quality-adjusted life years (QALY) was the main outcome in the current study. The local cost of treatment was converted to US dollars based on the exchange rate in 2017. A lifetime time horizon was used to model costs and QALYs for different alternatives.

2.2. Measurement of effectiveness

A systematic search of PubMed, Scopus, Web of Science, and Cochrane library databases was conducted prior to December 2018 to identify the best available published evidence on the effectiveness of ERT for IOPD. The details of this systematic review are presented elsewhere (*17*).

2.3. Assessing costs and cost-effectiveness

The perspective of the payer for healthcare was considered when calculating the cost of medication and relevant care. Only direct medical costs were measured when calculating the cost of treatment. In addition to the cost of Myozyme, the cost of injection and the treatment of adverse reactions were calculated in the ERT arm.

The price of Myozyme was obtained from the Iran Food and Drug Administration (IFDA), which is the only organization in charge of approving medicines in Iran. The cost of Myozyme was calculated based on the Myozyme dosage, which was 20 mg/Kg every two weeks. In order to calculate the cost of Myozyme, the average weight of patients was first estimated. As each Myozyme vial contains 50 mg of acid alpha-glucosidase, the number of vials per person was calculated based on the following formula (*18*):

$$\text{Number of vials} = (\text{Average weight} * 20)/50$$

In the no ERT arm, the cost of care in the PICU, as the only cost driver, was estimated based on the number of days hospitalized in the PICU and the per diem price of care in the PICU. The average number of days hospitalized in the PICU and the per diem price of care in the PICU were obtained from the Iranian Book of Medical Fees.

The incremental cost-effectiveness ratio (ICER) was estimated using the following formula (*19*):

$$\text{ICER} = (\text{Cost of ERT} - \text{Cost of no ERT})/(\text{QALYs gained with ERT} - \text{QALYs gained with no ERT})$$

2.4. Modeling and Model parameters

A combination of a decision tree and a Markov model was used to estimate total costs and QALYs in the ERT and no ERT arms by the end of the lives of patients with IOPD. The Markov model was based on the stages of Pompe disease. Although a published model evaluated the costs and effects of ERT in treating Pompe disease (*12*), that model was modified and improved based on the actual condition of patients. That is, a stage of "Alive, symptomatic" was added as the first stage because when patients with IOPD receive ERT they are alive and also have symptoms of the disease. Figure 1 shows all phases of both ERT treatment and conventional therapy. Every Markov cycle was considered to be one year. The model was run using TreeAge pro 2011.

Model parameters including health status, transition probabilities, and utility scores were obtained from literature (Table 1). The utility scores for different health statuses were obtained from two studies (*12,16*). In a study by Castro *et al.*, the utility score was 0.70 for ERT and 0.388 for no ERT (*12*). However, a study by Kanters *et al.* reported that the ERT group had an average utility score of 0.62 (*16*). The utility scores of Castro *et al.* were used in the current model and the utility scores of Kanters *et al.* were used for sensitivity analysis. Discount rates were not used because both costs and effects were incurred during the same period (*20,21*).

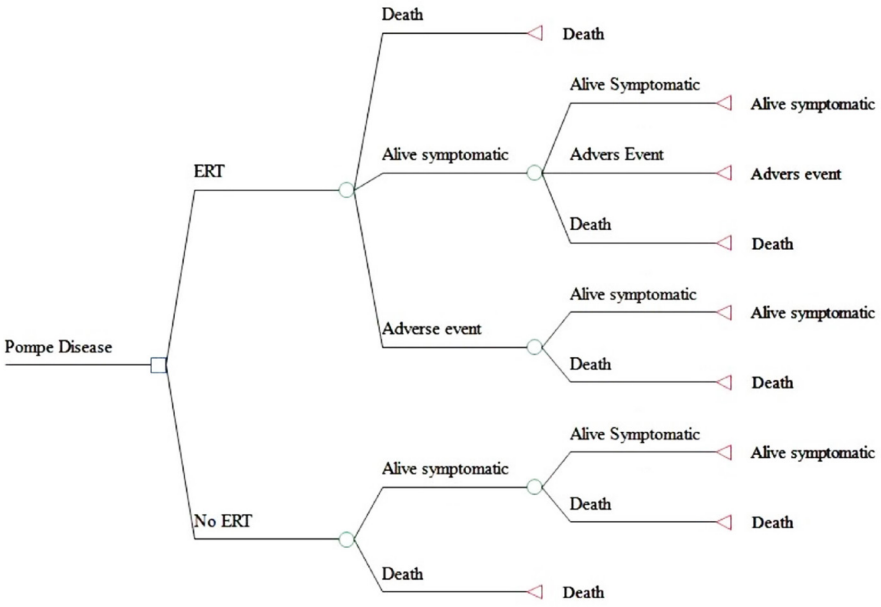

Figure 1. Model designed to analyze treatment of infantile-onset Pompe disease. This figure shows the phases of ERT treatment and Conventional therapy. ERT, enzyme replacement therapy.

Table 1. Transition probabilities for enzyme replacement therapy (ERT) and conventional therapy

Pompe disease	Stages		Probabilities	*Ref.*
	From	To		
ERT	Alive, symptomatic	Alive, symptomatic	0.33	(*12*)
	Alive, symptomatic	Adverse event	0.56	(*29,30*)
	Alive, symptomatic	Death	0.11	(*12*)
	Adverse event	Death	0.259	(*12*)
	Adverse event	Alive, symptomatic	0.741	(*12*)
Conventional therapy	Alive, symptomatic	Alive, symptomatic	0.08	(*12*)
	Alive, symptomatic	Death	0.92	(*12*)

2.5. Model assumptions

The model was designed based on the following assumptions:

i) All patients receiving conventional therapy (no ERT) die at the age of six months (*22*).

ii) The utility score for the treatment group was 0.7 for all stages (*12*). That is, the adverse events of ERT were negligible and ignored in the current model.

iii) After the first symptoms of the disease develop, patients are normally hospitalized due to the severity of the disease (*2*).

iv) In the ERT arm, a fixed rate survival of 75% was used for each cycle (*12*).

v) Patients suffering from classic IOPD do not have a normal growth rate due to feeding problems (*22*). Nonetheless, a 5% weight gain was assumed for the patients' growth rate based on expert opinions.

2.6. Sensitivity analysis

In order to assess the robustness of the model, a one-way deterministic sensitivity analysis and a probabilistic sensitivity analysis were performed. The costs and utility scores were included in the sensitivity analysis.

3. Results

3.1. Effectiveness

The results of a systematic review indicated that only two studies met the inclusion criteria for analysis. Research questions included the population of interest (IOPD), intervention (ERT), comparator (no ERT), and outcome (survival or QALY). The details of the results of that systematic review are presented elsewhere (*17*).

3.2. The cost of Myozyme

In order to calculate the cost of Myozyme, the average weight of patients was first estimated. The average weight of the patients was determined from 12 patient profiles from the IFDA in 2018; patients included eight females and four males. The weight of patients varied from 5 to 15 Kg, with an average of 7.29 Kg. The acceptable dose of Myozyme was 20 mg/Kg every other

week. The number of vials per person was calculated based on the following formula (*18*):

Number of vials = (Average weight * 20)/50

The number of vials consumed per patient was 2.96-3.0 every two weeks and 6 vials per month. Therefore, 72 vials of Myozyme were consumed in the first year of treatment (the first Markov cycle) at a cost of $48,964.3. However, considering the cost of all medications, the total cost of the first cycle was $49,456.94 (Table 2). According to the model's assumption, the weight of patients will increase 5% each year. Thus, the cost of Myozyme was increased by 5% for the following years (cycles).

3.3. Other costs

The results of a literature review indicated that the probability of an adverse event occurring was 56% and that the probability of anaphylactic shock in particular occurring was 1%. The risk of death due to anaphylactic shock has been reported to be 50% (*12*). When patients suffer adverse events, they receive hydrocortisone, hydroxyzine, and an antihistamine. The respective cost of these drugs was $12.24, $13.6, and $13.6 (Table 2).

3.4. Cost-effectiveness

Figure 2 shows the results of modelling. The results of the 22-year model verified that no ERT resulted in 1.087 years (0.422 QALYs) while ERT resulted in 6.015 life years (4.210 QALYs) on average. Based on the calculated costs, the use of ERT increased the cost by $366,777 and increased the life expectancy of patients by 4.93 years (Table 3). That is, no ERT resulted in $15,075 per 0.422 QALY and ERT resulted in $381,852 per 4.210 QALYs. Therefore, the ICER for ERT was $74,852 per LYG (life year gained) and $96,809 per QALY gained (Table 4).

3.5. Deterministic sensitivity analysis

In order to assess the robustness of the results, the effect of the costs on ICER was first examined. The total cost of ERT was reduced by 5, 10, and 20% to ascertain how these changes would affect the results of ICER. Although these changes reduced the value of the ICER to $6,364, the current results were robust up to a 22%

Table 2. The cost of the first cycle

	Drug	Number	Cost ($)
1	Hydrocortisone	24	12.24
2	Hydroxyzine	24	13.6
3	Antihistamine	24	13.6
4	Administration	24	453.2
5	Myozyme	72	48,964.3

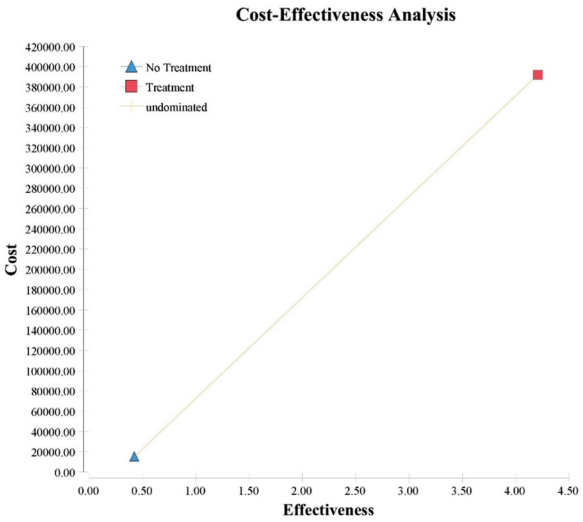

Figure 2. Cost effectiveness graph of treatment in comparison to no treatment. Although ERT resulted in more QALY in comparison to conventional therapy, it was not a cost-effective option due to its high cost. ERT, enzyme replacement therapy; QALY, quality-adjusted life year.

Table 3. Cost-utility analysis results

	Mean cost	QALY	ACER	Incremental cost	Incremental QALY	ICER
No ERT	15,075	0.42174	35,745	366,777	3.78864	96,809
ERT	381,852	4.21038	90,693			

ACER, average cost-effectiveness ratio; ERT, enzyme replacement therapy; ICER, incremental cost-effectiveness ratio; QALY, quality-adjusted life year.

Table 4. Cost-effectiveness results

	Mean cost	LYG	ACER	Incremental LYG	ICER
No ERT	15,075	1.08696	13,869	4.92787	74,429
ERT	381,852	6.01482	63,485		

ACER, average cost-effectiveness ratio; ERT, enzyme replacement therapy; ICER, incremental cost-effectiveness ratio; LYG, life years gained.

reduction in the cost of ERT.

The minimum and maximum value of utilities, which ranged from 0.24 to 0.82, were also used to assess the impact of these changes on the value of the ICER. These changes modified the value of the ICER from $358,945 to $81,318 per QALY, respectively, but none of the scenarios were cost-effective.

3.6. Probabilistic sensitivity analysis

Gamma and a normal distribution were used in order to determine the distribution of the costs and utilities (*23*). Table 5 shows the range of variables used for sensitivity analysis. A Monte-Carlo simulation was run for 1000 trials. The results of probabilistic sensitivity analysis indicated that 100% of the ERT trials were not cost-effective (Figure 3).

4. Discussion

The aim of this study was to assess the cost-effectiveness of ERT (Myozyme) in comparison to conventional therapy in the treatment of IOPD. The model indicated that ERT could increase the life expectancy of patients by 6.01 years, which is equal to 4.21 QALYs based on utility scores.

The past performance of the IFDA indicated that the IFDA has been using a cost-effectiveness threshold equal to the GDP per capita. This is compatible with World Health Organization (WHO) recommendation for developing countries (*24,25*). A report by the Central Bank of Iran indicated that the per capita GDP of Iran was $5,757 in 2018 (*26*). The current results indicated that the ICER was $96,809, which was 16.82 times the GDP per capita of Iran in 2018 (*24,25*). Uncertainties regarding parameters in the current study were addressed through probabilistic sensitivity analysis. This analysis indicated that the ICER was higher than the recommended threshold value in all cases (100 %) (Figure 3) and, therefore, confirmed the robustness of the current findings.

The results of the current study are consistent with the results of studies in many other countries (*12,16*). A cost-effectiveness analysis of ERT compared to no treatment was performed by Castro *et al.* (*12*). The ICER per QALY was £234.308 and £109.991 for England as a

Table 5. Range of variables for sensitivity analysis

	Variable	Base case	Range	Distribution
Utility	Treatment	0.7	0.5-0.9	Normal
	Conventional therapy	0.388	0.2- 0.576	Normal
Cost ($)	Adverse event	89,787	116,794-62,780	Gamma
	Alive, symptomatic	89,654	116,661-62,647	Gamma
	Conventional therapy	402	0-1,017	Gamma

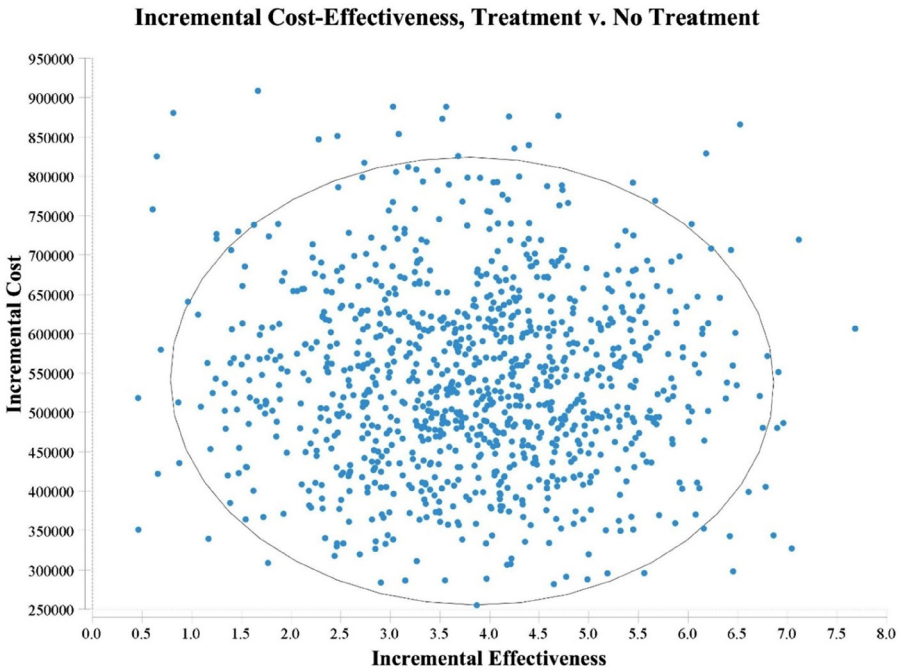

Figure 3. Incremental cost effectiveness scatterplot of ERT versus no ERT. A PSA graph shows that all trials were far from the threshold and that all trials were not cost-effective. ERT, enzyme replacement therapy.

high-income country and Colombia as a middle-income country, respectively. According to the National Institute of Health and Clinical Excellence (NICE), the cost-effectiveness threshold for England was £30,000 (*27*) and that for Columbia was equal to $10,615 USD (*28*). Therefore, the utilization of ERT was not a cost-effective option for treatment of IOPD in either country.

The manufacturer's price for ERT and its monopoly in England and Columbia had a great impact on the final results of previous studies, but in the current study the cost of Myozyme played a large role in the final results of cost-effectiveness analysis. In modelling of England, no treatment resulted in £149.187 per 0.16 QALY and ERT resulted in £1,337.12 per 5.23 QALYs. In modelling of Colombia, no ERT resulted in £49.676 per 0.16 QALY while ERT resulted in £607.329 and 5.23 QALYs. The main difference is due to the price variation in various countries. The difference between those costs might be associated with the different healthcare systems and health insurance. The costs of both ERT and no ERT differ from the costs in Iran. The QALY gained according to the study by Castro *et al.* differed from the findings of the current study. This could be attributed to both different sources of international data and different modeling. For example, the current study used data on an economic evaluation conducted by Castro *et al.* (*12*) and two quasi experimental studies (*29,30*).

The findings of this study are consistent with those of a study by Kanters *et al.* (*16*) who used a patient simulation model to assess the cost-effectiveness of ERT versus supportive therapy. Kanters *et al.* found that life expectancy in patients receiving ERT was 14 years and the incremental cost was £7 million. Likewise, the incremental QALY was 6.8 and thus the incremental cost per QALY gained was £1 million. One of the main causes of variations in the results of different studies could be attributed to the study's perspective. The perspective of society is recommended, but many studies adopt the perspective of the payer (*31*). The perspective of society is a wider one (*32*) and includes all cost and outcomes. The perspective of society was considered in the study by Kanters *et al.*, while the current study considered the perspective of the payer to economically evaluate care; indirect costs like lost productivity and transportation costs were not included in the analysis, so the overall costs may be underestimated. Therefore, different perspectives may result in different costs and outcomes.

This study has several limitations worth mentioning. First, there were few patients. Second, international data over a brief time period were used. And finally, a cost analysis was not performed due to the small number of patients.

In conclusion, Myozyme is effective for IOPD and could increase the life expectancy of patients significantly. Nonetheless, it imposes a heavy burden on the healthcare system and society. The calculated ICER was 17 times higher than per capita GDP of Iran in 2018. These findings suggest that the use of Myozyme for IOPD is not cost-effective in Iran.

Acknowledgements

This study was conducted as part of a MSc certification in Health Economics for Reza Hashempour at the Tehran University of Medical Science (TUMS). This MSc thesis was approved by the TUMS ethics committee (approval no. IR.TUMS.SPH.REC.1396.2902). The authors would like to thank Pharmaceutical Management & Economics Research Center for financial support.

Funding: This project funded by Pharmaceutical Management & Economics Research Center, Tehran University of Medical Science, Tehran, Iran.

References

1. van der Ploeg AT, Reuser AJ. Pompe's disease. Lancet. 2008; 372:1342-1353.
2. Chan J, Desai AK, Kazi ZB, Corey K, Austin S, Hobson-Webb LD, Case LE, Jones HN, Kishnani PS. The emerging phenotype of late-onset Pompe disease: A systematic literature review. Mol Genet Metab. 2017; 120:163-172.
3. Kanters TA, Hagemans ML, van der Beek NA, Rutten FF, van der Ploeg AT, Hakkaart L. Burden of illness of Pompe disease in patients only receiving supportive care. J Inherit Metab Dis. 2011; 34:1045-1052.
4. Regnery C, Kornblum C, Hanisch F, Vielhaber S, Strigl-Pill N, Grunert B, Müller-Felber W, Glocker FX, Spranger M, Deschauer M, Mengel E, Schoser B. 36 months observational clinical study of 38 adult Pompe disease patients under alglucosidase alfa enzyme replacement therapy. J Inherit Metab Dis. 2012; 35:837-845.
5. Papadimas GK, Spengos K, Konstantinopoulou A, Vassilopoulou S, Vontzalidis A, Papadopoulos C, Michelakakis H, Manta P. Adult Pompe disease: Clinical manifestations and outcome of the first Greek patients receiving enzyme replacement therapy. Clin Neurol Neurosurg. 2011; 113:303-307.
6. Chien YH, Goldstein JL, Hwu WL, *et al.* Baseline urinary glucose tetrasaccharide concentrations in patients with infantile- and late-onset Pompe disease identified by newborn screening. JIMD Rep. 2015;19:67-73.
7. Nilsson MI, Samjoo IA, Hettinga BP, Koeberl DD, Zhang H, Hawke TJ, Nissar AA, Ali T, Brandt L, Ansari MU, Hazari H, Patel N, Amon J, Tarnopolsky MA. Aerobic training as an adjunctive therapy to enzyme replacement in Pompe disease. Mol Genet Metab. 2012; 107:469-749.
8. Hamdan MA, El-Zoabi BA, Begam MA, Mirghani HM, Almalik MH. Antenatal diagnosis of Pompe disease by fetal echocardiography: Impact on outcome after early initiation of enzyme replacement therapy. J Inherit Metab Dis. 2010; 33:S333-339.
9. Wens SC, Schaaf GJ, Michels M, Kruijshaar ME, van Gestel TJ, In 't Groen S, Pijnenburg J, Dekkers DH, Demmers JA, Verdijk LB, Brusse E, van Schaik RH, van

der Ploeg AT, van Doorn PA, Pijnappel WW. Elevated plasma cardiac troponin T levels caused by skeletal muscle damage in Pompe disease. Circ Cardiovasc Genet. 2016; 9:6-13.
10. Schneider I, Zierz S. Profile of alglucosidase alfa in the treatment of Pompe disease: Safety, efficacy, and patient acceptability. Research and Reports in Endocrine Disorders. 2016; 6:1-9.
11. American Association of Neuromuscular & Electrodiagnostic Medicine. Diagnostic criteria for late-onset (childhood and adult) Pompe disease. Muscle Nerve. 2009; 40:149-160.
12. Castro-Jaramillo HE. The cost-effectiveness of enzyme replacement therapy (ERT) for the infantile form of Pompe disease: Comparing a high-income country's approach (England) to that of a middle-income one (Colombia). Rev Salud Publica (Bogota). 2012; 14:143-155.
13. Anderson LJ, Henley W, Wyatt KM, Nikolaou V, Waldek S, Hughes DA, Lachmann RH, Logan S. Effectiveness of enzyme replacement therapy in adults with late-onset Pompe disease: Results from the NCS-LSD cohort study. J Inherit Metab Dis. 2014; 37:945-952.
14. van der Ploeg AT, Kruijshaar ME, Toscano A, Laforêt P, Angelini C, Lachmann RH, Pascual Pascual SI, Roberts M, Rösler K, Stulnig T, van Doorn PA, Van den Bergh PYK, Vissing J, Schoser B; European Pompe Consortium. European consensus for starting and stopping enzyme replacement therapy in adult patients with Pompe disease: A 10-year experience. Eur J Neurol. 2017; 24:768-e31.
15. Han SO, Pope R, Li S, Kishnani PS, Steet R, Koeberl DD. A beta-blocker, propranolol, decreases the efficacy from enzyme replacement therapy in Pompe disease. Mol Genet Metab. 2016; 117:114-119.
16. Kanters TA, Hoogenboom-Plug I, Rutten-Van Mölken MP, Redekop WK, van der Ploeg AT, Hakkaart L. Cost-effectiveness of enzyme replacement therapy with alglucosidase alfa in classic-infantile patients with Pompe disease. Orphanet J Rare Dis. 2014; 9:75.
17. Davari M, Hashempour R, Pourreza A. Effectiveness of Enzyme Replacement Therapy for infantile onset Pompe disease (IOPD): A systematic review. Journal of Pharmacoeconomics and Pharmaceutical Management. 2020. (*in press*)
18. Genzyme Company. The production Monograph of Myozyme. *http://products.sanofi.ca/en/myozyme-en.pdf* (Accessed January 10, 2018)
19. Gustavsson E, Tinghög G. Needs and cost-effectiveness in health care priority setting. Health and Technology. 2020; 10:1-9.
20. Adla DN, Rowsell M, Pandey R. Cost-effectiveness of open versus arthroscopic rotator cuff repair. J Shoulder Elbow Surg. 2010; 19:258-261.
21. Robinson R. Costs and cost-minimisation analysis. BMJ. 1993; 307:726-728.
22. van den Hout HM, Hop W, van Diggelen OP, Smeitink JA, Smit GP, Poll-The BT, Bakker HD, Loonen MC, de Klerk JB, Reuser AJ, van der Ploeg AT. The natural course of infantile Pompe's disease: 20 original cases compared with 133 cases from the literature. Pediatrics. 2003; 112:332-340.
23. Alavian SM, Nikfar S, Kebriaeezadeh A, Lotfi F, Sanati E, Rezaei Hemami M, Keshavarz K. A cost-utility analysis of different antiviral medicine regimens in patients with chronic hepatitis C virus genotype 1 infection. Iran Red Crescent Med J. 2016; 18:e37094.
24. Bertram MY, Lauer JA, De Joncheere K, Edejer T, Hutubessy R, Kieny MP, Hill SR. Cost-effectiveness thresholds: pros and cons. Bull World Health Organ. 2016; 94:925-930.
25. WHO Commission on Macroeconomics and Health & World Health Organization. (2001). Macroeconomics and health: investing in health for economic development: executive summary/report of the Commission on Macroeconomics and Health. *https://apps.who.int/iris/handle/10665/42463* (accessed June 15, 2020)
26. Amiri A, Goudarzi R, Amiresmaili M, Iranmanesh F. Cost-effectiveness analysis of tissue plasminogen activator in acute ischemic stroke in Iran. J Med Econ. 2018; 21:282-287.
27. Picavet E, Cassiman D, Simoens S. What is known about the cost-effectiveness of orphan drugs? Evidence from cost-utility analyses. J Clin Pharm Ther. 2015; 40:304-307.
28. Parise H, Espinosa R, Dea K, Anaya P, Montoya G, Ng DB. Cost effectiveness of mirabegron compared with antimuscarinic agents for the treatment of adults with overactive bladder in Colombia. Pharmacoecon Open. 2020; 4:79-90.
29. Nicolino M, Byrne B, Wraith JE, *et al.* Clinical outcomes after long-term treatment with alglucosidase alfa in infants and children with advanced Pompe disease. Genet Med. 2009; 11:210-219.
30. Kishnani PS, Corzo D, Nicolino M, *et al.* Recombinant human acid α-glucosidase Major clinical benefits in infantile-onset Pompe disease. Neurology. 2007; 68:99-109.
31. Lamy A, Wang X, Kent R, Smith KM, Gafni A. Economic evaluation of the MEDENOX trial: A Canadian perspective. Medical patients with enoxaparin. Can Respir J. 2002; 9:169-177.
32. Jönsson B. Ten arguments for a societal perspective in the economic evaluation of medical innovations. Eur J Health Econ. 2009; 10:357-359.

Received April 29, 2020; Revised June 28, 2020; Accepted July 3, 2020

**Address correspondence to:*
Majid Davari, Department of Pharmacoeconomics and Pharmaceutical Administration, Faculty of Pharmacy, Tehran University of Medical Science, 16 Azar street, Tehran, Iran. Post Code:1417614411.
E-mail: M-Davari@TUMS.ac.ir

Released online in J-STAGE as advance publication July 25, 2020.

Brief Report

DOI: 10.5582/irdr.2020.03064

The challenge of managing comorbidities: a case report of primary Sjogren's syndrome in a patient with acute intermittent porphyria

Qing Teng[1], Liyan Ma[2], Yuelin Ma[1], Yiran Zhang[3], Ninglin Kang[4], Yuanxiang Hu[5], Songyun Zhang[1,*]

[1] Department of Endocrinology, The Second Hospital of Hebei Medical University, Shijiazhuang, Hebei, China;
[2] Department of Rheumatology, The Second Hospital of Hebei Medical University, Shijiazhuang, Hebei, China;
[3] School of First Clinical Medical College, Southern Medical University, Guangzhou, Guangdong, China;
[4] Hebei Provincial Hospital of Traditional Chinese Medicine, Shijiazhuang, Hebei, China;
[5] Geriatrics, First Affiliated Hospital of Hebei North University, Zhangjiakou, Hebei, China.

SUMMARY Acute intermittent porphyria (AIP) is a rare inherited metabolic disease associated with heme metabolism. Primary Sjogren's syndrome (PSS) is a common autoimmune disease. The combined presence of AIP and PSS complicates treatment. A rare case of concomitant AIP and PSS is reported in this paper. A 30-year-old woman with AIP had recurrent acute abdominal pain, nausea and vomiting, constipation, persistent chest, back, and waist pain, red urine, positivity for porphobilinogen (PBG) in urine and a pathogenic mutation of the HMBS gene. Two and a half years after she was diagnosed with AIP, she was diagnosed with PSS based on dryness of the eyes and mouth, the elevation of immunoglobulins (IgG and IgA) and positive results on an anti-SS-A antibody test, an anti-SS-B antibody test, Schirmer's test and a labial gland biopsy. A mutation in the HMBS gene was detected in the patient and her cousin, but the patient had more severe AIP and more severe symptoms (such as epilepsy and a limp), which may be related to the co-morbidity of PSS. According to her PSS activity score, the patient had an ESSDAI score of 9 and required systemic treatment. However, potential medications were limited by AIP, so mycophenolate mofetil was eventually added to delay the progression of the primary disease.

Keywords acute intermittent porphyria, primary Sjogren's syndrome, autoimmune disease, treatment

1. Introduction

Acute intermittent porphyria (AIP) is an autosomal dominant metabolic disease caused by gene mutations that results in decreasing heme synthase activity and accumulation of metabolic substrates, leading to neurological dysfunction (*1*). Primary Sjögren's syndrome (PSS) is a chronic inflammatory autoimmune disease that mainly affects exocrine glands such as the lacrimal and salivary glands (*2*) and that has a definite familial aggregation.

Many drugs cause the acute aggravation of AIP. If a patient with PSS has a score > 5 on the EULAR Sjögren's syndrome disease activity index (ESSDAI) (indicating moderately active PSS), the patient needs to receive systemic treatment in addition to local treatment. However, the key drugs used in systemic therapy, such as methylprednisolone and cyclophosphamide, can induce the acute onset of AIP. This poses major challenges to the treatment of AIP and other comorbidities in patients with PSS.

To date, there are few reports of patients with both AIP and autoimmune diseases, and most have AIP and systemic lupus erythematosus (SLE). At present, one case of AIP and PSS has been reported in Sweden (*3*). Reported here is a case of AIP and PSS, and this study explores its potential pathogenesis and difficulty in terms of treatment selection.

2. Patient and Methods

This study was reviewed and approved by the ethics committee of the Second Hospital of Hebei Medical University, and the patient and her family provided informed consent. All clinical data of the patient were collected. The patient and her cousin underwent exon gene sequencing, and genes related to AIP and immunodeficiency disorders were analyzed. The

ESSDAI scoring criteria were used to score the activity of PSS, and systemic treatment was required with an ESSDAI score > 5. The safety of glucocorticoids, immunosuppressants, and biological agents was analyzed based on references from the American Porphyria Foundation (*www.porphyriafoundation.com*) and the European Porphyria Network (*www.porphyria-europe.com*).

The current case involved a 30-year-old woman who had episodic abdominal pain for six years and a dry mouth and eyes for three and a half years.

Six years ago, in the fifth week of pregnancy, the woman developed acute and severe diffuse abdominal pain, accompanied by nausea, vomiting, constipation, persistent chest, back, and lower back pain, and red urine. Examinations revealed positivity for porphobilinogen (PBG) in urine and a mutation in the hydroxymethylbilane synthetase (HMBS) gene: c.806C>G (p.Thr269Arg) (Figure 1). The woman was diagnosed with severe AIP. In the six years after she was diagnosed, she had 17 acute episodes with two severe attacks. The first severe attack happened five years ago. The second day after undergoing a Cesarean section, the woman had severe abdominal pain, accompanied by headaches, dizziness, blurred vision, and seizures. Her blood pressure was 170/110 mmHg. A skull MRI revealed reversible encephalopathy syndrome. The second severe attack happened two years ago. The woman had severe abdominal pain after a cold, flaccid paralysis of the limbs, and muscle atrophy in the left hand. Each attack was treated with high concentration of glucose, heme arginate, an analgesic, and a beta blocker to lower blood pressure; the condition was relieved for one-three weeks.

Three and a half years ago, the woman developed a dry mouth and eyes and the sense of binocular gravel. Test results (Table 1) indicated that serum immunoglobulins (IgG and IgA) were elevated, and serum anti-SS-A antibody, serum anti-SS-B antibody, Schirmer's test were positive. A labial gland biopsy revealed moderate destruction of some of the acini, and interstitial scattering and multifocal infiltration of lymphocytes and plasma cells (grade 4) (Figure 2). Consequently, the woman was diagnosed with PSS. The woman was given artificial tears. PSS has gradually progressed over the past three and a half years. The woman developed mumps 3 times, and rampant dental caries and tooth loss gradually appeared. Serum immunoglobulin continued to rise (IgG: 16.70→28.00 g/L, IgA: 5.23→6.24 g/L). Complement C3 continued to decrease (C3: 0.91→0.59g/L).

Since the onset of AIP six years ago, routine urine testing has continued to reveal proteinuria (+), and 24-hour urine protein revealed proteinuria (0.65-1.05 g/day) that went untreated. Five years ago, the woman was diagnosed with Hashimoto's thyroiditis (subclinical hypothyroidism), and she was given Euthyrox 50 ug/d. Three years ago, intermittent purpura developed on the skin of the lower limbs after physical activity, though this was not treated.

Among the woman's family members, a cousin had similar attacks of abdominal pain, but the symptoms were mild, and there were no symptoms such as a dry mouth and dry eyes. Whole exon sequencing revealed a heterozygous missense mutation HMBS:NM_000190:exon12:c.806C>G (p.Thr269Arg) in the woman and her cousin. The results of first-generation sequencing indicated that the mutation was inherited from her father and not found in her mother. Analysis of the whole exon sequencing data from the woman and her cousin revealed three heterozygous missense variants related to immunodeficiency disorders: PSMB8: c.272G>A (p.Arg91Gln), IRF8: c.105G>C (p.Met35Ile), and CR2: c.3268C>A (p.Pro1090Thr) were carried by the woman but not by her cousin.

Table 1. Specific laboratory results related to dryness of the eyes and mouth

Laboratory test	Test result	Determination
IgA	5.23 g/L	H.
IgG	16.70 g/L	H.
Anti-SS-A antibody	114	+
Anti-SS-B antibody	71	+
Schirmer's test	R = 2/mm, L = 3/mm	+

H: elevated; Positive +

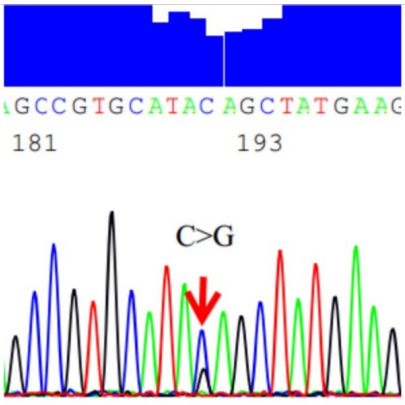

Figure 1. Detection of a mutation in the HMBS gene causing porphyria: c. 806C>G: p.T269R.

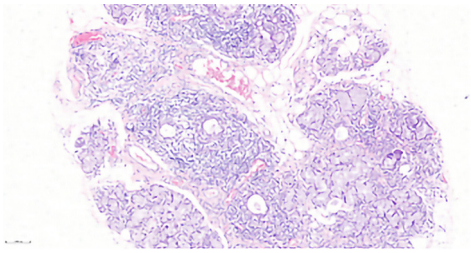

Figure 2. Microphotograph of a biopsied specimen from the patient's labial gland

3. Results and Discussion

This report has described a case of AIP and PSS. On the one hand, typical clinical manifestations of AIP and a known HMBS gene mutation (c. 806C>G (p.T269R)) were identified. On the other hand, there were typical clinical manifestations of PSS such as dry eyes and a dry mouth, the elevation of immunoglobulins (IgG and IgA) and the results of Schirmer's test, an anti-SS-A antibody test, an anti-SS-B antibody test, and a labial gland biopsy were all positive. A mutation in the HMBS gene was detected in the patient and her cousin, but the patient had more severe AIP, more frequent seizures, and more severe symptoms (such as epilepsy and a limp), which may be related to the co-morbidity of PSS.

SS is an autoimmune disease that primarily affects the exocrine glands and is thought to be the result of a combination of heredity and environment. Bacterial or viral infections activate the immune system, which may cause susceptible individuals with SS to develop SS (*4*). Accordingly, whole exon sequencing data from the patient and her cousin were analyzed. Three heterozygous missense variants related to immunodeficiency disorders were found: PSMB8: c.272G>A (p.Arg91Gln), IRF8: c.105G>C (p.Met35Ile), and CR2: c.3268C>A (p.Pro1090Thr) were carried by the patient but not by her cousin. However, whether these three variants are related to the clinical phenotype of patient needs to be studied further.

The treatment of AIP and PSS is more complex than treatment of PSS alone because drugs that may induce the acute onset of AIP must be avoided. The treatment of PSS includes symptomatic treatment and systemic treatment. According to the 2019 EULAR recommendations, patients with an ESSDAI score > 5 require systemic treatment. The patient also had cutaneous purpura, renal damage, hypothyroidism, and other extra-glandular lesions with dry mouth and eyes. Her ESSDAI score was 9 (Table 2), so systemic treatment must be given at the same time as symptomatic treatment. Glucocorticoids are the drug of choice for the systemic treatment of PSS, and medium-acting glucocorticoids are the first option. Prednisolone and triamcinolone can be safely used in patients with AIP, but the current patient refused to take them due to concerns of being overweight and having a family history of diabetes. Immunosuppressants are a second option, with cyclophosphamide being used most often, but it can induce the acute onset of AIP and thus could not be given to the current patient. Other immunosuppressants such as mycophenolate mofetil, azathioprine, cyclosporine, and methotrexate can all be used safely (Table 3). Mycophenolate mofetil can inhibit the proliferation of activated B cells and reduce serum immunoglobulin levels (*5*), and especially in patients with PSS associated with hyperglobulinemia and glomerulonephritis (*6*). Cyclosporine-A mainly inhibits T cell proliferation and is nephrotoxic (*7,8*). Azathioprine can not be used together with febuxostat (*9*), and has potent myelosuppressive action (*10*). Methotrexate is commonly used to alleviate the symptoms of arthritis (*11*) and skin lesions (*12*) in patients with PSS. In the current patient, hyperglobulinemia (-) was considered to be associated with purpura. Given renal damage and anemia in this patient, mycophenolate mofetil was

Table 2. Specific clinical manifestations indicated by a patient's disease activity score

Affected area	Level of disease activity	Specific manifestations
Glandular domain	Moderate activity = 2	Major glandular swelling: Enlarged parotid glands (ultrasound of the parotid gland reveals that the right parotid gland is about 5.5 × 2 cm in size and the left parotid gland is about 5 × 1.5 cm in size)
Cutaneous domain	Moderate activity = 2	Purpura of the ankle
Renal domain	Moderate activity = 2	Moderate renal involvement: Glomerular involvement with proteinuria (1.05 g/d)
Hematological domain	Low activity = 1	Cytopenia of auto-immune origin: Anemia (hemoglobin: 117 g/L)
Biological domain	Moderate activity = 2	High IgG level: IgG of 28.00g/L

Total ESSDAI score: 9.

Table 3. Safety of glucocorticoids, immunosuppressants, and biological agents commonly used for PSS in patients with AIP

Items	Glucocorticoid	Immunosuppressant	Biological agent
NP/PNP	Prednisolone (Medium-acting) Triamcinolone (Medium-acting) Betamethasone (Long-acting)	Mycophenolate mofetil Azathioprine Methotrexate cyclosporine-A	Rituximab
PSP	Hydrocortisone (Short-acting) Cortisone (Short-acting) Prednisone (Medium-acting) Methylprednisolone (Medium-acting) Dexamethasone (Long-acting)	Cyclophosphamide	

NP, not porphyrinogenic; PNP, probably not porphyrinogenic; PSP, possibly porphyrinogenic.

the most suitable. A biological agent is a third option. Rituximab can be safely used in patients with PSS and severe hemocytopenia or lymphoma (*13*), but this drug was not required in the current patient. Since the patient was given artificial tears to relieve dry eyes, she was given mycophenolate mofetil to delay the progression of the primary disease.

References

1. Benassi F, Righi E, Cimato P, Parravicini R. Cardiac surgery in patients with acute intermittent porphyria. J Card Surg. 2012; 27:331-4.
2. Ramos-Casals M, Brito-Zerón P, Sisó-Almirall A, Bosch X. Primary Sjogren syndrome. BMJ. 2012; 344:3821.
3. Floderus Y, Shoolingin-Jordan PM, Harper P. Acute intermittent porphyria in Sweden. Molecular, functional and clinical consequences of some new mutations found in the porphobilinogen deaminase gene. Clin Genet. 2002; 62:288-697.
4. Shen L, He J, Kramer JM, Bunya VY. Sjögren's Syndrome: Animal Models, Etiology, Pathogenesis, Clinical Subtypes, and Diagnosis. J Immunol Res. 2019; 2019:8101503.
5. Allison AC, Eugui EM. Mycophenolate mofetil and its mechanisms of action. Immunopharmacology. 2000; 47:85-118.
6. Bertsias GK, Tektonidou M, Amoura Z, *et al.* Joint European League Against Rheumatism and European Renal Association-European Dialysis and Transplant Association (EULAR/ERA-EDTA) recommendations for the management of adult and paediatric lupus nephritis. Ann Rheum Dis. 2012; 71:1771-1782.
7. Lai Q, Luo Z, Wu C, Lai S, Wei H, Li T, Wang Q, Yu Y. Attenuation of cyclosporine A induced nephrotoxicity by schisandrin B through suppression of oxidative stress, apoptosis and autophagy. Int Immunopharmacol. 2017; 52:15-23.
8. Caires A, Fernandes GS, Leme AM, Castino B, Pessoa EA, Fernandes SM, Fonseca CD, Vattimo MF, Schor N, Borges FT. Endothelin-1 receptor antagonists protect the kidney against the nephrotoxicity induced by cyclosporine-A in normotensive and hypertensive rats. Braz J Med Biol Res. 2017; 51:6373.
9. Logan JK, Wickramaratne Senarath Yapa S, Harinstein L, Saluja B, Muñoz M, Sahajwalla C, Neuner R, Seymour S. Drug interaction between febuxostat and thiopurine antimetabolites: a review of the FDA Adverse Event Reporting System and medical literature. Pharmacotherapy. 2020; 40:125-132.
10. Stoenoiu MS, Aydin S, Tektonidou M, *et al.* Repeat kidney biopsies fail to detect differences between azathioprine and mycophenolate mofetil maintenance therapy for lupus nephritis: Data from the MAINTAIN Nephritis Trial. Nephrol Dial Transplant. 2012; 27:1924-1930.
11. Mirouse A, Seror R, Vicaut E, *et al.* Arthritis in primary Sjögren's syndrome: characteristics, outcome and treatment from French multicenter retrospective study. Autoimmun Rev. 2019; 18:9-14.
12. Argyropoulou OD, Tzioufas AG. Common and rare forms of vasculitis associated with Sjögren's syndrome. Curr Opin Rheumatol. 2020; 32:21-28.
13. Leanna MW, Daniel GA. A patient with primary Sjogren's syndrome, cystic lung disease, and MALT lymphoma treated successfully with rituximab: A case-based review. Clin Rheumatol. 2020; 39:1357-136.

Received June 2, 2020; Revised July 18, 2020; Accepted July 29, 2020.

**Address correspondence to:*
Songyun Zhang, Department of Endocrinology, The Second Hospital of Hebei Medical University, Shijiazhuang 050000, Hebei, China.
E-mail: zsy2020@hebmu.edu.cn

Released online in J-STAGE as advance publication August 6, 2020.

Brief Report

DOI: 10.5582/irdr.2020.03065

An extremely rare combination of acute intermittent porphyria and Turner syndrome

Songyun Zhang[1,*], Jiahong Wu[2], Qing Teng[1], Yiran Zhang[3], Yuanxiang Hu[2], Ninglin Kang[4]

[1] Endocrinology, The Second Hospital of Hebei Medical University, Shijiazhuang, Hebei, China;
[2] Department of Geriatrics, The First Affiliated Hospital of Hebei North University Zhangjiakou, Hebei, China;
[3] The First Clinical Medical College Southern Medical University, Guangzhou, Guangdong, China;
[4] Hebei Provincial Hospital of Traditional Chinese Medicine, Shijiazhuang, Hebei, China.

SUMMARY A very rare case of acute intermittent porphyria (AIP) co-existing Turner syndrome (TS) is reported for the first time. A 32-year-old woman was diagnosed with AIP due to recurrent acute abdominal pain, red urine and pathogenic mutation of Hydroxymethyl synthetase (HMBS) gene. At the same time, TS was confirmed by Karyotype analysis results of 46,X,i(X)(q10), which accompanied by primary amenorrhea, elevated serum concentrations of follicle-stimulating hormone (FSH). Since the first attack of AIP, the patient has been increasingly depressed, and Psychiatry identified major depression. Duloxetine was chosen after careful deliberation, and the patient's mood stabilized. AIP had not recurred after half a year. Since sex hormones are the exacerbating factor of acute attack of AIP, sex hormone replacement therapy for TS was not administered. In conclusion, the conditions of AIP co-existing TS are complicate, and the treatment still needs to be improved by multiple disciplines in the follow-up.

Keywords acute intermittent porphyrin (AIP), Turner syndrome, HMBS gene, isochromosome, depression

1. Introduction

Acute intermittent porphyria (AIP) is a rare autosomal dominant genetic disease characterized by a deficiency in porphobilinogen deaminase (PBGD), the third enzyme in the heme biosynthesis pathway. The enzyme is coded for by the hydroxymethylbilane synthetase (HMBS) gene; mutations in that gene cause decreased PBGD activity and accumulation of precursors, leading to nerve dysfunction and clinical manifestations of acute abdominal pain and various neurological and mental disorders (*1*).

Turner syndrome (TS), also known as congenital ovarian dysplasia (*2*), is caused by complete or partial deletion of the X chromosome and is one of the most common chromosomal disorders in women. Clinical manifestations include primary amenorrhea, a short stature, abnormal bones, congenital heart disease, endocrine abnormalities, and autoimmune diseases (*3,4*). Reported here for the first time is a case of AIP and TS occurring together, and this study discusses this complex condition and difficulty in terms of treatment selection.

2. Patient and Methods

The design of this study was reviewed and approved by the Ethics Committee of the Second Hospital of Hebei Medical University, and the patient provided written informed consent. All clinical data on the patient were collected. The patient underwent whole exome sequencing and chromosome karyotype analysis. The safety of drugs used to treat the patient was determined based on standards of the American Porphyria Foundation (*www.porphyriafoundation.com*) and the European Porphyria Network (*www.porphyria-europe.com*). The PubMed database was searched in July 2020 using the keywords "acute intermittent porphyria AND Turner syndrome", and no articles were found.

This case involved a 32-year-old woman. The woman had paroxysmal abdominal pain and depression for two years.

Two years ago, she developed severe abdominal pain after exertion, nausea and vomiting, and oliguria and constipation. A physical examination was unremarkable. An abdominal X-ray suggested partial ileus that was alleviated with symptomatic treatment. Since then, the patient had gradually worsening depression, increased apathy, increased self-blame, fatigue, a poor appetite, difficulty falling asleep, and early waking. The patient had severe shortness of breath and was unable to talk

or walk. The results of electrocardiography and cardiac ultrasound were normal. The Hamilton Depression Scale indicated major depression. Consultation with a psychiatrist led to the diagnosis of major depression. Within 2 years, the patient had 6 acute episodes of AIP, 4 of which were induced by severe depression.

The patient had primary amenorrhea. Her father's height was 173 cm and her mother's height was 170 cm. Her parents are not cousins. Moreover, there are no similar diseases in the family. Her younger brother and sister are in good health. Physical findings from the patient were a height of 153 cm (lifetime height of 165.5 cm), a BMI of 17.5 kg/m^2, and no shield chest;short and webbed neck, cubitus valgus, and Madelung deformity of the forearm and wrist. The patient had Breast development Tanner stage 3, Pubic hair Tanner stage 2. Measurement of sex hormone levels revealed hypergonadotropic hypogonadism (FSH: 97.92 mIU/mL, LH: 21.05 mIU/mL, and E2: 28 pg/mL). A Pelvic ultrasound revealed an underdeveloped uterus, and neither ovary was evident. Karyotype analysis revealed an Isochromosome Xq(46,X,i(X)q), indicating Turner syndrome. Dual-energy absorptiometry (DXA) revealed severe osteoporosis with low bone mineral density (BMD) in the lumbar spine (Z-score of -4.7) and low BMD in the femoral neck (Z-score of -3.9)

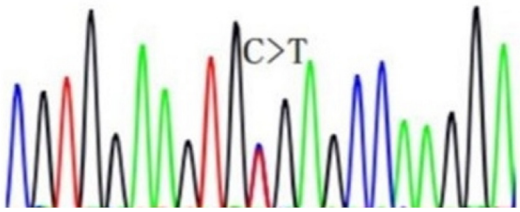

Figure 1. HMBS gene c. 673C>T (p. R225X).

3. Results and Discussion

AIP is a rare inherited disease, with an annual incidence of 0.13 per million and an estimated prevalence of 5.9 per million (*5*). TS is an uncommon sex chromosome aneuploidy (45,X) that affects approximately 1 in 2,000 to 1 in 2,500 live female births (*6-8*). Therefore, a combination of AIP and TS is a very rare clinical entity.

The patient was diagnosed with AIP based on genetic testing. A heterozygous missense variation, c. 673C>T, in the HMBS gene of the patient was identified (p.R225X) (Figure 1). According to the ACMG guidelines, it is a known pathogenic variation (PMID:8533808) (*9*), and it is also the most common HMBS gene variation observed in Chinese patients with AIP (research results to be published).This mutation occurs in exon 11, which is a termination mutation, resulting in the premature termination of the HMBS protein at position 225 during translation into amino acids, and the loss of all 136 amino acids in the C-terminal, including the C261 residue that is a binding site for a cofactor that facilitates 1-hydroxymethylbilane (HMB) formation, and the loss of function of PBGD.

The patient was diagnosed with Turner syndrome based on a karyotype analysis. The specific karyotype is 46,X,i(X)(q10) (Figure 2), that is, an isochromosome for the long arm of the X chromosome. The short arm of the X chromosome is missing and replaced by an accurate copy of the long arm, which is one of the most common structural abnormalities of sex chromosomes (*10*). The SHOX gene, located at the distal end of the short arm of the X chromosome, is associated with chondro-development and is a phenotype of human dwarfism. Deletion of the SHOX gene will lead to height defects. Thus, almost all patients with Turner syndrome have a short stature, *i.e*. a final height,

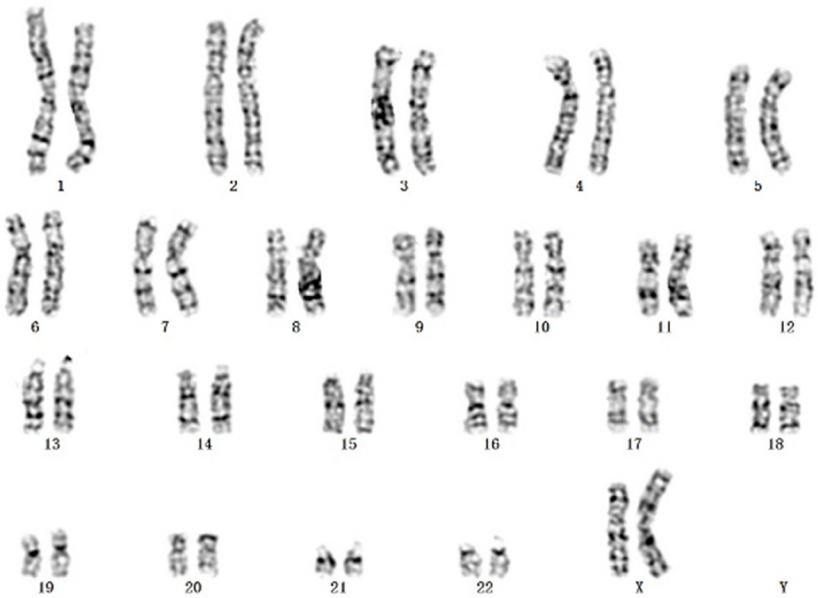

Figure 2. Karyotype analysis of the patient: An isochromosome for the long arm of the X chromosome 46,X,i(X)(q10).

usually no more than 150 cm, about 20 cm shorter than the expected lifetime height (*11*). However, the patient diagnosed with TS in the current case did not have a short stature but a natural height of 153 cm, which is just 10 cm shorter than the expected lifetime height (163 cm). The mechanism for this is unknown and worth exploring. The patient had natural breast development, suggesting partial prepubertal ovarian function.

Worsening depression is evident in patients with AIP and TS. A systematic review indicated that patients with TS had an increased risk of depression, and once depression developed, symptoms were more severe and more likely to recur. This is associated with decreased sex hormone levels and a short stature in patients with TS. The current patient was diagnosed with TS at the age of 32, and the delay in diagnosis resulted in a chronic deficiency of sex hormones and substantially increased the patient's risk of depression (*12*). According to the literature, patients with AIP can develop various mental and emotional issues at any time during the course of the disease, such as anxiety, depression, insomnia, behavioral abnormalities, personality changes, and even hallucinations and delirium. Depression is a very common one (*13*). In the current case, depression occurred after the first attack of AIP and gradually worsened, indicating that AIP caused the patient's depression. Various mood disorders, including depression, are aggravating factors for AIP (*14*). The untreated depression in the current patient markedly increased the incidence and severity of AIP attacks. In summary, the current patient had a high risk of depression due to TS. AIP induced depression , conversely , depression aggravated the severity of AIP, thus forming a vicious cycle. Accordingly, relief of depression is key to solving the problem.

First-line antidepressants are currently chosen based mainly on symptoms. Escitalopram and sertraline are chosen for anxiety. Duloxetine and venlafaxine are suggested for apathy. Mirtazapine is used for insomnia, loss of appetite, agitation, and suicidal ideation. The main symptom in the current patient was apathy. Because drugs can contribute to AIP, clinicians treating patients with AIP must choose drugs by carefully reviewing the latest drug safety information, including that from the American Porphyria Foundation (*www.porphyriafoundation.com*) and the European Porphyria Network (*www.porphyria-europe.com*). Duloxetine was deemed the most appropriate drug for the current patient. In this case, duloxetine was efficacious and symptoms were significantly alleviated. The patient had not suffered any acute AIP attacks in the half year prior to this report.

Severe osteoporosis is another major clinical manifestation that was noted the current patient. Osteoporosis is related to ovarian failure and an estrogen deficiency in patients with TS. The basic approach to preventing osteoporosis in women with TS is to start hormone replacement therapy as early as age 11-13, to titrate to the adult dose two years later, and to continue until menopausal age (*7*). Given that the current patient also had AIP, a sex hormone, and especially progesterone, would aggravate AIP, so hormone replacement therapy was not administered for the time being. Once AIP is stable, hormone replacement therapy may be cautiously attempted.

As mentioned earlier, the diagnosis of AIP or TS is often missed or delayed due to nonspecific symptoms, leading to increased morbidity and mortality. With that in mind, diagnosis requires a high index of suspicion, and treatment should be started as soon as possible.

In conclusion, AIP and TS may occur together, and the treatment for a patient with these comorbidities needs to be improved upon during follow-up by specialists in multiple disciplines.

References

1. Spiritos Z, Salvador S, Mosquera D, Wilder J. Acute intermittent porphyria: current perspectives and case presentation. Ther Clin Risk Manag. 2019; 15:1443-1451.
2. Classic pages in obstetrics and gynecology by Henry H. Turner. A syndrome of infantilism, congenital webbed neck, and cubitus valgus. Endocrinology. Am J Obstet Gynecol. 1972; 113:279.
3. Gravholt CH, Andersen NH, Conway GS, *et al*. Clinical practice guidelines for the care of girls and women with Turner syndrome: Proceedings from the 2016 Cincinnati International Turner Syndrome Meeting. Eur J Endocrinol. 2017; 177:G1-G70.
4. Gravholt CH, Viuff MH, Brun S, Stochholm K, Andersen NH. Turner syndrome: Mechanisms and management. Nat Rev Endocrinol. 2019; 15:601-614.
5. Elder G, Harper P, Badminton M, Sandberg S, Deybach JC. The incidence of inherited porphyrias in Europe. J Inherit Metab Dis. 2013; 36: 849-857.
6. Bondy CA, Turner Syndrome Study Group. Care of girls and women with Turner syndrome: a guideline of the Turner Syndrome Study Group. J Clin Endocrinol Metab. 2007; 92:10-25.
7. Stochholm K, Juul S, Juel K, Naeraa RW, Gravholt CH. Prevalence, incidence, diagnostic delay, and mortality in Turner syndrome. J Clin Endocrinol Metab. 2006; 91:3897-3902.
8. Cockwell A, MacKenzie M, Youings Sv, Jacobs P. A cytogenetic and molecular study of a series of 45,X fetuses and their parents. J Med Genet. 1991; 28:151-155.
9. Lee GY, Astrin KH, Desnick RJ. Acute intermittent porphyria: a single-base deletion and a nonsense mutation in the human hydroxymethylbilane synthase gene, predicting truncations of the enzyme polypeptide. Am J Med Genet. 1995; 58:155-158.
10. Wolff DJ, Van Dyke DL, Powell CM; Working group of the ACMG laboratory quality assurance committee. Laboratory guideline for Turner syndrome. Genet Med. 2010; 12:52-55.
11. C G Brook, G Mürset, M Zachmann, A Prader. Growth in children with 45,XO Turner's syndrome. Arch Dis

Child. 1974; 49:789-795.
12. Morris LA, Tishelman AC, Kremen J, Ross RA. Depression in Turner syndrome: a systematic review. Arch Sex Behav. 2020; 49:769-786
13. Duque-Serrano L, Patarroyo-Rodriguez L, Gotlib D, Molano-Eslava JC. Psychiatric aspects of acute porphyria: a comprehensive review. Curr Psychiatry Rep. 2018; 20:5.
14. Augoulea A, Zachou G, Lambrinoudaki I. Turner syndrome and osteoporosis. Maturitas. 2019; 130:41-49.

Received June 14, 2020; Revised July 13, 2020; Accepted July 28, 2020.

**Address correspondence to:*
Songyun Zhang, Endocrinology, The Second Hospital of Hebei Medical University, Hebei 050000, China.
E-mail: zsy2020@hebmu.edu.cn

Released online in J-STAGE as advance publication August 6, 2020.

Brief Report

DOI: 10.5582/irdr.2020.01026

array-CGH revealed gain of Yp11.2 in 49,XXXXY and gain of Xp22.33 in 48,XXYY karyotypes of two rare klinefelter variants

Somprakash Dhangar, Jagdeeshwar Ghatanatti, Babu Rao Vundinti

Department of Cytogenetics, National Institute of Immunohaematology (ICMR), K.E.M Hospital campus, Parel, Mumbai, India.

SUMMARY Klinefelter syndrome (KS) variants often share common features with classical syndrome but some of these variants present with a distinct phenotype. The incidence of sex chromosome tetrasomy and pentasomy are very less and generally diagnosed after prepubertal age. The early diagnosis of complex and unclassified syndromes and it's correlation with genotype is necessary for personalized treatment as well as genetic counselling of the affected families. We describe clinical presentation, and genetic diagnosis of two cases of variant KS. Our first case, a 4 year old male child presented with generalized tonic-clonic seizures (GTCSs), delayed milestones and dysmorphic features while case 2, a-21 years old male who had history of seizures and delayed puberty came to our lab for genetic diagnosis. The chromosomal analysis of case 1 and 2 showed 49,XXXXY and 48,XXYY karyotype respectively. The karyotype results were confirmed with fluorescence in situ hybridization (FISH) and array-CGH analysis. The FISH results were found to be consistent with karyotype but the array-CGH results showed the extra gain of region Yp11.2 in case 1 while the extra gain of region Xp22.33 in case 2. The cases were confirmed as variant KS on the basis of additional sex chromosomes and clinical presentation of deteriorated brain development. The present study suggests that the high doses of sex chromosome linked genes including pseudoautosomal region (PAR) caused the abnormal brain development. The combination of molecular techniques should be utilized for the diagnosis of such complex cases to understand the genotype-phenotype correlation and appropriate genetic counseling.

Keywords Klinefelter variants, sex chromosome polysomy, pseudoautosomal region, complex psychological behavior, deteriorated brain development

1. Introduction

Klinefelter syndrome (KS) variants are rare sex chromosome aneuploidy (SCA), which generally occur less frequently compared to classical KS (1:650 male births) (*1-3*). Sex chromosome tetrasomy and pentasomy individuals share many features including tall stature, undescended testis and hypergonadotropic hypogonadism. According to the literature the phenotypes in variant KS cases become more complex as number of sex chromosomes involvement increased (*4*). The presence of additional sex chromosomes causes an overdose of genes leading to overexpression of protein and affects the normal development of the phenotype. The variant 48,XXYY (tetrasomy) is found to be more common (1:18,000-1:40,000) SCA as compared to 49,XXXXY (pentasomy) which is estimated to be present in 1:85000-1:100000 male births (*5*). The chromosomal aneuploidy occurs through a non-disjunction mechanism in germ cells during gametogenesis or early embryonic development. However the number of extra chromosomes depends on the type of participating gametes and time of the events (*6*). The 46,XXYY variant mainly results due to fertilization of a normal oocyte with a aneuploid sperm and some times during postzygotic events while 49,XXXXY variant occurs from non- disjunction of the X chromosome during both meiosis- I and meiosis-II stage of oogenesis. Thus an aneuploid oocyte is fertilized with normal sperm (*7,8*).

The knowledge regarding complex psychological behavior with deteriorated brain development in rare cases of variant KFS are limited and only a few cases are reported in the literature (*9*). We report genetic analysis of two cases of variant KS present with complex features and abnormal brain development.

2. Materials and Methods

Two cases with dysmorphic features with delayed

milestones were referred to our cytogenetic laboratory for genetic diagnosis. Blood samples were collected in sodium heparin and ethylenediaminetetraacetic acid (EDTA) vacutainers (2 mL in each tube). The heparinized blood samples were used for cytogenetic analysis while EDTA samples were utilized for molecular analysis.

2.1. Conventional cytogenetics

The cytogenetic study was carried out by setting up peripheral blood cultures at 37°C for 72 hrs according to standard procedures (*10*). Briefly, the cultures were stimulated with phytohaemagglutinin (PHA) arrested with colchicine (50 µg/mL) and treated with hypotonic solution (KCL 0.56g/100 mL). The cells were fixed in Carnoy's solution (Methanol: Glacial acetic acid; 3:1). The chromosomal preparations obtained were subjected to GTG banding (*11*). At least 50 metaphases were scored and 10 were karyotyped (approximately 350 band resolution) according to International System of Chromosome Nomenclature 2016 (ISCN 2016) (*12*). The images were captured with a CCD camera attached to Nikon 90i microscope (Japan) and analysis was done using Applied Spectral Imaging software system (Inc. Carlsbad, USA).

2.2. Fluorescence in situ hybridization (FISH)

Metaphases obtained from conventional cytogenetic procedure were utilized for molecular cytogenetic study. Fluorescence in situ hybridization (FISH) was carried out using centromere specific (Vysis, Abbott Life Sciences, USA) probe for X (Cat. No.05J10-033) and Y (Cat. No. 05J08-035) chromosomes.

2.3. array-CGH

DNA was extracted from EDTA blood samples using a commercially available DNA kit (QIAamp DNA blood mini kit cat. No. 51104, Qiagen, Germany). Chromosomal microarray analysis (CMA) was performed using CytoPrime microarray. The cutoff filter settings for the CMA test analysis were 1MB for clinically relevant losses and 2 MB for gains.

2.4. Case 1

A 4-year old male child, the first born of a healthy non-consanguineous couple was referred to our cytogenetics laboratory for chromosomal analysis due to generalized tonic-clonic seizures (GTCSs) episodes, delayed milestones and dysmorphic features. This male patient was born at 8 months of pregnancy (preterm) through lower (uterine) segment caesarean section (LSCS) with moderately low birth weight. The mother of the child had no obvious history of illness or medication during pregnancy and her age was 30 years while the father was 32 years old. On clinical examination, the child had facial dysmorphic features such as slight downward slanting of the eyes with epicanthic folds, hypertelorism, low set ears, large pinnae, and flattened nasal bridge. The speech development was normal while the gross and fine motor development was poor. The proband also had limb anomalies including genu valgum and hyperlaxity of the upper limb. The Social Quotient (SQ) was 75. The magnetic resonance imaging (MRI) scan of the brain revealed demyelization of right parietal sub white matter, mild prominence at lateral and third ventricle with paucity of white matter. Brainstem Evoked Response Audiometric (BERA) test showed normal hearing ability. Ultra sonography (USG) of kidney, ureter and bladder and Barium swallow study revealed normal development. The study was carried out with the consent of the father of the proband.

2.5. Case 2

A 21- years old male was referred to our cytogenetic laboratory for chromosomal analysis. He had history of delayed puberty. This male patient was born at full term to non-consanguineous parents.. His mother brought him to the laboratory for the diagnosis of delayed puberty. The mother's age was 31 years while father was 36 years old at the time birth of the affected child. There was no obvious history of illness or medication of mother during pregnancy. The child birth history revealed that this affected patient was born with hypospadias and inguinal hernia and the volume of testis was comparatively low at the time of birth. The child also had history of delayed cry. The child was diagnosed with hydrocele at the age of 3 years and was corrected by surgery. The child had history of delayed puberty and convulsion disorder. During the prepubertal age of proband, mother of the child noticed aggressiveness and poor social behavior with family members. The proband also had history of tremalansness (tremors), which developed after the pubertal age. The clinical examination revealed absence of pubic and axillary hair. The proportion of upper and lower segment was not appropriate. The level of luteinizing hormone (LH) was 21.5 IU/mL (normal range 2.5-10 IU/mL) while follicular stimulating hormone (FSH) level was 63.0 IU/mL (normal range 2.5-10 IU/mL). The level of testosterone was very low (0.27 nmol/L). Thyroid stimulating hormone level was 212 µIU/mL (normal range 0.4- 4.0 µIU/mL). He also had an elevated level of creatine phosphokinase. The MRI brain of proband revealed periventricular gliotic changes in post parietal periventricular region with left subtle atrophy of right hippocampal tail. The sibling of the proband also had a similar history of medical problems such as protruding tongue, hypertelorism and seizures. The study was carried out with the consent of the parents of the proband.

3. Results and Discussion

The conventional cytogenetic analysis of case 1 revealed 49,XXXXY karyotype while case 2 was detected with 48,XXYY karyotype (Figure 1A and Figure 2A). The karyotypes of parents of both patients were normal. FISH results were consistent with conventional karyotype results and showed four copies of chromosome X and one copy of chromosome Y in case 1 while one extra copy of chromosome X and Y in case 2 (Figure 1B and Figure 2B). Mosaicism was not observed in both cases.

Further the chromosome gain and breakpoint were confirmed by array-CGH analysis (750K CytoPrime microarray system with Chromosome Analysis Suite software designed by Affymetrix). The array-CGH analysis of case 1 revealed a four copy number gain of entire chromosome X (cytoband Xp22.33-q28) and one extra partial copy number gain of chromosome Y for region Yp11.2 along with entire Y chromosome *i.e.* arr[GRCh38] Xp22.33q28(251879-156004066)×4, and arr[GRCh38]Yp11.2(2931110-6204020)×2 (Figure 1C). The array-CGH analysis of case 2 revealed a copy number gain of chromosome X and Y *i.e.* arr[GRCh38] Xp22.33q21.31(2785591-89149355)×2, arr[GRCh38] Xq21.31-q28(9110165-155641381)×2 and arr[GRCh38] Yp11.2(2782099-26653790)×2 respectively. The array-CGH analysis of case 2 also showed a gain at Xp22.33 region, which encompassed 24 genes *i.e.* arr[GRCh38] Xp22.33(251879-2771493)×4 (Figure 2C). The array-CGH analysis of the sibling of case 2 showed a normal result. Apart from the entire intact chromosome the array- CGH detected the extra gain of chromosome Y with accurate break point (Yp11.2) in case 1 and extra gain of chromosomal region Xp22.33 in case 2 which could not be detected by conventional method. The array-CGH result confirmed the diagnosis as variant KS in both patients with tetrasomy of chromosome X and disomy (partial) of chromosome Y in case 1 while tetrasomy (partial) of chromosome X and disomy of Y in case 2.

The variants of KFS are generally defined on the basis of variable number of sex chromosomes. The incidence of KFS variants vary and it depends on the type of chromosome involved. The incidence of variants of KFS is reported to be 1:18,000 to 1:1,000,000 male births and found to be rarer than classical KS (*13*). Our literature search revealed lack of information regarding incidence, and genotype phenotype correlation on

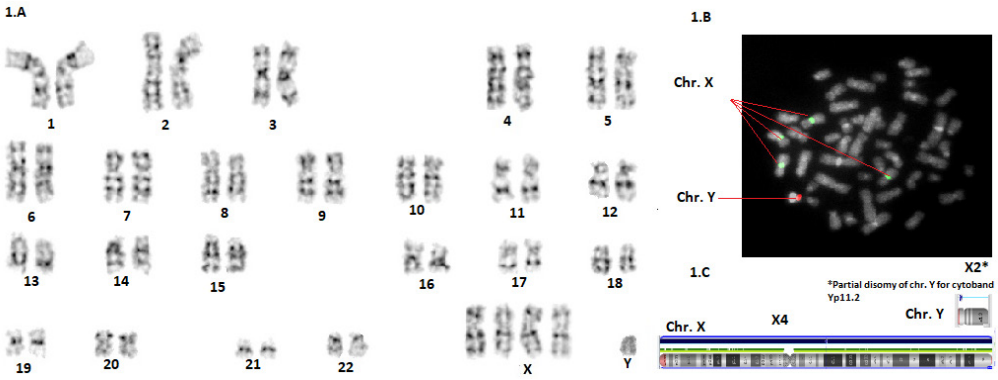

Figure 1. Conventional and molecular cytogenetic analysis of case 1. (A) GTG banded karyotype showing 49,XXXXY karyotype. **(B)** Tetrasomy of chromosome X (green) and single copy of chromosome Y (red) by FISH. **(C)** Array- CGH image showing tetrasomy of chromosome X and partial disomy of chromosome Y for region Yq11.2.

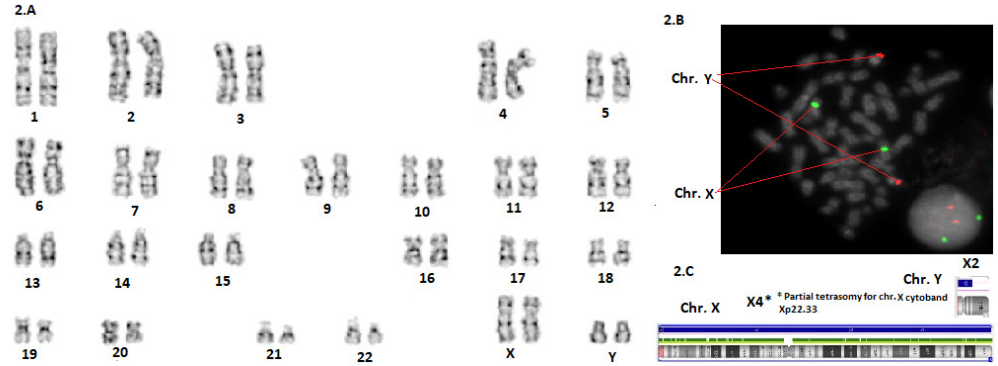

Figure 2. Conventional and molecular cytogenetic analysis of case 2. (A) GTG banded karyotype showing 48,XXYY karyotype. **(B)** Disomy of X (green) and Y (red) chromosomes by FISH. **(C)** Array- CGH image showing partial tetrasomy of chromosome X for region Xp22.33 and disomy of chromosome Y.

Table 1. Comparison of clinical abnormalities of present cases with reported clinical presentations of SCAs

S. No.	Clinical presentation of sex chromosome polysomy in males*	Clinical abnormalities observed in present study	
		Case 1	Case 2
1	Hypotonia in childhood	+ (mild)	-
2	Hypergonadotropic hypogonadism	+	+
3	Dental problems	-	-
4	Asthma/ Reactive airways disease	-	-
5	Food/ Environmental allergies	-	-
6	Cardiac malformations	-	-
7	Intention and postural tremor	-	+
8	Radioulnarsynostosis/Congenital elbow dislocation	+	-
9	Congenital hip dysplasia	-	-
10	Pes planus/ Flat feet	+	+
11	Club foot	-	-
12	Inguinal hernia/Undescended testis	-	+
13	Deep vein thrombosis/ Pulmonary embolism	-	-
14	Hypothyroidism	-	+
15	Type II diabetes	-	-
16	Scoliosis	-	-
17	Seizure disorder	+	+
18	Strabismus	+	-
19	Recurrentotitis	+	-
20	Gastroesophagealreflux	-	+
21	Constipation	-	+
22	Obstructive sleep apnoea	-	-
23	Osteoporosis	-	-

*The clinical presentations mentioned in the above table are not necessary to be present in all cases of sex chromosome aneuploidies (SCAs).

variants of SCA. However the Genetic and rare disease information center (GARD) is one of the important rare genetic disease databases and included these aneuploidies as numeric sex chromosome variations (*14*). Our extensive literature survey found that different types of KS variants (47,XYY; 48,XXXY; 48,XXYY; 48,XYYY; 49, XXXYY; 49,XXXXY) including copy number variations (CNV's) in sex chromosomes have been reported. However the literature related to CNV's are limited (*15*). The SCA's occurs due to error in cell division (non-disjunction) during gametogenesis or post zygotic events. In case of mosaic trisomy (46,XY/ 46,XXY), the non- disjunction takes place in somatic cells during fetal development (*7,8,16,17*). The classical features of KS include tall stature with eunuchoid skeleton, pes planus, clinodactyly of fifth finger and primary testicular insufficiency. The small volume of testis is the major clinical presentation in KS individuals, which leads to decreased production of testosterone and ultimately affects male sexual development. However, the clinical presentation of KS variants differs from case To case and affects different systems of the body (Table 1) (*18*). Despite multiple reports on effects of SCA and disease severity, the knowledge of abnormal brain development is limited (*19,20*). In our study we have identified aneuploidy of sex chromosomes in both cases, and it is evident that these anomalies occur denovo in the index cases because parental cytogenetic analysis revealed normal karyotypes. The non- disjunction mechanism taking place during gametogenesis in one of the parents may be the reason for the aneuploidy in the proband. In addition, the microarray analysis showed duplication of pseudoautosomal regions (PAR) PAR 1 and PAR 2 on the sex chromosomes. The abnormal crossing over taking place in the sex chromosome during gametogenesis involving the PAR1 and PAR 2 regions could be the reason for Copy number Variations (*21*).

In the present study, both cases were diagnosed as Variant KS with novel karyotype. In Case 1, the proband was diagnosed with 49,XXXXY karyotype. The proband also had partial disomy of chromosome Y for region Yp 11.2. Apart from the classical features (undescended testis, genu valgum and hyperlaxity of the upper limb) the proband also had brain anomalies like demyelination of the right parietal sub white matter, and mild prominence at lateral and third ventricle with paucity of white matter. The gene dosage of sex chromosomes were found to be associated with learning disabilities and language development, because the genes lying on the sex chromosome have a crucial role in brain development and language pathways (*22*).

The 48,XXYY karyotype is an uncommon chromosomal abnormality in humans. These anomalies occur due to non- disjunction of homologous chromosome during gametogenesis. The individual with 48,XXYY karyotype generally presented with tall stature, which became more significant during adolescence (*18*). In the present study, the proband (case 2) was diagnosed with 48,XXYY karyotype and also had partial tetrasomy X for the PAR region. The proband presented with tall stature and detoriated brain

development. Though Attention Deficit Hyperactivity Disorders (ADHD) are more common (70%) in 48,XXYY cases, evidence related to etiological genetic factors are limited. In our study we have identified brain anomalies in both cases, which are found to be associated with genotype. In our first case MRI study revealed demyelination of right parietal sub white matter, mild prominence at lateral and third ventricle with paucity of white matter while the second case shows periventricular gliotic changes in post parietal periventricular region with left subtle atrophy of right hippocampal tail. Similar clinical features also reported as case reports suggested that the gene dosage of X chromosome plays an important role in development of white matter tracts and ventricles of the brain and also reduces brain volume (*9,22*). Our CMA (CytoPrime microarray) analysis identified copy number gain at position Xp22.33 in case two, and the genes lying on this chromosomal region (Xp22.33) are found to be associated with ADHD and autism spectrum disorder, however pathogenicity is not yet clear (*23*). In case 1 apart from 49,XXXY Karyotype, our CMA analysis also identified a copy number gain at cytoband Yp11.2, which encompasses five genes (*ZFY, ZFY-AS1*, *LINC00278*, *TGIF2LY*, *PCDH11Y*) about 3.2MB in size. According to the literature, the gene *PCDH11Y* (paralogue of *PCDH11X*) has an important role in cell- cell recognition during development of the central nervous system which might play a role in brain development and reduced brain volume (*24*). Moreover the genes present in pesudoautosomal region expressed (2.0- fold in 48,XXYY, 48XXXY or 2.5- fold in 49,XXXXY) more as compared to classical KFS cases because these genes can escape X-inactivation. The over expression of these genes are found to be associated with different developmental problems (*25,26*).

In conclusion, the diagnosis of variants of clinical syndromes is important to understand the genetic nature and phenotype presentation. Though chromosomal aneuploidies are identified with routine cytogenetic investigation, the microarray analysis helps in identification of submicroscopic losses and gains, which greatly helps in genotype-phenotype correlation and appropriate genetic counseling.

Acknowledgements

The study was carried out with an Institutional core grant.

References

1. Evans J A, de von Flindt R, Greenberg C *et al*. A cytogenetic survey of 14,069 new born infants, IV, further follow-up on the children with sex chromosome anomalies. In: Birth Defects: Original Article Series (Stewart D, Ed.). Alan R. Liss, Inc, New York, USA, 1982; pp.169-184.
2. Fruhmesser A, Kotzot D. Chromosomal variants in klinefelter syndrome. Sex Dev. 2011; 5:109-123.
3. Asirvatham AR, Pavithran PV, Pankaj A, Bhavani N, Menon U, Menon A, Abraham N, Nair V, Kumar H, Thampi MV. Klinefelter syndrome: clinical spectrum based on 44 consecutive cases from a South Indian Tertiary Care Center. Indian J Endocr Metab. 2019; 23:263-266.
4. Radicioni AF, Ferlin A, Balercia G, Pasquali D, Vignozzi L, Maggi M, Foresta C, Lenzi A. Consensus statement on diagnosis and clinical management of Klinefelter syndrome. J Endocrinol Invest. 2010; 33:839-850.
5. Kleczkowska A, Fryns J, Van den Berghe H. X-chromosome polysomy in the male. Hum Genet. 1988; 80:16-22.
6. Maiburg M, Repping S, Giltay J. The genetic origin of Klinefelter syndrome and its effect on spermatogenesis. Fertil Steril. 2012; 98:253-260.
7. Hassold T, Hunt P. To err (meiotically) is human: the genesis of human aneuploidy. Nat Rev Genet. 2001; 2:280-291.
8. Hassold T, Hall H, Hunt P. The origin of human aneuploidy: where we have been, where we are going. Hum Mol Genet. 2007; 16:R203-208.
9. Blumenthal JD, Baker EH, Lee NR, Wade B, Clasen LS, Lenroot RK, Giedd JN. Brain morphological abnormalities in 49,XXXXY syndrome: a pediatric magnetic resonance imaging study. Neuroimage Clin. 2013; 2:197-203.
10. Moorhead PS, Nowell PC, Mellman WJ, Battips DM, Hungerford DA. Chromosome preparations of leukocytes cultured from human peripheral blood. Exp Cell Res.1960; 20:613-616.
11. Seabright M: A rapid banding technique for human chromosomes. Lancet.1971; 2:971-972.
12. McGowan-Jordan J, Simons A, Schmid M, (eds.). An international system for human cytogenomic nomenclature. Reprint of Cytogenetic and Genome Res, S Karger, Basel, New York, 2016, 149:1-2.
13. Linden MG, Bender BG, Robinson A. Sex chromosome tetrasomy and pentasomy. Pediatrics. 1995; 96:672-682.
14. The Genetic and Rare Diseases Information Center (GARD). Numeric-sex-chromosome-variations. *https://rarediseases.info.nih.gov/diseases/11919/numeric-sex-chromosome-variations* (accessed January 5, 2020).
15. Alberto F, Maria SR, Vanna P, Riccardo S, Nicola C, Carlo F. Copy number variations in the X chromosome of Klinefelter syndrome. Endocrine Abstracts 2015; 37 EP221.
16. Rinaldi A, Archidiacono N, Rocchi M, Filippi G. Additional pedigree supporting the frequent origin of XXYY from consecutive meiotic non-disjunction in paternal gametogenesis. J Med Genet. 1979; 16:225-226.
17. Lorda-Sanchez I, Binkert F, Hinkel K G, Moser H, Rosenkranz W, Maechler M, Schinzel A. Uniparental origin of sex chromosome polysomies. Hum Hered. 1992; 42:193-197.
18. Tartaglia N, Davis S, Hench A, Nimishakavi S, Beauregard R, Reynolds A, Fenton L, Albrecht L, Ross J, Visootsak J, Hansen R, Hagerman R. A new look at XXYY syndrome: Medical and psychological features. Am J Med Genet Part A. 2008; 146A:1509-1522.
19. Galasso C, Arpino C, Fabbri F, Curatolo P. Neurologic Aspects of 49,XXXXY Syndrome. J Child Neurol. 2003;

18:501-504.
20. Haeusler G, Frisch H, Guchev Z, Hadziselimovic F, Neuhold A, Vormittag W. Hypoplasia of the corpus callosum and growth hormone deficiency in the XXXXY syndrome. Am J Med Genet. 1992; 44:230-232.
21. Helena MA, Morris BJ. The human pseudoautosomal region (PAR): origin, function and future. Curr Genomics. 2007; 8:129-136.
22. Dhakar MB, Ilyas M, Jeong JW, Behen ME, Chugani HT. Frontal aslant tract abnormality on diffusion tensor imaging in an aphasic patient with 49, XXXXY syndrome. Pediatr Neurol. 2016; 55:64-67.
23. Green T, Flash S, Reiss AL. Sex differences in psychiatric disorders: what we can learn from sex chromosome aneuploidies. Neuropsychopharmacology. 2019; 44:9-21.
24. Shamsi MB, Kumar K, Dada R. Genetic and epigenetic factors: role in male infertility. Indian J Urol. 2011; 27:110-120.
25. Vawter MP, Harvey PD, and De Lisi LE. Dysregulation of X-linked gene expression in Klinefelter's syndrome and association with verbal cognition. Am J Med Genet. 2007; 144B:728-734.
26. Geschwind DH, Gregg J, Boone K, Karrim J, Pawlikowska- Haddal A, Rao E, Ellison J, Ciccodicola A, D'Urso M, Woods R, Rappold GA, Swerdloff R, Nelson SF. Klinefelter's syndrome as a model of anomalous cerebral laterality: Testing gene dosage in the X chromosome pseudoautosomal region using a DNA microarray. Dev Genet. 1998; 23:215-229.

Received March 4, 2020; Revised May 19, 2020; Accepted May 30, 2020

*Address correspondence to:
Babu Rao Vundinti, Department of Cytogenetics, National Institute of Immunohaematology (ICMR), 13th floor, new multistoried building, K.E.M Hospital campus, Parel, Mumbai-400012, India
E-mail: vbaburao@hotmail.com

Released online in J-STAGE as advance publication June 27, 2020.

Brief Report

DOI: 10.5582/irdr.2020.03033

A novel variant c.3706C>T p.(Avg 1236Cys) in the *ABCA7* gene in a Saudi patient with susceptibility to Alzheimer's disease 9

Hussein Algahtani[1,*], Bader Shirah[2], Alhusain Alshareef[3], Mohammad H. Al-Qahtani[4], Angham Abdulrahman Abdulkareem[4], Muhammad Imran Naseer[4,5]

[1] King Abdulaziz Medical City/King Saud bin Abdulaziz University for Health Sciences, Jeddah, Saudi Arabia;
[2] King Abdullah International Medical Research Center/King Saud bin Abdulaziz University for Health Sciences, Jeddah, Saudi Arabia;
[3] King Saud bin Abdulaziz University for Health Sciences, Jeddah, Saudi Arabia;
[4] Center of Excellence in Genomic Medicine Research, King Abdulaziz University, Jeddah, Saudi Arabia;
[5] Department of Medical Laboratory Technology, Faculty of Applied Medical Sciences, King Abdulaziz University, Jeddah, Saudi Arabia.

SUMMARY Alzheimer's disease (AD) is the most common cause of dementia with around 50 million people suffering from this disease worldwide. Mutations in the ATP-binding cassette sub-family A member 7 (*ABCA7*) have been reported to cause susceptibility to AD 9 (OMIM #608907). In this study, we report a novel variant in *ABCA7* in a Saudi patient with susceptibility to AD 9 and a strong family history of neurodegenerative disorders, which may be explained by the same variant. We studied a single 57-year-old female patient with typical symptoms of AD supported by MRI findings from a Saudi family with a positive history of a similar disease in multiple individuals. The case study was conducted in King Abdulaziz Medical City in Jeddah, Saudi Arabia. Whole-exome sequencing identified the novel heterozygous variant c.3706C>T p.(Avg 1236Cys) in the *ABCA7* gene, which leads to an amino acid exchange. Furthermore, bioinformatics *in silico* programs predict a pathogenic effect for this variant. To the best of our knowledge, the variant has not been described in the literature so far as evidenced by a thorough literature review using multiple databases such as Ovid, Medline, EMBASE, ProQuest, Science Direct, Google Scholar, and PubMed. In this article, we reported a middle-aged Saudi woman with a novel variant in *ABCA7* who had clinical features of both AD and Parkinson's disease. Given the reported function of this gene, it is most likely that it is etiological and pathological because of the presenting complex neurological disease due to decreased clearance of β-amyloid and α-Synuclein. We illustrate the importance of this interesting gene that could be implicated in several neurodegenerative disorders.

Keywords *ABCA7*, Alzheimer disease, dementia, mutation, Saudi Arabia

1. Introduction

Alzheimer's disease (AD) is a major public health issue because of the rising cost of caring for the increasing number of people suffering from this disorder (*1*). It is a neurodegenerative protein-conformational disease in which soluble neuronal proteins attain altered conformations leading to abnormal neuronal function and cell death. AD is the most common cause of dementia with around 50 million people suffering from this disease worldwide. It usually affects people above the age of 65 years (*2*). The early cardinal cognitive symptoms of AD are impairment of memory, executive function, and problem-solving ability. Behavioral and psychological manifestations such as apathy, social disengagement, and psychosis constitute the middle-late manifestations of the disease. Atypical presentation in which memory loss is not the initial manifestation could occur, especially in those with an early-onset disease in the fourth and fifth decade of life (*3*). Despite advances in medical therapy and intensive research efforts, currently available treatments have only marginal benefits with no cure or preventive intervention (*4*).

The sporadic form of AD is the most frequent type of AD with an age of onset usually after 60 years. The familial form represents less than 1% of all cases with early onset of the disease (the fourth and fifth decades of life) (*5*). A Mendelian autosomal dominant pattern of inheritance is seen in early-onset AD. The identified causative mutations in 60 to 70% of early-onset AD are in the following three genes: *APP*, *PSEN1*, and *PSEN2* located at ch 21q, ch14q, and ch 1q, respectively (*6*).

In contrast to early-onset AD, the genetic basis of late-onset AD is more complex with various and more common genetic factors but with a lesser degree of penetrance. However, the most penetrating genetic factor acknowledged is the presence of the Apolipoprotein E (APOE) epsilon 4 (ε4) allele on chromosome 19. The presence of two ε4 copies increases odds of AD by 8-12 fold, while one ε4 allele increases odds of AD by 2-3 fold compared with non-carriers (*7*). More than 20 other genes were identified by genome-wide association studies, yet the increased AD odds ratio is modest, ranging from 1-1.5 fold. These genes include *CLU*, *PICALM*, *BIN1*, *EPHA1*, and *ABCA7* (*8-10*). Mutations in the ATP-binding cassette sub-family A member 7 (*ABCA7*) have been reported to cause susceptibility to AD 9 (OMIM #608907). In this study, we report a novel variant in *ABCA7* for the first time in a Saudi patient with susceptibility to AD 9 and a strong family history of neurodegenerative disorders, which could be explained by the same variant.

2. Materials and Methods

2.1. Genetic analysis

We included a female patient with typical symptoms of AD supported by MRI findings from a Saudi family with a positive history of a similar disease in other family members. The diagnosis of AD was made according to the DSM-5 (Diagnostic and Statistical Manual of Mental Disorders, fifth edition) criteria. The case study was conducted in King Abdulaziz Medical City in Jeddah, Saudi Arabia. The genetic analysis was done by DNA fragmentation, and the exons of the known genes in the human genome, as well as the corresponding exon-intron boundaries, were enriched using Roche NimbleGen (SeqCap MedExome) capture technology, amplified and sequenced simultaneously by Illumina technology (next-generation sequencing, NGS) using an Illumina system. The target regions were sequenced with an average coverage of 106 fold. For about 99% of the regions of interest, a 15 fold coverage and for about 98%, a 20 fold coverage was obtained.

NGS data were aligned to the hg19 genome assembly. Variant calling and annotation was performed using an in-house developed bioinformatics pipeline. Identified single nucleotide variants and indels were filtered against external and internal databases focusing on rare variants with a minor allele-frequency (MAF) in genomAD of 1% or less and removing known artifacts and variants in regions with highly homologous regions. Classification of variants was conducted based on the American College of Medical Genetics guidelines considering database entries (including the Human Gene Mutation Database), bioinformatics prediction tools, and literature status. Variants annotated as common polymorphisms in databases or the literature or that were classified as (likely) benign were neglected.

Putatively pathogenic differences between the wildtype sequence (human reference genome according to the University of California Santa Cruz genome browser, hg19 GRCh37) and the patient's sequence mentioned and interpreted in this report were assessed using the in-house established quality score. Variants not passing the quality threshold were verified using polymerase chain reaction amplification followed by conventional Sanger sequencing. The sample identity was ensured by internal quality management procedures. This study was approved by the Institutional Review Board (IRB) of the King Abdullah International Medical Research Center (KAIMRC).

2.2. Case report

A 57-year-old lady presented to the neurology clinic with memory impairment, difficulty in walking, and abnormal muscle twitches of both upper and lower extremities. The onset of her complaints started four years ago after the death of her brother (her age at onset was 53 years). In addition, her family has noticed low mood, sleep deprivation, and episodic irritability. The course of the disease has been gradually progressive, and she struggles to remember her work-related tasks as she is a school administrator. She is a university graduate with a bachelor's degree in education. Her memory loss has worsened over a period of two years, which eventually has caused social impairment since she cannot remember the names of her relatives. In addition, she has complained of urinary incontinence for more than two years. In terms of her medical background, she is a known case of hypertension, diabetes, and hypothyroidism for more than ten years as well as atrial fibrillation for more than six years. She has been on aspirin, levothyroxine, simvastatin, omeprazole, gliclazide, insulin, propranolol, and mirtazapine. She is wheelchair-bound and dependent on others in most of her daily living activities. She is divorced and lives with her nephew. There is a strong family history of neurodegenerative diseases in both the central and peripheral nervous system affecting her mother, sisters, and brothers (Figure 1). Two brothers died at the age of 1 and 4 years, respectively, with no obvious medical illness. Two other brothers died at the ages of 38 and 45 years, respectively, with a neurological disorder manifesting as gait difficulty, ataxia, dysarthria, and nystagmus with normal cognitive functions. Two sisters died at the ages of 4 years and three days, respectively, with severe hypotonia and weakness. Her mother and one older sister who died at the age of 60 years had similar clinical features to our index case. On physical examination, she was afebrile and alert but disoriented to time, place, and person. She recalled 0/3 objects upon short memory testing with a mini-mental status examination score of 19/30. General knowledge questions showed a partial impairment of her long term

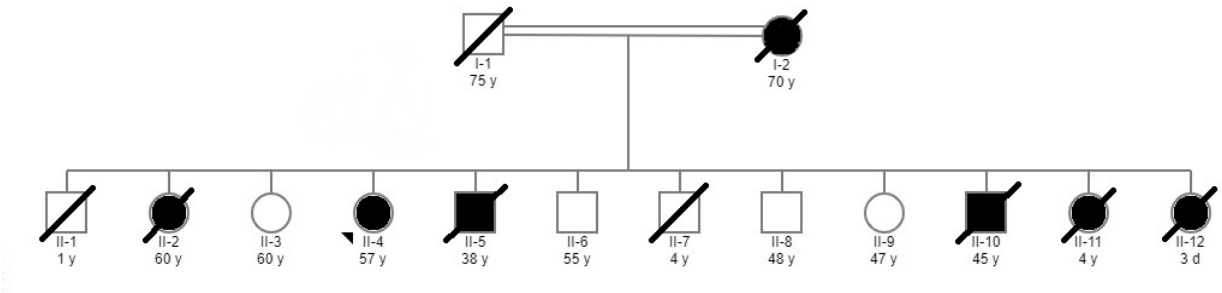

Figure 1. Family pedigree showing the details of the members of the family. Arrowhead indicates the proband included in this study.

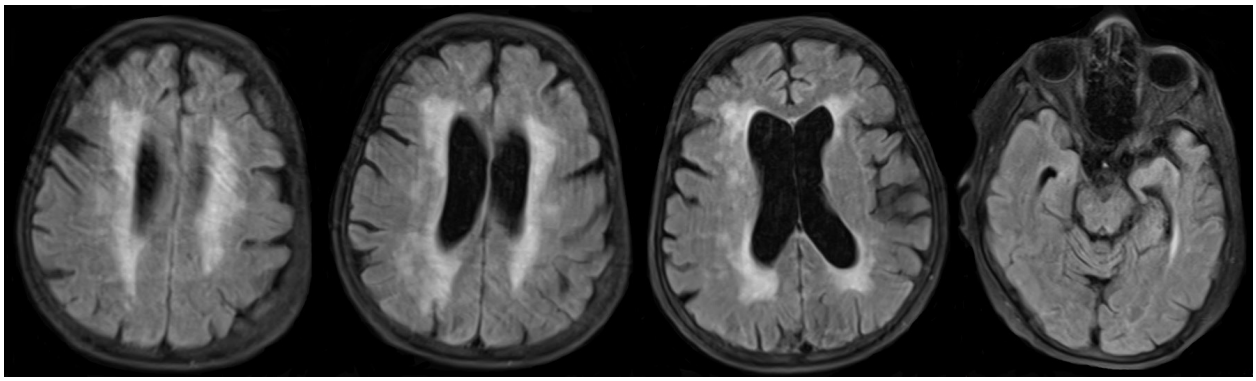

Figure 2. MRI of the brain showing severe diffuse atrophy for her age with confluent periventricular white matter and bilateral centrum semiovale abnormal signal intensity in keeping with moderate to severe microangiopathic leukoencephalopathic changes.

memory as well. However, her language was intact, and her speech tone, volume, and fluency were normal. Her cranial nerve examination from 2 to 12 was normal. She has pyramidal signs with increased tone in both upper and lower extremities and brisk symmetrical reflexes, but her plantar responses were downgoing. She also has extrapyramidal signs in the form of mild axial rigidity. She was not able to walk, and her legs were stiff and weak with a power of 2/5 in both proximal and distal muscles. MRI of the brain showed severe diffuse atrophy for her age with confluent periventricular white matter and bilateral centrum semiovale abnormal signal intensity in keeping with moderate to severe microangiopathic leukoencephalopathic changes (Figure 2). To exclude other differential diagnoses that may explain our patient's clinical and radiological findings, spinal cord MRI and electroencephalogram studies were done, which were unremarkable. The final diagnosis was familial AD, and her management was modified to include warfarin, memantine, rivastigmine, and aggressive physiotherapy.

3. Results and Discussion

Whole exome sequencing identified the heterozygous variant c.3706C>T p.(Avg 1236Cys) in the *ABCA7* gene, which leads to an amino acid exchange. Bioinformatics *in silico* studies predicted a pathogenic effect for this variant. To the best of our knowledge, the variant has not been described in the literature as far as is evident from a thorough literature review using multiple databases including Ovid, Medline, EMBASE, ProQuest, Science Direct, Google Scholar, and PubMed. The variant is found in 0.003% of the overall population (4 heterozygous (ages range from 40 – 45 to > 80), 0 homozygous; genomAD). No variants in other genes related to AD or genes related to leukoencephalopathy were identified. Considering the heterozygous variant in *ABCA7* and the supportive phenotype of the patient, a genetic diagnosis of susceptibility to AD 9 (OMIM #608907) was made. Genetic testing for the living family members was suggested, but the idea was rejected by the family.

The prevalence of AD in Arab countries is not accurately evaluated in comprehensive epidemiological studies (*11*). In Saudi Arabia, there are approximately 130,000 persons suffering from AD representing 0.4% of the Saudi population. Due to the shifting of the age of the population towards the elderly, this number is expected to increase in the coming two decades (*12*). In a recent study done by El Bitar *et al*. (*13*), a comprehensive screening for point mutations in 117 AD cases from Saudi Arabia was carried out by direct sequencing of coding regions in four AD-related genes (*PSEN1*, *PSEN2*, *APP*, and *SORL1*). They identified a total of eight potential pathogenic missense variants in all studied genes. The *ABCA7* gene was not tested in that cohort of patients. This indicates the importance of genetic testing of cases of AD, especially those with early-onset or strong family history of dementia. In addition, performing whole-exome sequencing yields more than targeted gene sequencing.

Familial AD (affecting three or more members in

a family) represents 25% of all cases of AD (*14*). Both familial and non-familial AD have the same clinical and pathologic phenotype, and the distinction can be made only by family history and/or molecular genetic testing. Familial AD can be either early-onset (before age 65 years) or late-onset (age 65 years and above) (*14*). Susceptibility genes in late-onset familial AD (more than 20 genes) have a role in brain development, immune functions, and cytoskeletal organization. In early-onset familial AD, more than four genes have been identified. Although the heritability of AD is about 70%, only 30% of those cases can be explained from the known genes. This can be explained by the phenomenon of complex genetic disease/traits (*15*).

ATP-binding cassette sub-family A member 7, abbreviated as (*ABCA7*) gene, is located on chromosome 19p13.3. This gene encodes a protein member of the superfamily ATP-binding cassette (ABC) transporters (*16*). *ABCA7* expression is widely distributed in the human body since it is found in the brain, lung, adrenal gland, kidney, spleen, thymus, lymph node, testis, keratinocytes, and pancreatic islets. In the brain, the mRNA of *ABCA7* was most abundant in microglial cells. The exact function of these (ABC) transporters are not fully understood, yet it is proposed that they interfere with lipid metabolism as well as phagocytosing apoptotic cells (*17*). In mouse models, *ABCA7* knock-out results in an interruption of the uptake and the proteolytic functions of microglial cells to degrade amyloid-beta peptides (Aβ). Therefore, brain aggregations of Aβ plaques were enhanced in those mice. Additionally, it is established that even the production of (Aβ) is increased and accelerated in primary neurons of mice in the absence of ABCA7 by further activation of the amyloid precursor protein (APP) cleaving enzymes (*18*). These findings provide us with a better insight into the *ABCA7* role in the pathogenesis of AD. However, human model-based research studies are needed for better understanding.

To date, the most common *ABCA7* mutation variants, with minor allele frequency (MAF) of more than 5%, are rs3764650, rs3764647, rs115550680, rs142076058, rs4147929, and rs3752246. These variants' genetic penetrating capability and the predisposition of developing AD are largely dependent on the ethnicity of the studied population. *ABCA7* variants rs3764650, rs3752246, and rs4147929 are significantly linked and reproduced among Caucasians (*19-21*). The African American population shows a large susceptibility for the following *ABCA7* variants: rs3764647, rs115550680, and rs142076058 (*22-24*). In addition, a rare (MAF < 1%) *ABCA7* missense variant, rs3752239, was detected within African Americans as well (*25*). A low frequency (MAF 1-5%) *ABCA7* variant, rs78117248, with high penetrating capability was reported by a Belgian cohort study (*26*). It is hypothesized that the characteristics of *ABCA7* are different, and only loss of function variants can be causal variants. Missense mutations of this gene are considered risk variants and not causal variants. More time and further research are needed to clarify such a theory.

In our patient, the presence of an *ABCA7* variant in this patient with early-onset AD with the presence of clinical features of both AD and Parkinson's disease suggests that this gene might be a risk factor for neurodegeneration. This gene is hypothesized to be involved in transport of phospholipid and cholesterol across membranes to APOE. In addition, it has been implicated in the activation of phagocytosis to clear amyloid plaques and apoptotic cells. It is functional throughout the brain and has been reported to be involved in several disorders including Parkinson's disease, cystic fibrosis, and tangier disease (*27*).

The definitive diagnosis of AD requires a histopathological confirmation through biopsy. However, this is rarely done in clinical practice due to its inconvenience (*28*). Therefore, the diagnosis is made upon the insidious progression of cognitive symptoms and the implementation of the National Institute on Aging and the Alzheimer's Association (NIA-AA) diagnosing criteria (*29*). Radiological evaluation is of great value in all suspected AD cases. MRI is the modality of choice in which a characteristic focal reduced hippocampal volume or medial temporal lobe atrophy is demonstrated. In addition, functional brain imaging with 18-F fluorodeoxyglucose positron emission tomography (FDG-PET) or single-photon emission computed tomography (SPECT) could be utilized as well (*30*). In our patient, we think that the MRI findings of severe white matter hyperintensity with subcortical white matter changes are not related to her genetic abnormality. This was confirmed by a thorough literature review that yielded no articles discussing the relationship between *ABCA7* variants and such radiological abnormality.

The limitation of this study involves the lack of confirmation of the presence of amyloid in the brain, which can be detected through amyloid PET imaging or cerebrospinal fluid analysis. In addition, the pathogenicity was not supported by a segregation study since the other family members either have died or refused genetic study. Furthermore, functional studies of the variant in animal models were not performed due to the unavailability of such technology in our center.

In this article, we reported a middle-aged Saudi woman with a novel variant in *ABCA7* who had clinical features of both AD and Parkinson's disease. Given the reported function of this gene, it is most likely that it is etiological and pathological of the presenting complex neurological disease due to decreased clearance of Aβ and α-Synuclein. We illustrate the importance of this interesting gene that could be implicated in several neurodegenerative disorders. Further studies using whole-exome sequencing should be utilized to screen familial cases of AD in the Saudi population.

References

1. Scheltens P, Blennow K, Breteler MM, de Strooper B, Frisoni GB, Salloway S, Van der Flier WM. Alzheimer's disease. Lancet. 2016; 388:505-517.
2. Prince M, Ali GC, Guerchet M, Prina AM, Albanese E, Wu YT. Recent global trends in the prevalence and incidence of dementia, and survival with dementia. Alzheimers Res Ther. 2016; 8:23.
3. Ballard C, Gauthier S, Corbett A, Brayne C, Aarsland D, Jones E. Alzheimer's disease. Lancet. 2011; 377:1019-1031.
4. Cummings J, Lee G, Ritter A, Zhong K. Alzheimer's disease drug development pipeline: 2018. Alzheimers Dement (N Y). 2018; 4:195-214.
5. Cacace R, Sleegers K, Van broeckhoven C. Molecular genetics of early-onset Alzheimer's disease revisited. Alzheimers Dement. 2016; 12:733-748.
6. Reitz C. Genetic diagnosis and prognosis of Alzheimer's disease: challenges and opportunities. Expert Rev Mol Diagn. 2015; 15:339-348.
7. Balasa M, Gelpi E, Antonell A, Rey MJ, Sánchez-Valle R, Molinuevo JL, Lladó A. Clinical features and APOE genotype of pathologically proven early-onset Alzheimer disease. Neurology. 2011; 76:1720-1725.
8. Chouraki V, Seshadri S. Genetics of Alzheimer's disease. Adv Genet. 2014; 87:245-294.
9. Seshadri S, Fitzpatrick AL, Ikram MA, *et al*. Genome-wide analysis of genetic loci associated with Alzheimer disease. JAMA. 2010; 303:1832-1840.
10. Le guennec K, Nicolas G, Quenez O, *et al*. ABCA7 rare variants and Alzheimer disease risk. Neurology. 2016; 86:2134-2137.
11. El-metwally A, Toivola P, Al-rashidi M, Nooruddin S, Jawed M, AlKanhal R, Abdul Razzak H, Albawardi N. Epidemiology of Alzheimer's disease and dementia in Arab Countries: a systematic review. Behav Neurol. 2019; 2019:3935943.
12. Algahtani H, Shirah B, Alhazmi A, Alshareef A, Bajunaid M, Samman A. Perception and attitude of the general population towards Alzheimer's disease in Jeddah, Saudi Arabia. Acta Neurol Belg. 2020; 120:313-320.
13. El bitar F, Qadi N, Al rajeh S, Majrashi A, Abdulaziz S, Majrashi N, Al Inizi M, Taher A, Al Tassan N. Genetic study of Alzheimer's disease in Saudi population. J Alzheimers Dis. 2019; 67:231-242.
14. Dorszewska J, Prendecki M, Oczkowska A, Dezor M, Kozubski W. Molecular basis of familial and sporadic Alzheimer's disease. Curr Alzheimer Res. 2016; 13:952-963.
15. Kim JH. Genetics of Alzheimer's Disease. Dement Neurocogn Disord. 2018;17:131-136.
16. Allen M, Lincoln SJ, Corda M, Watzlawik JO, Carrasquillo MM, Reddy JS, Burgess JD, Nguyen T, Malphrus K, Petersen RC, Graff-Radford NR, Dickson DW, Ertekin-Taner N. ABCA7 loss-of-function variants, expression, and neurologic disease risk. Neurol Genet. 2017; 3:e126.
17. Aikawa T, Holm ML, Kanekiyo T. ABCA7 and Pathogenic Pathways of Alzheimer's Disease. Brain Sci. 2018; 8:27.
18. Kim WS, Li H, Ruberu K, Chan S, Elliott DA, Low JK, Cheng D, Karl T, Garner B. Deletion of Abca7 increases cerebral amyloid-β accumulation in the J20 mouse model of Alzheimer's disease. J Neurosci. 2013; 33:4387-4394.
19. Hollingworth P, Harold D, Sims R, *et al*. Common variants at ABCA7, MS4A6A/MS4A4E, EPHA1, CD33 and CD2AP are associated with Alzheimer's disease. Nat Genet. 2011; 43:429-435.
20. Naj AC, Jun G, Beecham GW, *et al*. Common variants at MS4A4/MS4A6E, CD2AP, CD33 and EPHA1 are associated with late-onset Alzheimer's disease. Nat Genet. 2011; 43:436-441.
21. Lambert JC, Ibrahim-verbaas CA, Harold D, *et al*. Meta-analysis of 74,046 individuals identifies 11 new susceptibility loci for Alzheimer's disease. Nat Genet. 2013; 45:1452-1458.
22. Logue MW, Schu M, Vardarajan BN, *et al*. A comprehensive genetic association study of Alzheimer disease in African Americans. Arch Neurol. 2011; 68:1569-1579.
23. Reitz C, Jun G, Naj A, *et al*. Variants in the ATP-binding cassette transporter (ABCA7), apolipoprotein E ϵ4,and the risk of late-onset Alzheimer disease in African Americans. JAMA. 2013; 309:1483-1492.
24. Cukier HN, Kunkle BW, Vardarajan BN, *et al*. ABCA7 frameshift deletion associated with Alzheimer disease in African Americans. Neurol Genet. 2016; 2:e79.
25. N'Songo A, Carrasquillo MM, Wang X, Burgess JD, Nguyen T, Asmann YW, Serie DJ, Younkin SG, Allen M, Pedraza O, Duara R, Custo MTG, Graff-Radford NR, Ertekin-Taner N. African American exome sequencing identifies potential risk variants at Alzheimer disease loci. Neurol Genet. 2017; 3:e141.
26. Cuyvers E, De roeck A, Van den bossche T, Van Cauwenberghe C, Bettens K, Vermeulen S, Mattheijssens M, Peeters K, Engelborghs S, Vandenbulcke M, Vandenberghe R, De Deyn PP, Van Broeckhoven C, Sleegers K. Mutations in ABCA7 in a Belgian cohort of Alzheimer's disease patients: a targeted resequencing study. Lancet Neurol. 2015; 14:814-822.
27. Nuytemans K, Maldonado L, Ali A, John-Williams K, Beecham GW, Martin E, Scott WK, Vance JM. Overlap between Parkinson disease and Alzheimer disease in ABCA7 functional variants. Neurol Genet. 2016; 2:e44.
28. Atri A. The Alzheimer's disease clinical spectrum: diagnosis and management. Med Clin North Am. 2019; 103:263-293.
29. Mckhann GM, Knopman DS, Chertkow H, *et al*. The diagnosis of dementia due to Alzheimer's disease: recommendations from the National Institute on Aging-Alzheimer's Association workgroups on diagnostic guidelines for Alzheimer's disease. Alzheimers Dement. 2011; 7:263-269.
30. Risacher SL, Saykin AJ. Neuroimaging in aging and neurologic diseases. Handb Clin Neurol. 2019; 167:191-227.

Received May 11, 2020; Revised July 5, 2020; Accepted July 9, 2020.

**Address correspondence to:*
Hussein Algahtani, King Abdulaziz Medical City/King Saud bin Abdulaziz University for Health Sciences, P.O. Box: 12723, Jeddah 21483, Saudi Arabia.
E-mail: halgahtani@hotmail.com

Released online in J-STAGE as advance publication July 17, 2020.

Case Report

DOI: 10.5582/irdr.2020.01027

Benign adrenal and suprarenal retroperitoneal schwannomas can mimic aggressive adrenal malignancies: case report and review of the literature

Mitchell P. Wilson[1], Prayash Katlariwala[1], Jingyang Huang[2], Gavin Low[1], Edward Wiebe[1]

[1] Department of Radiology and Diagnostic Imaging, University of Alberta, Edmonton, Canada;
[2] Department of Laboratory Medicine and Pathology, University of Alberta, Edmonton, Canada.

SUMMARY The suprarenal retroperitoneum and adrenal gland is a rare site of origin for benign schwannomas which frequently present as larger and more aggressive lesions than schwannomas identified elsewhere. These tumors are often surgically excised. We present a case of an 81-year-old asymptomatic man presenting with an incidental 10 cm left suprarenal retroperitoneal mass identified on CT. The mass was indiscernible from the adrenal gland, demonstrating heterogeneous enhancement with a centrally cystic/necrotic core, and punctate calcifications. Subsequent core needle biopsy demonstrated a benign adrenal schwannoma. The lesion has been managed conservatively with imaging follow up and without complication. DISCUSSION: Our review of the literature identifies 121 reported in vivo benign adrenal and suprarenal schwannomas published to date with imaging features available for 90 cases (74%). All cases were encapsulated with the average size measuring over 6.5 cm. Fifteen percent (13/84) of reported lesions measured over 10 cm at presentation. Punctate calcification was present in 50% (26/52) of reporting cases. Nearly 50% (40/86) of cases demonstrate cystic/necrotic appearances on imaging. Despite aggressive appearances, our case demonstrates that biopsy and surveillance may represent a reasonable alternative to surgery in suboptimal surgical candidates.

Keywords adrenal, schwannoma, retroperitoneal, suprarenal, malignancy, nerve

1. Introduction

Non-malignant masses account for around 20% of primary retroperioneal (RP) tumors with benign schwannomas representing a subset of only 5% of primary RP tumors (*1*). Adrenal and suprarenal RP schwannomas represent an even rarer origin subset. Schwannomas presenting in this location tend to be larger and more heterogeneous at time of presentation than schwannomas presenting elsewhere in the body (*2-5*). Surgical resection is often the treatment of choice for these tumors (*2*).

2. Case Report

An 81-year-old otherwise asymptomatic man presented *via* ambulance to our tertiary care hospital after falling from a ladder. He remained hemodynamically stable throughout his presentation. On account of his mechanism and multifocal pain, he underwent a trauma scan of his chest, abdomen, and pelvis. An incidental 8 × 5 × 10 cm (anteroposterior × transverse × craniocaudal) left suprarenal lesion indiscernible from the left adrenal gland was identified (Figure 1). The lesion demonstrated peripheral arterial and portal venous enhancement with a centrally cystic/necrotic core. There were punctate calcifications scattered throughout. The right adrenal gland was normal. No regional lymph node enlargement was present. No other primary or metastatic lesions were seen elsewhere throughout the body.

A 24-hour urine metanephrine study was negative for PCC. Bloodwork was otherwise non-contributory. A subsequent ultrasound-guided core needle biopsy was performed. Histopathology demonstrated a tumor composed of spindle cells with minimal atypia and/or mitotic activity (Figure 2). The spindle cells were dense, wavy, and with tapered ends. Hyalinized blood vessels were readily present. Subsequent immunohistochemical analysis demonstrated a diffusely positive S100 stain while markers for other RP tumors including MART1, HMB45, DOG1, CD117, MDM2, actin, desmin,

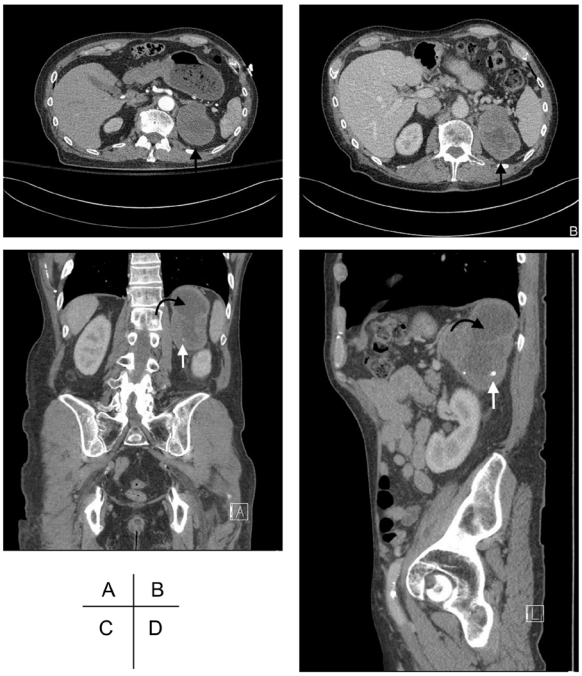

Figure 1. The 81-year-old male with left suprarenal schwannoma. Findings: CT images demonstrate a large heterogeneously enhancing aggressive appearing left suprarenal mass (arrow) with central necrosis (curved arrow) and punctate calcifications (white arrow). Technique: Arterial axial **(A)** CT imaging of the abdomen and portal venous axial **(B)**, coronal **(C)**, and sagittal **(D)** CT imaging of the abdomen and pelvis, variable (40-55) mAs, 120 kV, 2 mm slice thickness, 83 ml Omnipaque 350 IV contrast.

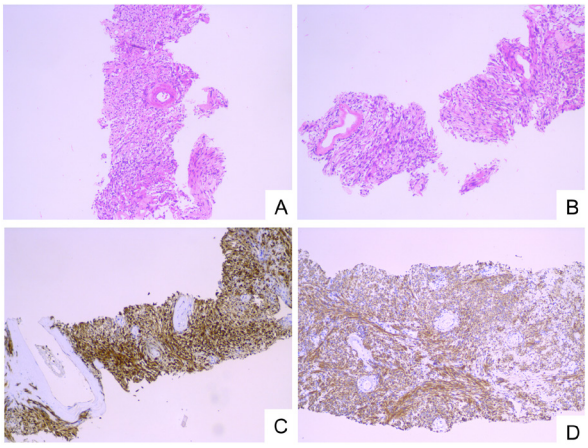

Figure 2. The 81-year-old male with left suprarenal schwannoma. Findings: Core needle biopsy demonstrating a tumor composed of dense wavy spindle cells with minimal atypia or mitotic activity **(A, B)**. Immunohistochemical analysis demonstrates diffusely positive S100 **(C)** and GFAP **(D)** stains. Pathology was consistent with a benign schwannoma of cellular subtype.

caldesmon, AE1/AE3, CD34 and STAT6 were all negative. Pathological features were consistent with a benign adrenal schwannoma. A glial fibrillary acidic protein (GFAP) stain was performed for the purposes of this report and was positive.

Following consultation with urology, the lesion was managed conservatively with observation. The patient has remained free of symptoms relating to the tumor. As of a six-month follow-up CT scan, no change in size or appearance of the lesion has been documented and the patient remained otherwise clinically asymptomatic.

3. Discussion

3.1. Literature review

An English language search of MEDLINE and Google Scholar from inception to July 24, 2019 with search terms including "schwannoma" AND ("retroperitoneal" OR "adrenal") was performed to evaluate for in vivo cases of adrenal or suprarenal RP schwhannomas. A total of 121 reported cases were identified with 90 cases documenting imaging characteristics (Table 1) (*2-44*). The rarity of these reports is demonstrated by Li *et al.* who identified only 19 adrenal schwannomas in a series of almost 4,000 adrenal lesions (26). Patients in our literature review ranged in age between 14-81, with our report representing the oldest known patient described to date. As seen in our study, male gender accounts for less than half of the identified reports.

3.2. Clinical and imaging findings

Clinical and imaging features are summarized in Table 2. Similar to more than half of reported cases, the RP schwannoma in our patient was identified incidentally when investigating for another purpose. Most patients who did present with symptoms complained of non-specific symptoms including flank and abdominal pain and rarely abdominal distention. It is possible that several of these patients' tumors were also identified incidentally with the symptoms attributable to an alternative otherwise undetected cause. This would correspond with a study by Zhou *et al*. assessing pathologic features of 31 patients with adrenal schwannomas identifying 84% of patients as presenting incidentally (Table 3) (*44*). The high frequency of incidental and often delayed presentation likely accounts for why the average size of suprarenal RP schwannomas is larger than the average size of schwannomas identified elsewhere. In our review, the average size of identified tumors was over 6.5 cm with 15% (13/84) of reporting cases demonstrating tumors at least 10 cm in size.

All reported cases including ours demonstrated well encapsulated margins typical of a benign schwannoma. Punctate calcifications described in our case were present in 50% (26/52) of reporting imaging cases. The number of cases with calcifications may even be under-reported as several studies evaluated lesions with only ultrasound and/or MRI features but lacking spatial resolution necessary to identify small calcifications. This would correspond with Li *et al.*'s study where 84% (16/19) of their patients had some calcification

Table 1. Clinical and imaging characteristics of suprarenal retroperitoneal schwannomas

Author, Year (*Ref.*)	Age/ Gender	Presentation	Size (cm)	Margin	Heterogeneity	Solid/ Cystic	Calcification	Suspected Diagnosis	Diagnosis
Abdessater 2018 (*2*)	50/F	Asymptomatic	10	En	Heg	Cystic	Present	ACC	Surgery
Adas 2013 (*3*)	32/F	Flank Pain	10	En	Heg	Cystic	NR	ACC	Surgery
Babaya 2017 (*4*)	69/M	Abdominal Pain	4	En	Hog	Solid	None	NAA	Surgery
Bakhshi 2011 (*5*)	34/F	Asymptomatic	9	En	Heg	Cystic	NR	NAA	Surgery
Bedard 1986 (*6*)	63/F	Abdominal Pain	6	En	Hog	Solid	NR	NC	Surgery
Damodaran 2015, Case 1 (*7*)	36/F	Flank Pain	9	En	Heg	Cystic	NR	ACC	Surgery
Damodaran 2015, Case 2 (*7*)	50/F	Flank Pain	NR	En	Hog	NR	NR	NAA	Surgery
Fernandez 2016 (*8*)	56/F	Asymptomatic	10	En	Heg	Cystic	NR	ACC	Surgery
Fu 2015 (*9*)	71/M	Asymptomatic	15	En	Heg	Cystic	NR	NC	Surgery
Garg 2007 (*10*)	50/F	Abdominal Pain	9	En	Hog	Solid	NR	ACC	Surgery
Gazula 2007 (*11*)	42/M	Flank Pain	12	En	Heg	Cystic	NR	ACC	Surgery
Goh 2006, Case 1 (*12*)	46/M	Asymptomatic	NR	En	Heg	Cystic	NR	ACC	Surgery
Goh 2006, Case 2 (*12*)	28/F	Asymptomatic	NR	En	Heg	Cystic	Present	ACC	Surgery
Goh 2006, Case 3 (*12*)	49/M	Asymptomatic	NR	En	Heg	Cystic	None	ACC	Surgery
Goh 2006, Case 4 (*12*)	58/M	Flank Pain	NR	En	Heg	Cystic	None	ACC	Surgery
Grasso 2015 (*13*)	45/M	Asymptomatic	12	En	Heg	Cystic	None	ACC	Surgery
Hsiao 2008 (*14*)	49/M	Asymptomatic	5	En	Hog	Solid	None	NAA	Surgery
Igawa 1998 (*15*)	45/M	Abdominal Pain	6.5	En	Hog	Solid	NR	ACC	Surgery
Ikemoto 2002 (*16*)	62/F	Abdominal Pain	12	En	Hog	Solid	None	NC	Surgery
Inokuchi 2006 (*17*)	35/F	Asymptomatic	7	En	Heg	Cystic	Present	ACC	Surgery
Jakowski 2008 (*18*)	51/F	Asymptomatic	5.5	NR	NR	NR	NR	NC	Surgery
Jeshtadi 2014 (*19*)	55/F	Flank Pain	6.5	En	Hog	Solid	NR	NC	Surgery
Khurram 2015 (*20*)	64/M	Asymptomatic	2	En	Hog	Solid	None	NAA	Surgery
Kleiman 2011 (*21*)	31/F	Asymptomatic	4.5	En	Heg	Solid	NR	NAA	Surgery
Konstantinos 2012 (*22*)	71/F	Flank Pain	8	En	Heg	Cystic	Present	ACC	Surgery
Korets 2007 (*23*)	70/M	Hematuria	3	En	Heg	Cystic	None	NC	Surgery
Kostakopoulos 1991 (*24*)	38/F	Abdominal Pain	18	En	Heg	Cystic	None	ACC	Surgery
Lau 2006, Case 1 (*25*)	73/M	Abdominal Pain	9	NR	NR	NR	NR	NC	Surgery
Lau 2006, Case 2 (*25*)	26/F	Abdominal Pain	10	NR	NR	NR	NR	NC	Surgery
Li 2015, Case 1 (*26*)	38/F	NR	7	En	Hog	Solid	Present	NAA	Surgery
Li 2015, Case 2 (*26*)	31/F	NR	4	En	Hog	Solid	Present	ACC	Surgery
Li 2015, Case 3 (*26*)	50/F	NR	4	En	Hog	Solid	Present	ACC	Surgery
Li 2015, Case 4 (*26*)	55/F	NR	6	En	Hog	Solid	Present	PCC	Surgery
Li 2015, Case 5 (*26*)	50/F	NR	9	En	Heg	Cystic	None	Schwannoma	Surgery
Li 2015, Case 6 (*26*)	23/M	NR	6	En	Hog	Solid	Present	PCC	Surgery
Li 2015, Case 7 (*26*)	54/F	NR	7	En	Hog	Solid	None	PCC	Surgery
Li 2015, Case 8 (*26*)	66/F	NR	6.5	En	Hog	Solid	Present	PCC	Surgery
Li 2015, Case 9 (*26*)	56/F	NR	5.5	En	Hog	Solid	Present	NAA	Surgery
Li 2015, Case 10 (*26*)	61/M	NR	6	En	Hog	Solid	Present	Schwannoma	Surgery
Li 2015, Case 11 (*26*)	65/F	NR	8	En	Hog	Solid	None	Teratoma	Surgery
Li 2015, Case 12 (*26*)	34/M	NR	5	En	Heg	Cystic	Present	ACC	Surgery
Li 2015, Case 13 (*26*)	64/F	NR	6	En	Hog	Solid	Present	NAA	Surgery
Li 2015, Case 14 (*26*)	44/F	NR	6	En	Hog	Solid	Present	Schwannoma	Surgery
Li 2015, Case 15 (*26*)	46/F	NR	6.5	En	Hog	Solid	Present	PCC	Surgery
Li 2015, Case 16 (*26*)	50/F	NR	7	En	Heg	Cystic	Present	ACC	Surgery
Li 2015, Case 17 (*26*)	40/F	NR	5	En	Hog	Solid	Present	NAA	Surgery
Li 2015, Case 18 (*26*)	32/F	NR	6	En	Hog	Solid	Present	Schwannoma	Surgery
Li 2015, Case 19 (*26*)	58/F	NR	7	En	Hog	Solid	Present	ACC	Surgery
Liu 2012, Case 1 (*27*)	14/M	Abdominal Pain	7	En	Hog	Solid	None	NAA	Surgery
Liu 2012, Case 2 (*27*)	51/M	Abdominal Distension	4	En	Heg	Cystic	NR	ACC	Surgery
Liu 2012, Case 3 (*27*)	57/M	Flank Pain	7	En	Hog	Solid	NR	NAA	Surgery
Oberoi 2019 (*28*)	50/F	Asymptomatic	12	En	Heg	Solid	NR	ACC	Surgery
Onoda 2008 (*29*)	62/M	Asymptomatic	4	En	Hog	Solid	NR	NAA	Surgery
Pittasch 2000 (*30*)	56/F	Abdominal Pain	12	En	Hog	Solid	NR	ACC	Surgery
Richter 2011 (*31*)	30/F	Abdominal Pain	14	En	Heg	Solid	NR	NAA	Surgery
Said 2017 (*32*)	64/M	Asymptomatic	9	En	Heg	Cystic	Present	ACC	Surgery
Shabana 2019 (*33*)	32/M	Flank Pain	5	En	Heg	Solid	NR	NAA	Surgery
Suzuki 2007 (*34*)	33/M	Asymptomatic	8	En	Hog	Solid	None	NC	Surgery
Tang 2018, Case 1 (*35*)	47/F	Asymptomatic	5.5	En	Heg	Cystic	None	NC	Surgery
Tang 2018, Case 2 (*35*)	65/F	Asymptomatic	5	En	Heg	Cystic	None	NC	Surgery
Tang 2018, Case 3 (*35*)	64/F	Asymptomatic	4	En	Heg	Cystic	None	NC	Surgery
Tang 2018, Case 4 (*35*)	50/F	Abdominal Pain	8	En	Heg	Cystic	None	NC	Surgery
Tang 2018, Case 5 (*35*)	31/F	Asymptomatic	3.5	En	Hog	Solid	None	NC	Surgery

NR: Not Reported; En: Encapsulated; Heg: Heterogenous; Hog: Homogenous; NC: not clear; ACC: adrenal cortical carcinoma; NAA: nonfunctional adrenal adenoma; PCC: Pheochromocytoma.

Table 1. Clinical and imaging characteristics of suprarenal retroperitoneal schwannomas (continued)

Author, Year (*Ref.*)	Age/ Gender	Presentation	Size (cm)	Margin	Heterogeneity	Solid/ Cystic	Calcification	Suspected Diagnosis	Diagnosis
Tang 2018, Case 6 (*35*)	30/M	Asymptomatic	6.5	En	Heg	Cystic	None	NC	Surgery
Tang 2018, Case 7 (*35*)	49/F	Asymptomatic	3.5	En	Heg	Cystic	None	NC	Surgery
Tang 2018, Case 8 (*35*)	34/F	Asymptomatic	3	En	Hog	Solid	None	NC	Surgery
Tang 2018, Case 9 (*35*)	35/M	Asymptomatic	4	En	Heg	Cystic	Present	NC	Surgery
Tang 2018, Case 10 (*35*)	58/F	Abdominal Pain	8	En	Heg	Cystic	None	NC	Surgery
Tang 2018, Case 11 (*35*)	56/F	Abdominal Pain	9	En	Heg	Cystic	None	NC	Surgery
Tang 2018, Case 12 (*35*)	28/M	Asymptomatic	2.5	En	Heg	Cystic	None	NC	Surgery
Tang 2018, Case 13 (*35*)	39/M	NR	5.5	En	Heg	Cystic	NR	NC	Surgery
Tang 2018, Case 14 (*35*)	35/F	NR	4.5	En	Heg	Cystic	NR	NC	Surgery
Tang 2018, Case 15 (*35*)	48/F	NR	3.5	En	Heg	Cystic	NR	NC	Surgery
Tang 2018, Case 16 (*35*)	46/F	NR	5.5	En	Heg	Cystic	NR	NC	Surgery
Tang 2018, Case 17 (*35*)	31/F	NR	3	En	Hog	Solid	NR	NC	Surgery
Tarcoveanu 2009 (*36*)	55/NR	Asymptomatic	4	En	Hog	Solid	NR	Metastasis	Surgery
Tezel 2005 (*37*)	46/F	Asymptomatic	8	En	NR	Solid	NR	ACC	Surgery
Thomas 2018 (*38*)	56/F	Abdominal Pain	5	En	Heg	Cystic	None	ACC	Surgery
Tommaselli 1996 (*39*)	44/M	Asymptomatic	4	En	Heg	Cystic	Present	ACC	Surgery
Wilson (Present Case)	81/M	Asymptomatic	10	En	Heg	Cystic	Present	ACC	Biospy
Xiao 2011, Case 1 (*40*)	38/F	Asymptomatic	3.5	En	Hog	Solid	NR	NAA	Surgery
Xiao 2011, Case 2 (*40*)	46/F	Asymptomatic	4.5	En	Hog	Solid	NR	NAA	Surgery
Xiao 2011, Case 3 (*40*)	39/M	Flank Pain	3.5	En	Hog	Solid	NR	NAA	Surgery
Xiao 2011, Case 4 (*40*)	43/F	Abdominal Pain	5	En	Hog	Solid	NR	NAA	Surgery
Xiao 2011, Case 5 (*40*)	47/M	Asymptomatic	6	En	Heg	Cystic	Present	PCC	Surgery
Xiao 2011, Case 6 (*40*)	30/F	Asymptomatic	3	En	Hog	Solid	NR	NAA	Surgery
Yang 2009 (*41*)	30/F	Flank Pain	NR	En	Heg	Cystic	NR	NC	Surgery
Yonou 1999 (*42*)	67/F	Abdominal Pain	6	En	Heg	Cystic	Present	ACC	Surgery
Yun 2016, Case 1 (*43*)	39/F	NR	1.4	En	Hog	Solid	NR	NC	Surgery
Yun 2016, Case 2 (*43*)	45/F	NR	4	En	Hog	Solid	NR	NC	Surgery

NR: Not Reported; En: Encapsulated; Heg: Heterogenous; Hog: Homogenous; NC: not clear; ACC: adrenal cortical carcinoma; NAA: nonfunctional adrenal adenoma; PCC: Pheochromocytoma.

Table 2. Summary table of retroperitoneal adrenal and suprarenal schwannomas based on a review of 121 reported cases

Etiology	• Tumors of Schwann cell origin.
Incidence	• All RP schwannomas represent 5% of RP tumors. • Suprarenal RP schwannomas are a rare subtype of RP schwannomas.
Gender Ratio	• ~1.8F:1M.
Age	• Range between 14-81.
Risk Factors	• Most are sporadic. There is an association with NF2.
Treatment	• Typically surgical resection. • Surveillance following pathology confirmation in suboptimal surgical candidates may represent a viable alternative.
Prognosis	• Slow growing benign lesions.
Imaging Features	• Often present larger and more aggressive appearing than schwannomas elsewhere. • Encapsulated. • Typically large (average size 6.5 cm; 15% >10 cm at presentation). • 45-50% demonstrate centrally cystic/necrotic cores. • ~ 50% demonstrate punctate calcifications .

RP: retroperitoneal; NF2: neurofibromatosis type 2.

present on pathologic assessment (*26*). Our case also demonstrated marked heterogeneity with a centrally cystic/necrotic core, a feature which has been described in nearly 50% (40/86) of reported suprarenal RP schwannomas. The high frequency of central cystic changes may relate to a frequently delayed presentation with increased size of these tumors at presentation. A study by Hirose *et al*. identify a higher proportion of GFAP positive schwannomas in the retroperitoneum compared to elsewhere (*45*). They attribute this to the origin and subtype of RP schwannomas and could provide an alternative reason for the more aggressive appearance of many suprarenal RP schwannomas at presentation. Of identified cases in our review, a GFAP stain was only performed prospectively by Fernandez *et al*. and retrospectively in our case with both cases

Table 3. Clinical and pathological characteristics of suprarenal retroperitoneal schwannomas published by Zhou *et al.* (*44*)

Cases	Age/Gender	Presentation	Size (cm)	Margin	Heterogeneity	Solid/Cystic	Calcification	Suspected Diagnosis	Diagnosis
Case 1	45/F	Asymptomatic	3	En	NR	Solid	None	NAA	Surgery
Case 2	53/M	Asymptomatic	8	En	NR	Cystic	None	NAA	Surgery
Case 3	66/M	Hypotension	5	En	NR	Cystic	Present	FAA	Surgery
Case 4	43/M	Asymptomatic	6.5	En	NR	Solid	None	NAA	Surgery
Case 5	62/F	Asymptomatic	5	En	NR	Solid	None	PCC	Surgery
Case 6	32/F	Asymptomatic	6	En	NR	Solid	None	NAA	Surgery
Case 7	42/F	Asymptomatic	6	En	NR	Solid	None	NAA	Surgery
Case 8	44/F	Flank Pain	5	En	NR	Solid	Present	FAA	Surgery
Case 9	26/F	Asymptomatic	3	En	NR	Solid	None	NAA	Surgery
Case 10	50/M	Flank Pain	4	En	NR	Solid	None	FAA	Surgery
Case 11	58/M	Asymptomatic	2.5	En	NR	Solid	None	FAA	Surgery
Case 12	56/F	Asymptomatic	1	En	NR	Solid	Present	FAA	Surgery
Case 13	38/M	Asymptomatic	3.5	En	NR	Solid	None	NAA	Surgery
Case 14	61/F	Asymptomatic	12	En	NR	Solid	None	NAA	Surgery
Case 15	57/F	Cushing Syndrome	6	En	NR	Solid	None	FAA	Surgery
Case 16	47/F	Asymptomatic	12	En	NR	Solid	None	NAA	Surgery
Case 17	48/F	Asymptomatic	8	En	NR	Solid	None	NAA	Surgery
Case 18	40/M	Asymptomatic	3	En	NR	Solid	Present	NAA	Surgery
Case 19	42/M	Asymptomatic	3	En	NR	Solid	None	NAA	Surgery
Case 20	42/F	Asymptomatic	4	En	NR	Solid	None	NAA	Surgery
Case 21	52/F	Asymptomatic	4.5	En	NR	Solid	Present	NAA	Surgery
Case 22	31/M	Asymptomatic	7	En	NR	Cystic	None	NAA	Surgery
Case 23	69/M	Asymptomatic	2.5	En	NR	Cystic	None	NAA	Surgery
Case 24	67/M	Asymptomatic	6	En	NR	Cystic	None	PCC	Surgery
Case 25	46/F	Asymptomatic	12	En	NR	Solid	Present	NAA	Surgery
Case 26	29/F	Abdominal Pain	2	En	NR	Solid	None	NAA	Surgery
Case 27	31/F	Asymptomatic	4	En	NR	Solid	None	NAA	Surgery
Case 28	54/M	Asymptomatic	8.5	En	NR	Solid	None	NAA	Surgery
Case 29	67/F	Asymptomatic	7	En	NR	Cystic	Present	NAA	Surgery
Case 30	71/M	Asymptomatic	1	En	NR	Cystic	None	NAA	Surgery
Case 31	33/F	Asymptomatic	4	En	NR	Solid	None	NAA	Surgery

En: Encapsulated; NR: Not Reported; ACC: adrenal cortical carcinoma; NAA: nonfunctional adrenal adenoma; FAA: functional adrenal adenoma; PCC: Pheochromocytoma.

Table 4. Differential diagnosis table for retroperitoneal adrenal and suprarenal schwannomas

Adrenal adenoma	• Typically small. • Typically homogenous. • Typically low density (HU < 10 on non-contrast imaging) and/or demonstrates washout characteristics (> 60% absolute washout; > 40% relative washout). • Increasing size raises concern for malignancy.
Adrenal cortical carcinoma	• Typically large (> 6 cm). • Irregularly shaped (main differentiating factor from RP suprarenal schwannomas). • Typically heterogeneous with central necrosis and/or hemorrhage. • Calcification in up to 30%.
Adrenal metastasis	• Variable appearance. • Typically < 50% washout.
Pheochromocytoma	• Typically large. • Typically heterogeneous. • Avid enhancement. • Calcification in < 10%. • Typically "light bulb bright" on T2 MRI sequence.
Suprarenal Schwannoma	• Typically large (mean 6.5 cm). • Encapsulated. • Nearly 50% are heterogeneous with central necrosis and/or hemorrhage. • Calcification in ~50%. • Can be indistinguishable from adrenal metastasis on imaging.

demonstrating positivity (*8*). Hirose *et al*. identified GFAP positivity in 92% of their RP cellular/fascicular type schwannomas, which would be consistent with GFAP positivity seen in our cellular type schwannoma.

3.3. Differential diagnoses

Irrespective of cause, our case and review of the literature demonstrates the high proportion of aggressive appearing

suprarenal schwannomas at imaging presentation. These tumors are frequently misattributed as malignant etiologies of adrenal origin such as adrenal cortical carcinoma and metastasis. Other adrenal lesions such as adrenal adenomas and PCCs are frequently considered as well. Solid lesions of retroperitoneal origin such as lymphoid tumors, sarcomas, teratomas, and other non-schwannoma neurogenic tumors can be considered but rarely represent the predominant differential in these lesions (*46*). Features for typical differential diagnoses for adrenal and suprarenal retroperitoneal schwannomas are described in Table 4.

4. Conclusion

Although rare, our case and review demonstrates that benign schwannoma is a differential consideration for suprarenal malignant lesions. All other known reported cases utilized resection for pathological diagnosis. While publication bias is likely a factor, resection may not be a preferable approach in older patients and/or poor surgical candidates. As in our case of an 81-year-old man reluctant to undergo aggressive surgery, a core needle biopsy and close imaging follow up may be sufficient for management despite the aggressive appearance on initial presentation.

References

1. Rajiah P, Sinha R, Cuevas C, Dubinsky TJ, Bush WH, Kolokythas O. Imaging of uncommon retroperitoneal masses. Radiographics. 2011; 31:949-976.
2. Abdessater M, Mokdad ME, Gas J, Sleiman W, Coloby P, Bart S. Juxta-adrenal schwannoma presenting as a giant adrenal tumor: A case report and a literature review. Int J Surg Case Rep. 2018; 53:132-136.
3. Adas M, Ozulker F, Adas G, Koc B, Ozulker T, Sahin IM. A rare adrenal incidentaloma: Adrenal schwannoma. Case Rep in Gastroenterol. 2013; 7:420-427.
4. Babaya N, Makutani Y, Noso S, Hiromine Y, Ito H, Taketomo Y, Ueda K, Ushijima H, Komoike Y, Yamazaki Y, Sasano H, Kawabata Y, Ikegami H. Case report: Schwannoma arising from the unilateral adrenal area with bilateral hyperaldosteronism. Endocr Disord. 2017; 17:74.
5. Bakhshi GD, Borisa A, Tayade MB, Bhandarwar AH, Mogal HD. Primary schwannoma of adrenal gland: A case report. J Indian Med Assoc. 2011; 109:762-763.
6. Bedard YC, Horvarth E, Kovacs K. Adrenal schwannoma with apparent uptake of immunoglobulins. Ultrastruct Pathol. 1986; 10:5050-513.
7. Damodaran S, Mahimairaj G, Velaichamy K. A series of two cases of juxta-adrenal schwannoma presenting as adrenal mass lesion and review of the literature. Urol Ann. 2015; 7:254-258.
8. Fernandez RB, Villamil LR, Montes FP, Mendez BD, Fonseca JMP, Menendez CL, Garcia CP, Ugarteburu RG, Rodriguez IG, Madera JM. Management of retroperitoneal schwannoma: Case reports and review of the literature. World J Nephrol Urol. 2016; 5:58-62.
9. Fu H, Lu B. Giant retroperitoneal schwannoma: A case report. Int J Clin Exp Med. 2015; 8:11598-11601.
10. Garg S, Mathew M, Goel T. Adrenal schwannoma: a case report and review of the literature. Indian J Pathol Microbiol. 2007; 50:587-588.
11. Gazula S, Mammen KJ. Schwannoma with concomitant tuberculosis in the adrenal gland. Indian J Urol. 2007; 23:469-470.
12. Goh BKP, Tan YM, Chung YFA, Chow PKH, Ooi LLPJ, Wong WK. Retroperitoneal schwannoma. Am J Surg. 2006; 192:14-18.
13. Grasso E, Simone M. Adrenal schwannomas: Rare tumor of the retroperitoneum. Case Rep Surg. 2015:547287.
14. Hsiao HL, Li CC, Lin HC, Yeh HC, Huang CH, Wu WJ. Adrenal schwannoma treated with laproscopic adrenalectomy: A case report. Kaohsiung J Med Sci. 2008; 24:553-557.
15. Igawa T, Hakariya H. Primary adrenal schwannoma. Nihon Hinyokika Gakki Zasshi. 1998; 8:567-570.
16. Ikemoto I, Yumoto T, Yoshino Y, Furuta N, Kiyota H, Oishi Y. Schwannoma with purely cystic form originating from the adrenal area: A case report. Acta Urol Jpn. 2002; 48:289-291.
17. Inokuchi T, Takiuchi H, Moriwaki Y, Ka T, Takahashi S, Tsutsumi Z, Shima H, Hirota S, Yamamoto T. Retroperitoneal ancient schwannoma presenting as an adrenal incidentaloma: CT and MR findings. Mag Res Imag. 2006; 24:1389-1393.
18. Jakowski JD, Wakely PE, Jimenez RE. An uncommon type of adrenal incidentaloma: A case report of the arenal medulla with cytological, histological, and ultrastructural correlation. Ann Diag Pathol. 2008; 12:356-361.
19. Jeshtadi A, Govada N, Somalwar SB, Nagulapally S. Schwannoma of the adrenal gland. J Med Allied Sci. 2014; 4:77-80.
20. Khurram M, Hamza A, Briski L, Ibrahim A. Schwannoma of the adrenal gland: A rare adrenal incidentaloma: Case report and review of the literature. Am J Clin Pathol. 2015; 144:A318.
21. Kleiman DA, Hughes DB, Joshi ART. Surgical management of incidental adrenal schwannomas. Am Surg. 2011; 77:E89-E90.
22. Konstantinos TG, Dimitrios T, Panagiotis KB, Nikolaos MV, Ioannis F, Andreas M. Laproscopic resection of an adrenal schwannoma. JSLS. 2012; 16:663-667.
23. Korets R, Berkenblit R, Ghavamian R. Incidentally discovered adrenal schwannoma. JSLS. 2007; 11:113-115.
24. Kostakopoulos A, Pilramenos D, Livadas K, Antonopoulos P, Demonakou M. Malignant schwannoma of the adrenals: A rare case. Acta Urologica Belgica. 1991; 51:129-132.
25. Lau SK, Spagnolo DV, Weiss LM. Schwannoma of the adrenal gland: Report of two cases. Am J Surg Pathol. 2006; 30:630-634.
26. Li SQ, Zhang YS, Shi J, Li HZ. Clinical features and retroperitoneal laproscopic resection of adrenal schwannoma in 19 patients. Endocr Pract. 2015; 21:323-329.
27. Liu QY, Gao M, Li HG, Lin XF, Huang SQ, Liang BL. Juxa-adrenal schwannoma: Dynamic multi-slice CT and MRI findings. Eur J Radiol. 2012; 81:794-799.
28. Oberoi A, Kataria K, Prakash O, Yadav R, Goyal A. Management of giant adrenal schwannoma. Int Surg J. 2019; 6:2605-2608.
29. Onoda N, Ishikawa T, Toyokawa T, Takashima T, Wakasa K, Hirakawa K. Adrenal schwannoma treated

with laproscopic surgery. JSLS. 2008; 12:420-425.
30. Pittasch D, Klose S, Schmitt J, Roessner A, Ridwelski K, Lippert H, Lehnert H. Retroperitoneal schwannoma presenting as an adrenal tumor. Exp Clin Endocrinol Diabetes. 2000; 108:318-321.
31. Richter KK, Premkumar R, Yoon HS, Mercer P. Laproscopic adrenalectomy for a rare 14 cm adrenal schwannoma. Surg Lacrosc Endosc Percutan Tech. 2011; 21:E339-E343.
32. Said S, Muhammad R, Othman HA, Othman S, Rashid NFA, Zin RRM. Adrenal schwannoma: A rare type of adrenal incidentaloma. World J Endocr Surg. 2017; 9:111-114.
33. Shabana W, Raslan W, Hassan S, Al-Tartir T. Schwannoma mascquerading as adrenocortical tumor: A case report and review of literature. Urol Case Rep. 2019; 26:100926.
34. Suzuki K, Nakanishi A, Kurosaki Y, Nogaki J, Takaba E. Adrenal schwannoma: CT and MRI findings. Radiat Med. 2007; 25:299-302.
35. Tang W, Yu XR, Zhou LP, Gao HB, Wang QF, Peng WJ. Adrenal schwannoma: CT, MR manifestations and pathological correlation. Clin Hemorheol Microcirc. 2018; 68:401-412.
36. Tarcoveanu E, Dimofte G, Bradea C, Moldovanu R, Vasilescu A, Anton R, Ferariu D. Adrenal schwannoma. JSLS. 2009; 13:116-119.
37. Tezel GG, Karaman N, Karakoc D, Yorganci K. Giant juxtadrenal and adrenal schwannoma with concurrent adrenal myelolipoma mimicking an adrenal malignant tumor. Turk J Med Sci. 2005; 35:255-258.
38. Thomas MB, Stephen J. Adrenal schwannoma: A rare adrenal incidentaloma. Int Surg J. 2018; 5:1967-1969.
39. Tommaselli AP, Valentino R, Rossi R, Savastano S, Luciano A, Battista C, Troncone G, Lombardi G. Usefulness of 123I-Metaiodobenzylguanidine scintiscan in the diagnosis of juxta-adrenal schwannoma. JCE&M. 1996; 81:843-846.
40. Xiao C, Xu B, Ye H, Yang Q, Wang L, Sun YH. Experience with adrenal schwannoma in a Chinese population of six patients. J Endocrinol Invest. 2011; 34:417-421.
41. Yang CY, Chou CW, Lin MB, Li CF. Schwannomas of the left adrenal gland and posterior mediastinum. J Chin Med Assoc. 2009; 72:83-87.
42. Yonou H, Goya M, Miyazato M, Miyazato T, Suaya K, Koyama Y, Hatano T, Ogawa Y. Retroperitoneal schwannoma arising from the adrenal area: A case report. Acta Urol Jpn. 1999; 45:403-405.
43. Yun HJ, Kim SY, Kim SM, Lee YS, Chang HS, Park CS. Adrenal schwannoma: Rare entity of adrenal incidentaloma. Korean J Endocr Surg. 2016; 16:107-111.
44. Zhou J, Zhang D, Li W, Zhou L, Xu H, Zheng S. Primary adrenal schwannoma: A series of 31 cases emphasizing their clinicopathologic features and favorable prognosis. Endocrine. 2019; 65:662-674.
45. Hirose T, Ishizawa K, Sakaki M, Fujii Y. Retroperitoneal schwannoma is characterized by a high incidence of cellular type and GFAP-immunoreactivity. Pathol Int. 2012; 62:456-462.
46. Scali EP, Chandler TM, Heffernan EJ, Coyle J, Harris AC, Chang SD. Primary retroperitoneal masses: what is the differential diagnosis? Abdom Imaging. 2015; 40:1887-1903.

Received March 6, 2020; Revised July 1, 2020; Accepted July 7, 2020.

Address correspondence to:
Mitchell P. Wilson, Department of Radiology and Diagnostic Imaging, University of Alberta, 2B2.41 WMC, 8440-112 Street NW, Edmonton, Alberta, T6G 2B7, Canada.
E-mail: mitch.wislon@ualberta.ca

Released online in J-STAGE as advance publication July 9, 2020.

Case Report

DOI: 10.5582/irdr.2020.03003

Successful endoscopic biopsy for Primary central nervous system lymphoma of the corpus callosum in the splenium with bilateral visuomotor ataxia

Yusuke Morinaga[1,*], Kouhei Nii[1], Kimiya Sakamoto[1], Ritsurou Inoue[1], Takafumi Mitsutake[1], Hayatsura Hanada[1], Seiji Haraoka[2]

[1] Department of Neurosurgery, Fukuoka University Chikushi Hospital, Chikushino, Fukuoka, Japan;
[2] Department of Pathology, Fukuoka University Chikushi Hospital, Chikushino, Fukuoka, Japan.

SUMMARY Primary central nervous system lymphoma (PCNSL) is a rare malignant tumor of the central nervous system. It is associated with poor prognosis. Early diagnosis and subsequent planning of adequate treatment strategy are relevant to improve survival and reduce neurological deficit. Specifically, there are no reports of successful endoscopic biopsy for PCNSL of the corpus callosum in the splenium with bilateral visuomotor ataxia. An 74-year-old woman presented to our hospital with anorexia, depression and ataxia beginning six months earlier. Head computed tomography and magnetic resonance imaging showed malignant tumor suspected in the corpus callosum. Endoscopic biopsy was performed via the low parieatal approach, suspecting GBM or PCNSL. She had no new postoperative neurological deficits and was pathologically diagnosed with diffuse large B-cell lymphoma (DLBCL). She is currently undergoing radiation chemotherapy with a modified Rankin Scale score of 2. Regarding preoperative symptoms, ataxia was considered to be bilateral visuomotor ataxia caused by damage to the corpus callosum in the splenium, and anorexia and depression were considered symptoms of the surrounding limbic system. Delay in the diagnosis of PCNSL can lead to a poor prognosis. Visuomotor ataxia should also consider the potential for the corpus callosum in the splenium lesion, including PCNSL, and appropriate imaging and pathological diagnosis with endoscopic biopsy can contribute to a good clinical outcome.

Keywords PCNSL, DLBCL, visuomotor ataxia, corpus callosum in the splenium, endoscopic biopsy

1. Introduction

Primary central nervous system lymphoma (PCNSL) is a rare malignant tumor of the central nervous system. It is associated with poor prognosis and accounts for 0.7-0.9% of all lymphomas and only 0.3-1.5% of intracranial tumors. Typically, these lesions are in the cerebral white matter near the corpus callosum, the central gray matter, the basal ganglia-thalamus-hypothalamic region, the posterior fossa and the periventricular region (*1*). PCNSLand glioblastoma multiforme (GBM) are malignant cerebral neoplasms associated with poor prognosis. Early diagnosis and subsequent planning of adequate treatment strategy are relevant to improve survival and reduce neurological deficit (*2*). Specifically, there are no reports of successful endoscopic biopsy for PCNSL of the corpus callosum with bilateral visuomotor ataxia. Here, we describe a rare case where PCNSL of the corpus callosum with bilateral visuomotor ataxia was diagnosed early and successfully by endoscopic biopsy.

2. Case Report

A 74-year-old woman presented to our hospit anorexia, depression, and ataxia beginning six months earlier. She had history of dyslipidemia and had taken atorvastatin. Neurological assessments revealed a Japan Coma Scale grade I-1, ataxia, and no limb paralysis and cerebellar symptoms. Upon hospitalization, his heart rate was 62 bpm and his blood pressure was 120/72 mmHg. Blood sampling revealed normal IL-2 receptor (417 U/mL) and no other abnormalities. Plain head computed tomography (Figure 1A) and magnetic resonance imaging (MRI) (Figure 1B, 1C) showed malignant tumor suspected on the corpus callosum in the splenium with perifocal edema. Neuronavigation-guided endoscopic biopsy was performed using a 10 mm cylinder via the low parieatal approach, suspecting

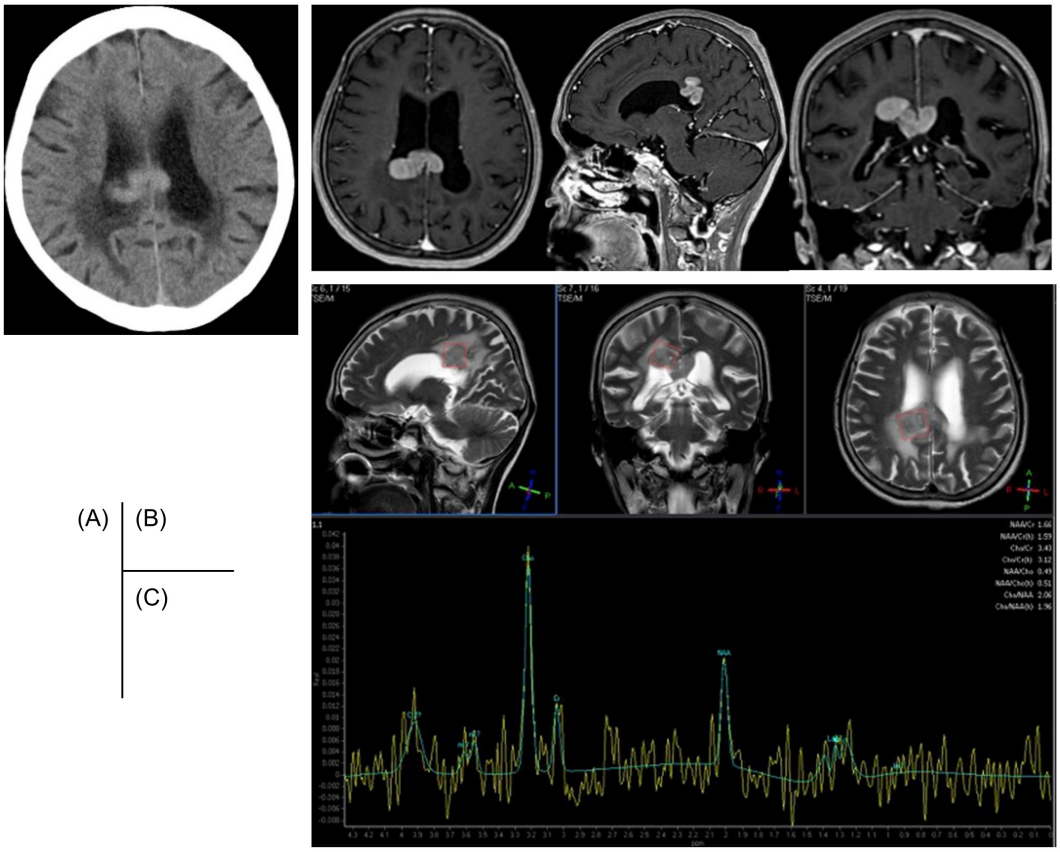

Figure 1. Clinical imaging at hospitalization. (A) Head plane computed tomography show tumor suspected on the corpus callosum in the splenium with perifocal edema. **(B)** Head gadolinium-T1-weighted (Gd-T1) magnetic resonance imaging reveals malignant tumor suspected on the corpus callosum in the splenium (left; axial view, median; sagittal view, right; coronal view). **(C)** Magnetic resonance spectroscopy reveals a malignant pattern.

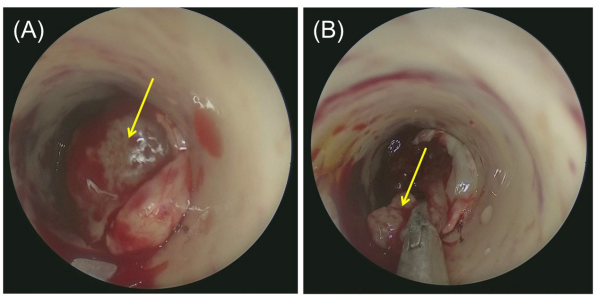

Figure 2. Intaraoperative imaging. Neuronavigation-guided endoscopic biopsy is performed via the low parieatal approach. **(A)** Yellow arrows indicate the tumor on the corpus callosum in the splenium. **(B)** The tumor is biopsied with forceps.

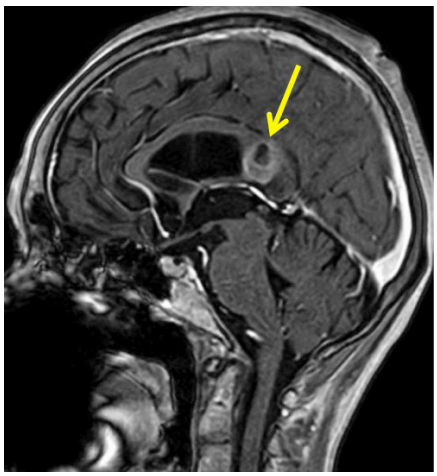

Figure 3. Postoperative imaging. Postoperative Gd-T1 magnetic resonance imaging reveals the good enucleation of the tumor and no bleeding.

GBM or PCNSL (Figure 2A, 2B). Postoperative MRI revealed good enucleation and no bleeding (Figure 3). She had no new postoperative neurological deficits and was pathologically diagnosed with diffuse large B-cell lymphoma (DLBCL). She is currently undergoing radiation chemotherapy with a modified Rankin Scale score of 2. Regarding preoperative symptoms, ataxia was considered to be visuomotor ataxia caused by damage to the corpus callosum in the splenium, and anorexia and depression were considered symptoms of the surrounding limbic system.

Informed consent was obtained from the patient for publication of this case report and the accompanying images, and the study design was approved by the appropriate ethics review board.

3. Discussion

To the best of our knowledge, reports of successful early diagnosis by endoscopic biopsy for PCNS of the corpus callosum with optic ataxia, such as the present one, are rare (*1,2*).

Rondot P, *et al*. (*3*) reports that visuomotor ataxia (*3,4*) is a disorder of movement performed under visual control. It can occur in the absence of disturbance of ocular fixation and in the absence of spatial agnosia. This disorder may extend over the whole visual field or it may be localized to one visual half-field, right or left. It may involve both hands or one hand only, so that visuomotor ataxia may be divided into: (*1*) Unilateral visuomotor ataxia, localized to a single field. In this case it may affect both hands or a single hand. It is direct when the hand is ataxic in the ipsilateral visual field and it is crossed when the hand is ataxic in the contralateral visual field; (*2*) Bilateral visuomotor ataxia, involving the whole visual field. Each hand may be ataxic only in the contralateral visual field, that is, bilateral crossed visuomotor ataxia; or in the ipsilateral field when it is called bilateral direct visuomotor ataxia. The observed clinical variations which are described here imply the existence of both direct and crossed visuomotor connections, the latter probably crossing the corpus callosum in the splenium (*3,4*). Callosal disconnection syndrome (*5*) refers to conduction aphasia, visuomotor ataxia, apraxia of the left hand, agraphia of the left hand, alien hand syndrome (*6*). In the corpus callosum in the splenium, visual and auditory information integration and memory functions are impaired (*3,4*). These symptoms may not show any noticeable disability in daily life and are often not recognized without a special callosal function test. In our case, regarding preoperative symptoms, ataxia was considered to be bilateral visuomotor ataxia caused by damage to the corpus callosum in the splenium, and anorexia and depression were considered symptoms of the surrounding limbic system (*7*).

Marion R, *et al*. reports that fluorescence-guided endoscopic visualization identified 5-aminolevulinic acid (5-ALA)-positive tissue not sufficiently exposed by conventional microscopic visualization (*8*). Although 5-ALA was not used in our case, safe endoscopic biopsy could be performed under the neuronavigation, and it was considered to be a minimally invasive treatment.

In conclusion, delay in the diagnosis of PCNSL can lead to a poor prognosis. bilateral visuomotor ataxia should also consider the potential for the corpus callosum in the splenium lesion, including PCNSL, and appropriate imaging and pathological diagnosis with endoscopic biopsy can contribute to a good clinical outcome.

Acknowledgements

We would like to thank Editage (www.editage.com) for English language editing. This research did not receive any specific grants from funding agencies in the public, commercial, or not-for-profit sectors.

References

1. Rizq H, Aisha A, Issam Al B, Abdulrazzaq H, Sirajeddin B. Solitary Primary Central Nervous System Lymphoma Mimicking Third Ventricular Colloid Cyst-Case Report and Review of Literature. World Neurosurg. 2019; 123:286-294.
2. Cerqua R, Balestrini S, Perozzi C, Cameriere V, Renzi S, Lagalla G, Mancini G, Montanari M, Leoni P, Scerrati M, Iacoangeli M, Silvestrini M, Luzzi S, Provinciali L. Diagnostic delay and prognosis in primary central nervous system lymphoma compared with glioblastoma multiforme. Neurol Sci. 2016; 37:23-29.
3. Rondot P, Recondo JD, Dumas JL. Visuomotor ataxia. Brain. 1977; 100:355-376.
4. Ohigashi Y, Hamanaka T, Yamashita S, Tokuriki Y, Tana H. Bilateral crossed visuomotor ataxia — a case report. No to shinkei. 1983; 35:1217-1222. (in Japanese)
5. Nocentini U, Borghese NA, Caltagirone C, Fadda L, Lacquaniti F. A callosal disconnection syndrome of vascular origin. J Neurosurg Sci. 1997; 41:107-111.
6. Hidalgo-Borrajo R1, Belaunzaran-Mendizábal J, Hernáez-Goñi P, Tirapu-Ustárroz J, Luna-Lario P. Alien hand syndrome: a review of the literature. Rev Neurol. 2009; 48:534-539. (in Spanish)
7. Hu H. Advances in molecular and circuitry mechanisms of depressive disorder — A focus on lateral habenula. Adv Exp Med Biol. 2019; 1180:135-146.
8. Marion R, Marcel K, Hans-Jakob S, Michael S. Endoscopic-assisted visualization of 5-aminolevulinic acid-induced fluorescence in malignant glioma surgery: a technical note. World Neurosurg. 2014; 82:e277-9.

Received March 23, 2020; Revised May 9, 2020; Accepted May 13, 2020.

**Address correspondence to:*
Yusuke Morinaga, Department of Neurosurgery and Neuroscience, Fukuoka University Chikushi Hospital, 1-1-1 Zokumyoin, Chikushino-shi, Fukuoka 818-8502, Japan.
E-mail: yu_the_morio@yahoo.co.jp

Released online in J-STAGE as advance publication May 15, 2020.

Case Report

DOI: 10.5582/irdr.2020.03014

Pseudohypoparathyroidism presenting with seizures: a case report and literature review

Mostafa Suhail Najim*, Riyadh Ali Mohammed Hammamy, Mohammed Awad Azzam Ashour, Asaad Omer Ahmed Imameldin

Department of Internal Medicine, Hamad Medical Corporation, Doha, Qatar.

SUMMARY Symptomatic hypocalcemia is frequently encountered in the Emergency Department, necessitating admission. It has a variety of underlying etiologies, with hypoparathyroidism and vitamin D deficiency being the most common. However, rarer etiologies such as pseudohypoparathyroidism, as was present in the current case, should not be overlooked. Reported here is a case of a young female patient presenting with generalized tonic clonic seizures. Electrocardiography revealed a prolonged QT interval which pointed towards a metabolic cause, and this was confirmed by laboratory results which indicated a low calcium level. A parathyroid pathology was obvious as the phosphate level was elevated. Pseudohypoparathyroidism, rather than hypoparathyroidism, was identified since the parathyroid hormone level was elevated. Other relevant differential diagnoses were excluded. The patient was treated with intravenous calcium initially and given regular oral calcium, calcitriol, and sevelamer.

Keywords hypocalcemia, pseudohypoparathyroidism, seizures

1. Introduction

Symptomatic hypocalcemia is frequently encountered in the Emergency Department, necessitating admission. It has a variety of underlying etiologies, with vitamin D deficiency being the most common (*1*). Pseudohypoparathyroidism (PHP) is an uncommon cause of hypocalcemia attributed to parathyroid hormone (PTH) resistance, with a prevalence of 3.4 per 1 million according to one Japanese study (*2*) and 0.79 per 100,000 according to the Orphanet Report Series, November 2008 (*3*). PHP is diagnosed based on the exclusion of other differential diagnoses, and it can be confirmed by genetic analysis (*3*).

2. Case Report

A 34-year-old woman, with a medical history of three seizures in the past for which she did not seek medical treatment, presented with generalized body weakness and a subjective fever for two days prior. While being assessed in the Emergency Department, she developed generalized tonic clonic seizures that resolved spontaneously, followed by post-ictal confusion.

On examination, vital signs were within normal limits. A systemic physical exam was unremarkable, including a neurological and a musculoskeletal examination. Laboratory results (Table 1) revealed a very low corrected serum calcium level of 1.2 mmol/L [2.1-2.6 mmol/L] combined with a high serum phosphorus level of 1.86 mmol/L [0.87-1.45 mmol/L] in the absence of hypomagnesaemia (serum magnesium of 0.72 mmol/L [0.66-1.07 mmol/L]). These biochemical changes were combined with a high serum intact PTH of 108 pg/mL [15-65 pg/mL]. All of these findings are indicative of PHP. The low serum vitamin D level of 15 ng/mL [30-80 ng/mL] potentially added to the already low serum calcium level. Other pertinent laboratory abnormalities that suggested recent seizure activity were a high white blood cell count of $16.4 \times 10^3/\mu L$ [4-$10 \times 10^3/\mu L$] and elevated serum creatine kinase of 426 U/L [26-192 U/L].

Chest x-ray (CXR) revealed clear costophrenic angles and lung zones. The mediastinum and hila appeared normal. Cardiac size was within normal limits. Electrocardiography (ECG) (Figure 1) revealed a sinus rhythm with a prolonged QT interval (a corrected QT interval of 552), suggestive of hypocalcemia. A plain CT scan of the head (Figure 2) was unusual in that it revealed extensive bilateral symmetrical calcifications of basal ganglia, cerebellar dentate nuclei, and subcortical white matter. These calcium deposits substantiate the biochemical changes caused by PHP as mentioned above. Magnetic resonance imaging

Table 1. Laboratory results*

Laboratory results	Patient values	Normal reference range
General hematology		
White blood cell count (10^3/μL)	16.4	4 -1 0
Hemoglobin (g/dL)	11.6	12 - 15
MCV (fL)	75.8	83 - 101
Platelet count (10^3/μL)	273	150 - 400
General chemistry		
Urea (mmol/L)	3.5	2.76 - 8.07
Creatinine (μmol/L)	48	53 - 97
Sodium (mmol/L)	137	135 - 145
Potassium (mmol/L)	3.1	3.6 - 5.1
Chloride (mmol/L)	92	96 - 110
Magnesium (mmol/L)	0.72	0.66 - 1.07
Glucose (mmol/L)	6.4	3.3 - 5.5
C-reactive protein (mg/L)	< 5	0 - 5
Bicarbonate (mmol/L)	17.5	24 - 30
Albumin (g/L)	47	35 - 50
Corrected calcium (mmol/L)	1.2 Low	2.1 - 2.6
Phosphorus (mmol/L)	1.86 High	0.87 - 1.45
Alkaline phosphatase (U/L)	76	45 - 129
Creatine kinase (U/L)	426	26 - 192
Myoglobin (ng/mL)	48	25 - 58
Urine chemistry		
24-hour calcium (mmol/24 hours)	2.2	2.5 - 7.5
Endocrinology		
Parathyroid hormone (pg/mL)	108 High	15 - 65
Vitamin D (ng/mL)	15 Low	30 - 80
Thyroid stimulating hormone (mIU/L)	2.51	0.27 - 4.20
Thyroxine (pmol/L)	12.1	12 - 22

*Urine cAMP was not done after PTH administration, as it was not available.

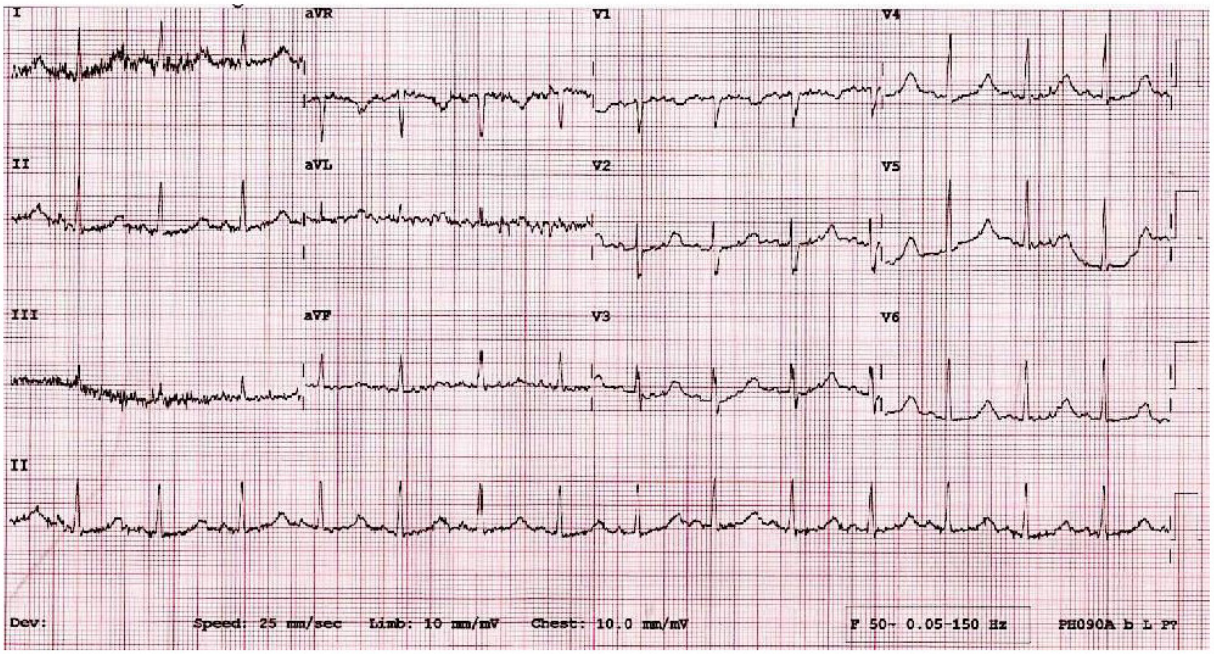

Figure 1. ECG. This ECG strip is showing sinus rhythm with prolonged QT interval (QTc 552).

(MRI) of the head (Figure 3) confirmed the findings from the head CT scan as imaging revealed bilaterally symmetric calcifications involving the dentate nuclei, basal ganglia, and subcortical white matter regions with no abnormal soft tissue component, perifocal oedema, or mass effect. Electroencephalography (EEG) revealed bilateral frontal cerebral dysfunction but was otherwise unremarkable.

Course of treatment and outpatient follow-up: The patient was given regular intravenous calcium gluconate, regular oral calcium carbonate, calcitriol, and sevelamer. She did not experience any further

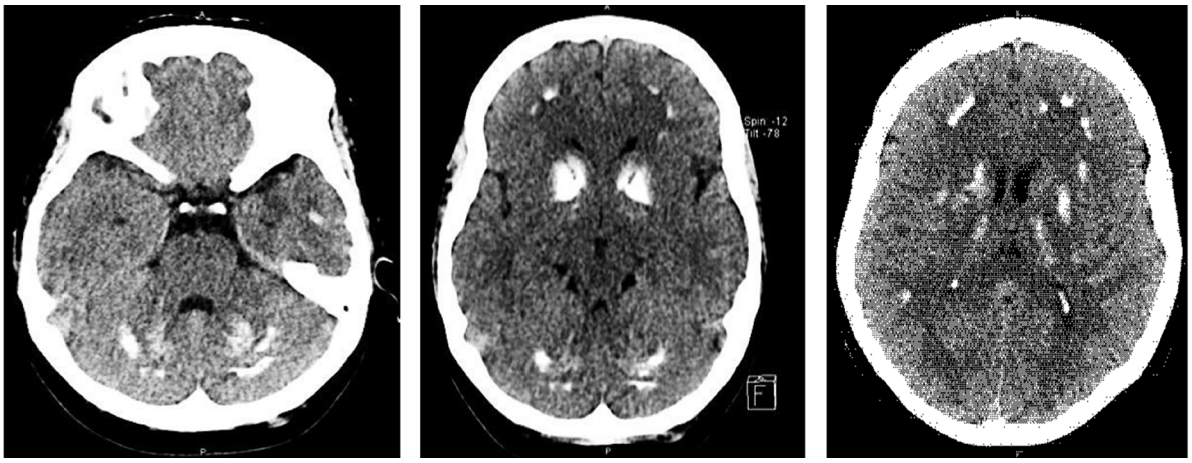

Figure 2. Plain CT head. These CT sections are showing extensive bilateral symmetrical calcifications of basal ganglia, cerebellar dentate nuclei and subcortical white matter.

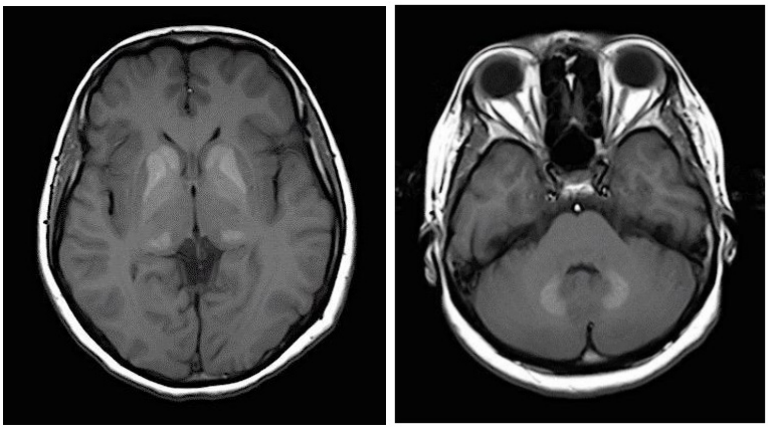

Figure 3. MRI head. These MRI sections are showing bilaterally symmetric calcifications involving dentate nuclei, basal ganglia, and subcortical white matter regions with no abnormal soft tissue component, perifocal oedema, or mass effect.

seizures during hospitalization. In a post-discharge visit 1 week later, the patient was asymptomatic, corrected calcium was 1.89 mmol/L, and PTH was still high at 106 pg/mL.

3. Discussion

PTH plays a major role in keeping the body's calcium levels in check. When the serum calcium level is low, the parathyroid glands send signals to bone and the kidneys to raise serum calcium levels and maintain calcium homeostasis. These processes involve bone resorption, calcium absorption in the distal tubules, and vitamin D production *via* 1 alpha hydroxylase enzyme activation in the kidneys. Active vitamin D (1,25 dihydroxy vitamin D) will enhance intestinal absorption of calcium. When calcium levels are above normal, in contrast, the parathyroid glands are suppressed (*4*).

PHP, in simple terms, is hypoparathyroidism despite elevated PTH levels. This is due to the fact that the peripheral organs are unresponsive to the action of PTH. PHP is subdivided into different subtypes with different genetic mutations that include deletions, small mutations, or methylation (loss of function) near the GNAS locus on chromosome 20q 13.3 (Table 2) (*5,6*). The latter normally mediates the action of G protein-coupled receptors *via* the transcription of a signaling protein called Gs alpha (*7*). PHP 1b involves a normal phenotype, which differentiates it from the other PHP 1 subtypes (PHP 1a and 1c) that have clinical features of Albright hereditary osteodystrophy (AHO); however, laboratory results, namely hypocalcemia, hyperphosphatemia, high serum PHP, and low urine cyclic adenosine 3′, 5′-monophosphate (cAMP) post PTH administration, are the same (Table 2). A high PTH level is usually apparent in childhood at the age of 2-3, and hypocalcemia is mostly symptomatic in adolescence before the age of 20 (*7,8*). Incidental PHP has also been reported in the literature based on the presence of asymptomatic hypocalcemia as part of a preoperative work-up (*9*). Later, genetic testing confirmed the diagnosis of PHP 1b. The inheritance of PHP 1b follows an autosomal dominant pattern, but sporadic cases of PHP 1b reported in the literature indicate that other exogenous and environmental factors may be in play (*10-12*). Based on the previous

Table 2. Characteristics of PHP subtypes (*5,6*)

Items	PHP 1a	PHP 1b	PHP 1c	PHP II	PPHP
Phenotype	AHO + Hormonal resistance (PTH, TSH, Gn, GHRH)	Hormonal resistance (PTH +/-TSH)	AHO + Hormonal resistance (PTH, TSH, Gn)	No hormonal resistance	No hormonal resistance
Main molecular determinants	Maternal LoF in GNAS	Deletions in GNAS	No mutations	Few mutations reported	Paternal LoF in GNAS
Serum Ca	Low	Low	Low	Low	Normal
Serum P	High	High	High	High	Normal
Serum PTH	High	High	High	High	Normal
Urine cAMP post PTH	Low	Low	Low	Normal	Normal

AHO, Albright hereditary osteodystrophy; Ca, calcium; cAMP, cyclic adenosine 3′, 5′-monophosphate; GHRH, growth hormone-releasing hormone; Gn, gonadotropin; LoF, loss of function; P, phosphorus; PHP, pseudohypoparathyroidism; PPHP, pseudo-pseudohypoparathyroidism; PTH, parathyroid hormone; TSH, thyroid stimulating hormone.

Table 3. Studies reporting late PHP 1b presentation

Author, year (*Ref.*)	Age, gender	Patient characteristics	Clinical manifestations	Vitamin D level	Brain imaging
Iglesias *et al.*, 2017 (*8*)	65 year-old, female	Normal phenotype	Asymptomatic	Normal	Not done
Chong *et al.*, 2013 (*13*)	46 year-old, female	Normal phenotype	Symptomatic	Low	Not done
Chale-Matsau *et al.*, 2018 (*14*)	33 year-old, female	Normal phenotype	Symptomatic	Normal	Not done
Aggarwal *et al.*, 2016 (*15*)	23 year-old, female	Normal phenotype	Symptomatic	Normal	Normal
Van Rooijen *et al.*, 2012 (*16*)	18 year-old, female	Normal phenotype	Symptomatic	Low	Not done
Zeniya *et al.*, 2014 (*17*)	22 year-old, female	AHO phenotype	Symptomatic	Normal	Bilateral calcifications
Garg *et al.*, 2011 (*18*)	34 year-old, male	Normal phenotype	Symptomatic	Normal	Normal

AHO, Albright hereditary osteodystrophy; PHP: pseudohypoparathyroidism.

discussion, the current patient was deemed to be a late presenter of sporadic PHP 1b.

While there are numerous case reports addressing PHP 1b in the pediatric population, there are few PHP 1b cases involving a late presentation. Moreover, most of the published articles focus on the genetic mutations of the disease rather than the clinical aspects and disease implications. A review of the literature identified 7 relevant case reports that share some similarities as well as differences with the current case (Table 3) (*8,13-18*).

Hypoparathyroidism and PHP are the most common causes of basal ganglia calcifications. Together, they account for more than two-thirds of cases (*19*). There is some evidence that extracellular phosphate accumulation may play a major role in the formation of these calcifications (*20*). Widespread calcifications beyond the basal ganglia, as were present in the current case, are uncommon in PHP (*21*). Such extensive calcifications might be asymptomatic or have been likened to seizures or more severe neurological manifestations such as parkinsonism and impaired mental function (*19*). Other rarer causes of basal ganglia calcifications include Down's syndrome, Fahr's syndrome, tuberous sclerosis, and Cockayne syndrome (*22*).

PHP can cause serious skeletal complications if left untreated. This is attributable to the accompanying secondary hyperparathyroidism due to the resistance of renal receptors to the action of PTH. If this persists long enough, it can reduce bone density, and mainly that of cancellous bones, *via* accelerated bone turnover (*23*). Elevated serum alkaline phosphatase (ALP) can be a marker of PHP-related bone disease that warrants a thorough skeletal survey (*24*).

The current patient presented with seizures, and this can be explained by the effects of PHP; namely hypocalcemia and widespread cortical and basal ganglia calcifications as were mentioned earlier. In addition, vitamin D deficiency reduced the patient's calcium level even lower and might have contributed to clinically evident seizures. Normal serum ALP precluded the need for a detailed skeletal survey (Table 1). In conclusion, PHP is a rare cause of hypocalcemia that should be considered among differential diagnoses. The two aspects that distinguish the current case are the late presentation of the disease and the potentially preventable bone disease that may occur if the diagnosis of PHP is missed.

References

1. Cooper MS, Gittoes NJ. Diagnosis and management of hypocalcaemia. BMJ. 2008; 336:1298-1302.
2. Nakamura Y, Matsumoto T, Tamakoshi A, Kawamura T, Seino Y, Kasuga M, Yanagawa H, Ohno Y. Prevalence of idiopathic hypoparathyroidism and pseudohypoparathyroidism in Japan. J Epidemiol. 2000; 10:29-33.
3. Mantovani G. Clinical review: Pseudohypoparathyroidism: diagnosis and treatment. J Clin Endocrinol Metab. 2011;

96:3020-3030.
4. Poole K, Reeve J. Parathyroid hormone — A bone anabolic and catabolic agent. Curr Opin Pharmacol. 2005; 5:612-617.
5. Navaeifar MR, Zamanfar D. Calcification of soft tissues in a family, case report and review of pseudohypoparathyroidism. Journal of Rare Disorders: Diagnosis & Therapy. 2017; 3:16.
6. Mantovani G, Spada A, Elli FM. Pseudohypoparathyroidism and Gsα–cAMP-linked disorders: current view and open issues. Nat Rev Endocrinol. 2016; 12:347-356.
7. Jüppner H. Genetic and epigenetic defects at the GNAS locus cause different forms of pseudohypoparathyroidism. Ann Endocrinol (Paris). 2015; 76:92-97.
8. Iglesias Bolaños P, Gutierrez Medina S, Bartolomé Hernandez L. Late diagnosis of 1b pseudohypoparathyroidism. Med Clin (Barc). 2017; 149:508-509.
9. Goto M, Yamamoto Y, Ishii M, Nakamura A, Sano S, Kagami M, Fukami M, Saito R, Araki S, Kubo K, Kawagoe R, Kawada Y, Kusuhara K. Sporadic pseudohypoparathyroidism type-1b with asymptomatic hypocalcemia. Pediatr Int. 2016; 58:1229-1231.
10. Bastepe M, Fröhlich LF, Hendy GN, Indridason OS, Josse RG, Koshiyama H, Körkkö J, Nakamoto JM, Rosenbloom AL, Slyper AH, Sugimoto T, Tsatsoulis A, Crawford JD, Jüppner H. Autosomal dominant pseudohypoparathyroidism type Ib is associated with a heterozygous microdeletion that likely disrupts a putative imprinting control element of GNAS. J Clin Invest. 2003; 112:1255-1263.
11. Morgado J, Dias P, Sampaio M, Sousa A. A sporadic case of pseudohypoparathyroidism type Ib. Revista Portuguesa de Endocrinologia, Diabetes e Metabolismo. 2016; 11:212-214.
12. Donghi V, Mora S, Zamproni I, Chiumello G, Weber G. Pseudohypoparathyroidism, an often delayed diagnosis: a case series. Cases J. 2009; 2:6734.
13. Chong P, Meeking D. Pseudohypoparathyroidism: a rare but important cause of hypocalcaemia. BMJ Case Rep. 2013; 2013:bcr2012008040.
14. Chale-Matsau B, van Niekerk C, Kemp T, Pillay T. Discordant calcium and parathyroid hormone with presumed epileptic seizures. Clin Chem. 2018; 64:442-445.
15. Aggarwal A, Shah R, Mousa O, Patel A. Isolated PTH renal resistance pseudohypoparathyroidism 1b: a rare cause of hypocalcemia. JNMA J Nepal Med Assoc. 2016; 55:33-35.
16. Van Rooijen C, Kok M, Simsek S, Stam F. Ain't no sunshine when she's gone: pseudohypoparathyroidism discovered in an adult. Case Rep Endocrinol. 2012; 2012: 739375.
17. Zeniya S, Yuno A, Watanabe T, Usui T, Moriki Y, Uno Y, Miake H. A 22-year-old woman with hypocalcemia and clinical features of Albright hereditary osteodystrophy diagnosed with sporadic pseudohypoparathyroidism type Ib using a methylation-specific multiplex ligation-dependent probe amplification assay. Intern Med. 2014; 53:979-986.
18. Kharb S, Gundgurthi A, Dutta M, Garg M. Adult onset pseudohypoparathyroidism type-1b with normal phosphaturic response to exogenous parathyroid hormone. Indian J Endocrinol Metab. 2011; 15:337-340.
19. Koller WC, Cochran JW, Klawans HL. Calcification of the basal ganglia: computerized tomography and clinical correlation. Neurology. 1979; 29:328-333.
20. Mitchell D, Regan S, Cooley M, Lauter K, Vrla M, Becker C, Burnett-Bowie S, Mannstadt M. Long-term follow-up of patients with hypoparathyroidism. J Clin Endocrinol Metab. 2012; 97:4507-4514.
21. Montenegro A, Gelenske T, Carvalho É, Bandeira F, Sougey E. First description of pseudohypoparathyroidism with frontal lobe calcification and normal serum calcium at the initial manifestation in an otherwise healthy seven-year-old girl. Arq Bras Endocrinol Metabol. 2011; 55:349-352.
22. Basak R. A case report of basal ganglia calcification - a rare finding of hypoparathyroidism. Oman Med J. 2009; 24:220-222.
23. Tollin S, Perlmutter S, Aloia J. Serial changes in bone mineral density and bone turnover after correction of secondary hyperparathyroidism in a patient with pseudohypoparathyroidism type Ib. J Bone Miner Res. 2000;15:1412-1416.
24. Kidd G, Schaaf M, Adler R, Lassman M, Wray H. Skeletal responsiveness in pseudohypoparathyroidism. Am J Med. 1980; 68:772-781.

Received April 8, 2020; Revised May 10, 2020; Accepted May 24, 2020.

Address correspondence to:
Mostafa Suhail Najim, Department of Internal Medicine, Hamad Medical Corporation, Al Rayyan Street, Hamad General Hospital, P.O. Box 3050, Doha, Qatar.
E-mail: drmostafanajim@gmail.com

Released online in J-STAGE as advance publication June 2, 2020.

Case Report

DOI: 10.5582/irdr.2020.03015

Tuberculous choroiditis masquerading as sympathetic ophthalmia: a case report

Xiaoxu Huang[1,*], Xiaolin Qin[1], Zhengyang Luo[1], Luoxiang Li[2], Jianbin Hu[1,*]

[1] Chengdu Aier East Eye Hospital, Chengdu, Sichuan, China;
[2] Department of Pathology, Hospital of Chengdu University of Traditional Chinese Medicine, Chengdu, Sichuan, China.

SUMMARY A 26-year-old Chinese man was admitted to this clinic due to decreased vision in his right eye for 4 days and painful protrusion in his left eye for 20 days. He had no perception of light in his left eye and perception of hand motion (HM) in his right eye. Examinations revealed that the left eye's lens and iris had protruded, and corneoscleral perforation. The right eye had an anterior chamber reaction and severe exudative retinal detachment that were confirmed by fluorescein angiography. Systemic examinations failed to identify a cause. The presumptive diagnosis was sympathetic ophthalmia of the right eye. Therefore, systemic steroid treatment was administered and enucleation of the left eye was performed. Although steroid treatment had been initiated, exudative detachment did not vary markedly. A pathological examination of the left eye revealed ocular tuberculosis, and anti-tuberculosis treatment resulted in a gradual reduction in subretinal fluid as well as improved vision.

Keywords ocular tuberculosis, sympathetic ophthalmia, choroiditis

1. Introduction

The eye is an organ often affected by extrapulmonary tuberculosis, and all ocular tissues can be affected, such as the eyelids, orbit, conjunctiva, plica semilunaris, lacrimal caruncle, sclera, retina, choroid, and optic nerve. Because of its slow and abundant blood flow, the choroid is a tissue most often affected by ocular tuberculosis (*1*). This poses a diagnostic challenge because of its protean clinical manifestations (*2,3*). Ocular tuberculosis is often diagnosed empirically in the absence of a microbial culture or pathological evidence (*4*). Tuberculosis can also induce endophthalmitis or panophthalmitis (*5-8*), but such conditions are extremely rare. Fewer than 20 cases have been reported worldwide (*8*), most of which necessitated enucleation or evisceration (*9*).

Presented here is a case of severe ocular tuberculosis where corneoscleral perforation with tubercular panophthalmitis was diagnosed based on a histopathological examination of the patient's left eye, in addition to severe exudative retinal detachment due to tuberculous choroiditis in the right eye.

2. Case Report

A 26-year-old Chinese man from a medically underserved area was admitted to this clinic due to reduced vision for 4 months, complete loss of vision for 2 months, painful protrusion in the left eye for 20 days, and a sudden reduction in vision in the right eye for 4 days. There was no perception of light in the left eye and perception of hand motion (HM) in the right eye. Examinations revealed that his left eye's lens and iris had protruded, corneoscleral perforation was evident, and the cornea was highly opaque. B-scan ultrasonography revealed an irregular strong echo in the ocular cavity, and layers of retina and choroid were thickened inside the eye (Figure 1). An anterior segment examination of the right eye revealed conjunctival congestion, mild corneal edema , granulomatous keratic precipitates (KPs) (+), anterior chamber flare (+), cells (+), and a dilated pupil (diameter:4.5 mm); a posterior segment examination revealed vitreous cavity cells (+), optic disc swelling, retinal vascular dilation, and severe exudative retinal detachment (Figure 2A) that was confirmed by optical coherence tomography (OCT) (Figure 2B) and fluorescein angiography (FA) (Figure 2C). FA revealed multifocal hypofluorescent areas throughout all of the frames and progressive patchy hyperfluorescence in the late frames, and especially on the nasal side of the optic disc, indicating choroidal leakage. Systemic examinations that included chest radiography, routine blood tests, a human immunodeficiency virus (HIV) test, a syphilis test, and screening for immune diseases failed to identify a cause. Before admission, the patient's left eye had been treated despite lack of a definitive diagnosis. The

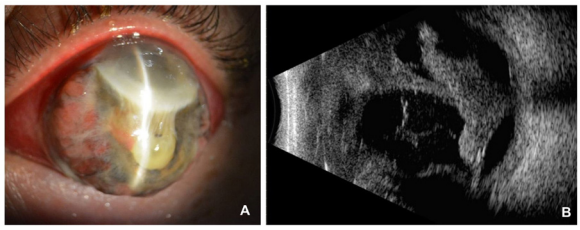

Figure 1. (A), The left eye had a protruded lens and iris at the corneoscleral perforation with an extensive opaque cornea. (B), The anterior segment could not be distinguished in B-scan ultrasonography, an irregular strong echo was present in the ocular cavity, and layers of retina and choroid had thickened.

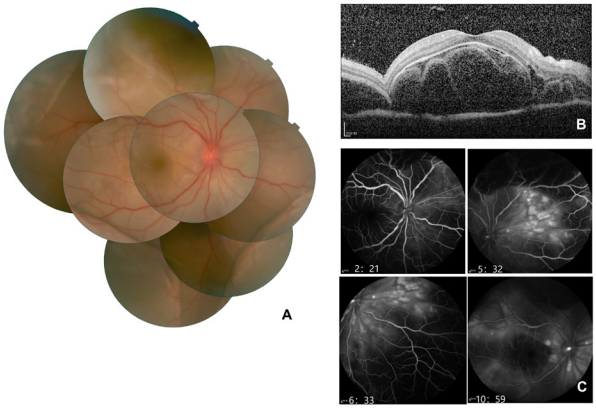

Figure 2. (A), Photography of the right eye revealed congestion and a blurred boundary of the optic disc, vascular dilation, retinal edema, and exudative retinal detachment. (B), OCT confirmed retinal edema and a large volume of subretinal fluid in the posterior area. (C), FA revealed multifocal hypofluorescent areas throughout all of the frames and progressive patchy hyperfluorescence in the late frames, and especially on the nasal side of the optic disc.

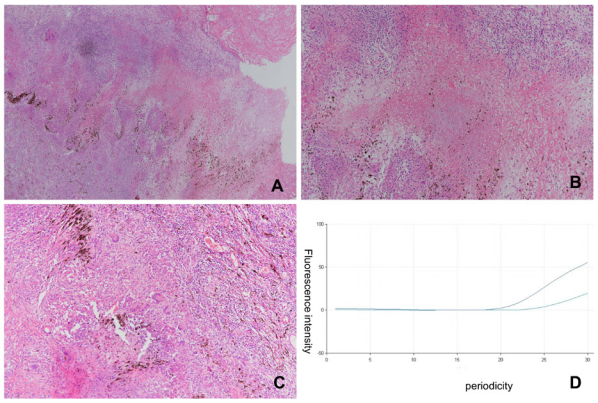

Figure 3. A pathological examination of the left eye revealed (A), part of the choroid had been entirely destroyed by granulomas, which were mainly infiltration by lymphocytes and monocytes/ macrophages. (B), caseous necrosis. (C), Langerhans cells were evident. (D), Results of fluorescent probe PCR of TB-DNA were positive: the curve matched the positive control curve.

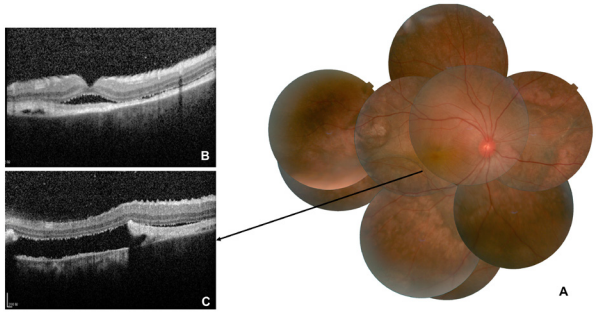

Figure 4. (A), 1.5 months after anti-tuberculosis treatment, previous retinal edema and detachment resolved; (B), OCT confirmed that the retinal edema and detachment had resolved; (C), Deposits and subretinal pigment accumulation in the posterior area.

patient had no previous history of systemic or infectious diseases. He also had no history of trauma. Considering granulomatous inflammation and severe exudative retinal detachment in the right eye and perforation in the left eye, the presumptive diagnosis was sympathetic ophthalmia of the right eye. Therefore systemic steroid treatment was administered (infusion of 1,000 mg of methylprednisolone per day). Anti-inflammatory eye drops (tobramycin dexamethasone, pranoprofen, and compound tropicamide) were administered to the right eye as well. Enucleation of the left eye was performed. After 4 days of steroid treatment, vision did not change, and both the anterior chamber reaction and exudative retinal detachment improved slightly. However, a final pathological examination of the left eye revealed ocular tuberculosis. Multiple choroidal granulomas with caseous necrosis were present and a polymerase chain reaction (PCR) to identify tuberculosis-DNA (TB-DNA) was positive (Figure 3), although Ziehl-Neelsen staining of histopathology specimens did not reveal acid-fast bacilli. Accordingly, systemic steroid treatment was stopped except for the focal eye drops, which were adjusted according to follow-ups. The patient was transferred to a tuberculosis hospital to undergo further examinations, which confirmed tuberculosis, and then started on anti-tuberculosis therapy. After 1.5 months, vision in the right eye improved to counting fingers (CF) 50 cm. The anterior chamber reaction in the right eye had almost disappeared except for the dilated pupil, and previous retinal edema and retinal detachment improved as well (Figure 4). Therapeutic efficacy confirmed tuberculous choroiditis in the right eye.

3. Discussion

Presented here is a rare case of severe ocular tuberculosis masquerading as sympathetic ophthalmia, and this condition was eventually corrected.

All of the ocular tissues may be affected by tuberculosis (*4*); in the current case, tuberculosis in the left eye manifested as panophthalmitis. Because of its slow and abundant blood flow, the choroid is a tissue most often affected (*1*). Tuberculous choroiditis presents in various ways such as granulomatous uveitis, inflammatory and non-inflammatory conditions such as tumors, macular degeneration, and non-infectious

autoimmune uveitis (*1,2*), posing a diagnostic challenge (Table 1).

In 60% of cases, extrapulmonary tuberculosis in not accompanied by pulmonary tuberculosis (*9*), indicating the difficulty of identifying that condition *via* routine screening of the lung. Ocular tuberculosis is difficult to diagnosed empirically in the absence of a microbial culture or pathological evidence (*11*). In the current case, there was no noteworthy history of conditions affecting the left eye, corneoscleral perforation was evident, and the patient was healthy except for his eye problems. Moreover systemic examinations did not identify a cause, so the condition was misdiagnosed as sympathetic ophthalmia of the right eye following a penetrating injury of the left eye. The diagnosis of exudative retinal detachment led to administration of high-dose systemic corticosteroid therapy, but improvement in exudative retinal detachment was limited. The left eye was enucleated, which may have helped to gauge preoperative diagnostic accuracy and to provide a safety net for any unsuspected pathology (*12*). The final pathological examination revealed tuberculosis despite negative acid-fast staining. However, negative results could not exclude tuberculosis because only 54-86% of Mycobacterium tuberculosis bacilli (MTB) can be detected by Ziehl-Neelsen acid-fast staining (*13*). After further confirmation, anti-tuberculosis treatment was initiated and had satisfactory efficacy.

Table 1. Clinical manifestations of intraocular tuberculosis (*10*)

Tissue	Possible presentations
Anterior uvea/Pars plana	Granulomatous anterior uveitis Iris nodules Iris atrophy Intermediate uveitis
Choroid	Tubercles Tuberculomas Abscesses Choroiditis
Retina	Macular edema Intra- or preretinal hemorrhage Retinitis Vasculitis Neovascularization Neuroretinitis Eales disease
Optic nerve	Optic neuritis Retrobulbar neuritis Papillitis Papilledema Tubercles
Globe	Panuveitis Endophthalmitis Panophthalmitis Globe rupture

The detailed stages of diagnosis and therapy are listed in the Table 2. The pathological examination as described here was crucial to making a precise diagnosis. In addition, there are only a handful of reported cases where histopathological evidence corroborated the existence of tuberculosis (*14,15*).

Although tuberculosis has been controlled quite well over the past several decades in China (*16*), ocular tuberculosis typically appears in atypical forms. The current case indicates that ophthalmologists should be extremely watchful to avoid a missed diagnosis or misdiagnosis.

Acknowledgements

The authors wish to thank Professor Hyoung Jun Koh, M.D in Ophthalmology at Severance Hospital, Yonsei University. His advice prompted this case report.

Table 2. Detailed diagnosis and therapy

Day 1 *Presumed diagnosis*: sympathetic ophthalmia	No history of systemic or infectious diseases. No trauma or surgery. Left eye: corneoscleral perforation; Right eye: anterior chamber reaction and severe exudative retinal detachment. OCT, FFA, Ultrasound B scan, *etc*. Chest radiography, blood routine, HIV, syphilis, immune diseases screening, *etc*.
Day 2	Systemic steroid venous transfusion; Anti-inflammatory eyedrops for the right eye; Enucleation of the left eye.
Day 5	Pathologic diagnosis of the left eye revealed ocular tuberculosis. Steroid treatment was stopped. Exudative retinal detachment improved only slightly; Vison did not change.
Day 7 *Modified diagnosis*: tuberculous choroiditis	Anti-tuberculosis therapy began.
Day 52	Anti-tuberculosis treatment had satisfactory efficacy.

References

1. Zhang M, Zhang J, Liu Y. Clinical presentations and therapeutic effect of presumed choroidal tuberculosis. Retina. 2012; 32:805-813.
2. Varma D, Anand S, Reddy AR Das A, Watson JP, Currie DC, Sutcliffe I, Backhouse OC. Tuberculosis: An under-diagnosed aetiological agent in uveitis with an effective treatment. Eye (Lond). 2006; 20:1068-1073.
3. Boonsopon S, Tesavibul N, Uiprasertkul M, Leeamornsiri S, Choopong P. Rare presentation of intractable tuberculous panophthalmitis with intraocular and intraorbital abscesses: A case report. J Med Case Rep. 2017; 11:180.
4. Gupta V, Shoughy SS, Mahajan S, Khairallah M, Rosenbaum JT, Curi A, Tabbara KF. Clinics of ocular tuberculosis. Ocul Immunol Inflamm. 2015; 23:14-24.
5. Manthey KF, Duncker G, Gronemeyer U. Endophthalmitis caused by mycobac-terium tuberculosis. Klin Monatsbl Augenheilkd. 1982; 180:556-558. (in German)
6. Raina UK, Tuli D, Arora R, Mehta DK, Taneja M. Tubercular endophthalmitis simulating retinoblastoma. Am J Ophthalmol. 2000; 130:843-845.
7. Wadhwani M, Sethi S, Beri S, Jain R, Dsouza P, Nangia A, Garg SP. An unusual case of metastatic tubercular panophthalmitis in a 14-year-old boy. J Pediatr Ophthalmol Strabismus. 2011; 48:318-319.
8. Hase K, Namba K, Saito W, Ohno S, Ishida S. A case of tuberculous endophthalmitis successfully treated with vitrectomy followed by antituberculous agents. J Ophthalmic Inflamm Infect. 2015; 8:14.
9. Cimino L, Herbort CP, Aldigeri R, Salvarani C, Boiardi L. Tuberculous uveitis, a resurgent and underdiagnosed disease. Int Ophthalmol. 2009; 29:67-74.
10. Dalvin LA, Smith WM. Intraocular manifestations of mycobacterium tuberculosis: a review of the literature. J Clin Tuberc Other Mycobact Dis. 2017; 7:13-21.
11. Mao Y, Peng XY, You QS, Wang H, Zhao M, Jonas JB. Tuberculous uveitis in China. Acta Ophthalmol. 2014; 92: e393-e397.
12. Thaung C. Changing indications for enucleation and selected unusual pathologies. Saudi J Ophthalmol. 2019; 33:238-242.
13. Ryan GJ, Shapiro HM, Lenaerts AJ. Improving acid-fast fluorescent staining for the detection of mycobacteria using a new nucleic acid staining approach. Tuberculosis (Edinb). 2014; 94:511-518.
14. Aggarwal K, Agarwal A, Sehgal S, Sharma S, Singh N, Sharma K, Samanta R, Invernizzi A, Sharma A, Gupta V. An unusual presentation of intraocular tuberculosis in a monocular patient: clinicopathological correlation. J Ophthalmic Inflamm Infect. 2016; 6:46.
15. Wroblewski KJ, Hidayat AA, Neafie RC, Rao NA, Zapor M. Ocular tuberculosis: a clinicopathologic and molecular study. Ophthalmology. 2011; 118:772-777.
16. Wang L, Zhang H, Ruan Y, *et al.* Tuberculosis prevalence in China, 1990-2010: a longitudinal analysis of national survey data. Lancet. 2014; 383:2057-2064.

Received April 10, 2020; Revised May 20, 2020; Accepted May 29, 2020

**Address correspondence to:*
Xiaoxu Huang and Jianbin Hu, Chengdu AIER East Eye Hospital, No. 388, Shuanglin Road, Chenghua District, Chengdu 610056, Sichuan, China.
E-mail: xpxiaoxu222@163.com (Huang XX), hujianbin@aierchina.com (Hu JB)

Released online in J-STAGE as advance publication June 2, 2020.

Case Report

DOI: 10.5582/irdr.2020.03038

Cranial intraosseous angiolipoma: case report and literature review

Katherine M. Morgan[1], Simon Hanft[2], Zhenggang Xiong[1,*]

[1] Department of Pathology and Laboratory Medicine, Robert Wood Johnson Medical School, Rutgers University, New Brunswick, New Jersey, USA;
[2] Department of Neurosurgery, Robert Wood Johnson Medical School, Rutgers University, New Brunswick, New Jersey, USA.

SUMMARY Angiolipomas are slow-growing, soft tissue tumors consisting of mature adipocytes and thin-walled blood vessels. While most angiolipomas are subcutaneous lesions in the trunk and upper extremities, intraosseous angiolipomas are rare at cranial site. We present the case of a 61-year-old female with an enlarging lesion in the left frontoparietal skull following minor head trauma. Radiography confirmed an expansile, enhancing, spiculated bony lesion in the left frontoparietal calvarium with extension outside the cortex into the soft tissues. She underwent a craniectomy for complete resection of the calvarial mass, which was histologically composed of mature adipocytes and disorganized blood vessels highlighted by an immunophenotype positive for S100 and CD34, respectively, consistent with a cranial intraosseous angiolipoma. The review of the literature that reported five cases of cranial intraosseous angiolipoma with our case representing the sixth case is discussed.

Keywords intraosseous angiolipoma, calvarium, cranium, skull bone, soft tissue tumor

1. Introduction

Angiolipomas are benign tumors composed of mature adipocytes admixed with thin-walled blood vessels. Most are found in the trunk and upper extremities (*1*). While angiolipomas are predominantly subcutaneous lesions, intraosseous angiolipomas are very rare tumors that occur most commonly in the rib (*2,3*) and mandible (*4,5*).

A literature review revealed only five reported cases of cranial intraosseous angiolipomas (*6-10*). These lesions can mimic lipomas, angiomas, fibrous dysplasia, meningiomas, or metastases on computed tomography (CT) and magnetic resonance imaging (MRI) and, thus, should be included in the differential diagnosis of an enlarging skull mass (*6,7,9*).

Herein, we describe a rare case of cranial intraosseous angiolipoma and further discuss this entity by reviewing the literature.

2. Case Report

2.1. Clinical history

A 61-year-old female with hypertension and arthritis, as well as a history of both squamous cell carcinoma and basal cell carcinoma, was referred to our institute for evaluation of an enlarging palpable left frontoparietal bone lesion. Six months prior to presentation, the patient hit her head on a closet rail and subsequently noted a lump on the left frontoparietal aspect of her scalp. She was then followed up with CT and MRI of the brain with and without contrast, revealing a growing expansile, striated, enhancing lesion in the left frontoparietal cranial bone, which appeared to abut the superior sagittal sinus. The lesion disrupted the inner and outer tables of the cranial bone and indented the extra-axial space of the left frontoparietal region with extension outside of the cortex into the soft tissues. There was no evidence of cerebral parenchymal involvement, except for cerebral compression (Figure 1A-E). The differential diagnosis including metastatic disease or an atypical hemangioma was radiologically considered. Subsequently, a total body bone scan was also performed and only revealed this solitary lesion in the skull (Figure 1F).

Given the rapid growth and etiological uncertainty of the bone lesion, a left frontoparietal craniectomy for complete resection of the mass with subsequent cranioplasty was performed. The excised lesional skull bone was sent for histopathological examination. Clinical follow-up with the patient showed no recurrence of this tumor.

2.2. Pathological examination

The craniectomy specimen grossly consisted of an oval mass lesion measuring approximately 4.0 × 3.0 × 0.6

cm in overall dimensions with cranial convex surface on one side demonstrating diffuse pitting of the bone (Figure 2A). Upon sectioning, the cut surface revealed a dark red-grey appearance spanning the entire thickness of the bone, including the aforementioned raised area (Figure 2B). After formalin fixation, the sections were decalcified in Immunocal (100% formic acid) for approximately two days. Representative sections were taken, including six full thickness sections from the central lesional portion of the bone. The tissue was then paraffin-embedded and 4-um sections were obtained. The resulting sections were stained with hematoxylin and eosin (H&E). Microscopic examination showed that the mass lesion was composed of mature adipose tissue admixed with disorganized thin-walled blood vessels. Cytological atypia, mitosis or necrosis was not identified (Figure 2C and 2D). Immunohistochemical (IHC) studies demonstrated that the vascular endothelium expresses CD34 (Figure 2E) and the mature adipocytes express S100 (Figure 2F).

Based on the above findings, the diagnosis of cranial intraosseous angiolipoma was generated.

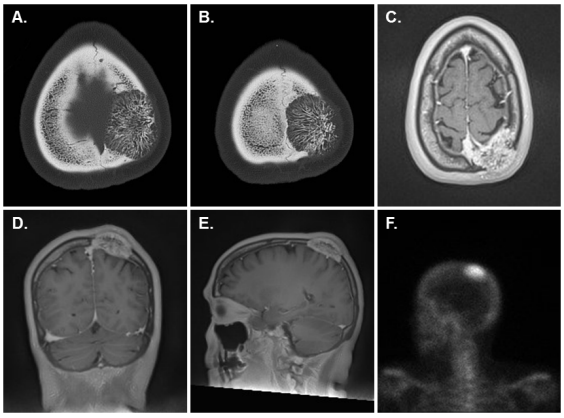

Figure 1. Radiographic images of the left frontoparietal mass. **(A, B)** CT without contrast revealed an expansile, spiculated osseous lesion in the left frontoparietal calvarium with a small soft tissue component along its superficial surface (A, B, axial). **(C, D, E)** T1-weighted MRI with and without contrast identified an expansile, striated, enhancing left frontoparietal bone lesion which indented the extra-axial space of the left parietal region with extension outside the cortex into the soft tissues (C, axial; D, coronal; E, sagittal). **(F)** Total body bone scan revealed a solitary lesion in the skull (left lateral view of the head is shown).

3. Discussion

Although intraosseous angiolipomas are seen at extra-cranial sites, cranial intraosseous angiolipoma is rarely encountered. Due to its non-specific clinical characteristics and presentation, histopathological evaluation plays an essential role in clinical management. Our literature search revealed only five reported cases of intraosseous angiolipoma involving the cranium, the salient clinicopathological features of which are summarized in Table 1 and discussed below.

Intraosseous angiolipomas are slow-growing and can take months to years to develop before coming to the attention of clinicians. Although our patient as well as one of the five literature-documented cases (*9*) had noted the enlarging skull mass following head trauma, whether there is an association between head trauma and cranial intraosseous angiolipomas remains unclear and requires further investigation. The clinical presentation of a cranial intraosseous angiolipoma varies depending on the location and size of the tumor. In the reported cases, the most common symptoms included headache and altered sensation or tenderness to palpation at the site of the mass (*6-8,10*), while others, including our patient, were asymptomatic (*9*). It is noted that the mass lesion involved the frontal and parietal area of the skull in all five previously reported cases as well as our case, which may suggest the site

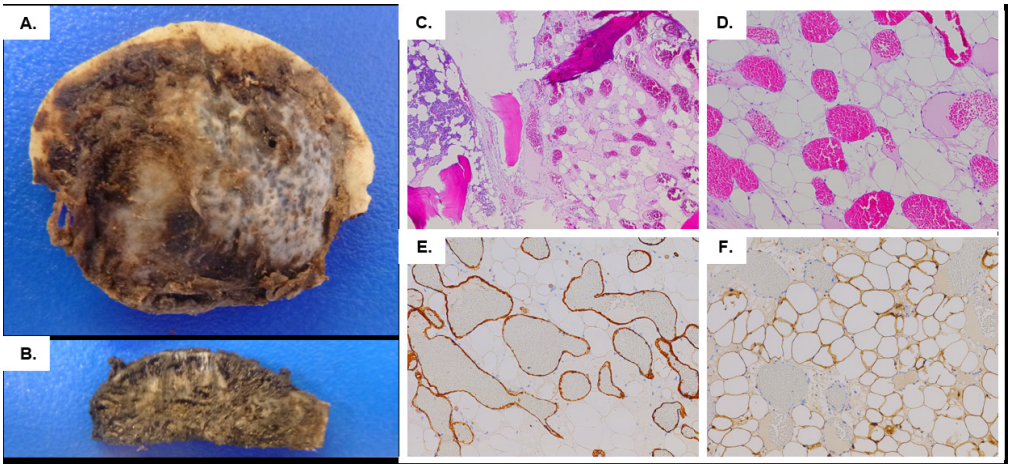

Figure 2. Resected left frontoparietal mass and microscopic findings. **(A)** The specimen grossly consisted of an oval portion of cranium with a raised area on the convex surface. **(B)** Upon sectioning, the cut surface revealed a dark red-gray appearance spanning the entire thickness of the bone and raised area. **(C, D)** Histologically, the calvarial mass was composed of mature adipose tissue and disorganized thin-walled blood vessels (H&E, C: 40×, D: 100×). **(E, F)** The immunophenotype was positive for CD34 staining the vascular endothelium (E, 100×) and S100 highlighting the adipocytes (F, 100×).

Table 1. Clinicopathological features of reported cases of cranial intraosseous angiolipoma

Author, Year (*Ref.*)	Age (years)/ Gender	Location	Period of Expansion	History of Head Trauma	Clinical Features/ Neurological Examination	Radiographic Findings	Histopathology*
Amirjamshidi *et al.*, 2014 (*10*)	41/Female	Right frontotemporo-parietooccipital	2 years	No	Tender to palpation, headache	X-ray, CT, & MRI: 20 cm expansile, non-enhancing lesion extending along the diploe and destroying the internal and external tables with cerebral compression	• Gross: yellow lipomatous bone with cancellous and vascular components; • Histo: Some lesional vessels with fibrin thrombi, no cellular atypia or mitotic figures; • IHC: S100 neg, CD34 pos, Sudan black pos
Atilgan *et al.*, 2014 (*7*)	16/Female	Right frontal	"long time"	No	Swelling, headache	CT: 2 cm well defined lesion with no bone destruction or soft tissue component	• Gross: yellow-brown solid lesion; • Histo: Some lesional vessels with neutrophils and fibrin thrombi, no mitosis or necrosis, average of 10 mast cells per 1 HPF; • IHC: CD34 pos, CD31 pos, VEGF pos, TGFbeta pos, TNFalpha pos
Nguyen *et al.*, 2014 (*8*)	55/Male	Right frontal	-	-	Headache, nausea, vomiting, diplopia, facial asymmetry [concurrently diagnosed with metastatic invasive ductal breast carcinoma]	CT & MRI: 4.3 cm heterogeneously enhancing lesion with cerebral compression, but without involvement of overlying soft tissue	• Gross: Well circumscribed, mixed areas of firm-to-soft tan and red lobulated tissue; • Histo: No cytologic atypia or mitoses; • IHC: pankeratin neg
Singh *et al.*, 2016 (*6*)	30/Female	Right parietal	5 years, following pregnancy	No	Altered sensation over area without pain on palpation	CT & MRI: 6.4 cm mass with expansion of diploid space and cerebral compression	• Histo: No cytologic atypia; • IHC: epithelial membrane antigen neg
Yu *et al.*, 2009 (*9*)	50/Male	Right parietal	11 years	Minor trauma	Swelling	CT: 7 cm spiculated, non-enhancing lesion with cerebral compression	• Gross: yellow-brown lesion of variable consistency; • Histo: well circumscribed nonencapsulated lesion, scattered mast cells, no thrombi
Our case	61/Female	Left frontoparietal	6 months	Minor trauma	Swelling	Bone scan, CT & MRI: 4.4 cm expansile, spiculated, enhancing lesion with superficial soft tissue component and cerebral compression	• Gross: dark red-grey cut surface; • Histo: no cytologic atypia or mitosis or necrosis; • IHC: CD34 pos, S100 pos

*All specimens histologically demonstrated an admixture of mature adipose tissue and thin-walled blood vessels. Histo: Histology; IHC: Immunohistochemistry; neg: negative; pos: positive; HPF: high power field.

predilection of intraosseous angiolipomas.

Every documented case of cranial intraosseous angiolipoma underwent at least CT imaging to evaluate the lesion. Radiographically, the depiction of the expansile masses varied, utilizing such descriptors as trabeculated, lytic, or spiculated. Enhancement of the lesional parenchyma depends upon the extent of the vascular component, with only our case and another reported case (*8*) documenting contrast enhancement of the angiolipoma. The majority of the cases, including our own, had radiographic evidence of some degree of mass effect and cerebral compression from the tumor, but the lesion did not invade the brain parenchyma.

While the slow-growing nature of these lesions may allow clinicians to initially employ an observational management strategy (*9*), the lack of lesion-specific clinical characteristics and concern for a malignant process result in eventual surgical resection of these cranial masses. Histopathologically, every resected intraosseous angiolipoma demonstrated mature adipose tissue admixed with thin-walled blood vessels without significant cytologic atypia or mitosis. In some instances, mast cells (*7,9*) and fibrin thrombi (*7,10*) were noted. Immunohistochemical staining was utilized to confirm the histology noted on H&E, including highlighting the vascular component with endothelial markers such as CD34 (*7,10*) and the adipose component with adipocyte markers such as S100 (our case) or Sudan black (*10*). In some cases, immunohistochemical studies were employed to rule out other possible diagnoses, such as intraosseous meningioma and carcinoma metastasis.

The prognosis for angiolipomas is excellent, with surgical excision being considered curative, along with a very low risk of local recurrence and no known risk of malignant transformation. The natural history of an intraosseous angiolipoma demonstrates that growth appears to be secondary to the vascular component, which is responsible for the progressive expansion of the bone (*9*). The expansile nature of cranial intraosseous angiolipomas result in skull deformity and, depending on location, may be accompanied by neurological sequelae.

Acknowledgements

The authors thank Wendy Reed, PA (ASCP) for photographing and grossing the specimen.

References

1. Lin JJ, Lin F. Two entities in angiolipoma. A study of 459 cases of lipoma with review of literature on infiltrating angiolipoma. Cancer. 1974; 34:720-727.
2. Celik A, Sezen CB, Ertunc O, Tastepe AI. Intraosseous Angiolipoma of the Rib. Indian J Surg. 2015; 77(Suppl 3):1409-1410.
3. Hall FM, Cohen RB, Grumbach K. Case report 377: Intraosseous lipoma (angiolipoma) of right third rib. Skeletal Radiol. 1986; 15:401-403.
4. Manganaro AM, Hammond HL, Williams TP. Intraosseous angiolipoma of the mandible: a case report and review of the literature. J Oral Maxillofac Surg. 1994; 52:767-769.
5. Hemavathy S, Roy S, Kiresur A. Intraosseous angiolipoma of the mandible. J Oral Maxillofac Pathol. 2012; 16:283-287.
6. Singh R, Josiah DT, Turner RC, Cantu-Durand DE, Williams HJ, Gyure K, Voelker JL. Giant calvarial intraosseous angiolipoma: a case report and review of the literature. J Surg Case Rep. 2016; 2016:rjw051.
7. Atilgan AO, Terzi A, Agildere M, Caner H, Ozdemir BH. Intraosseous angiolipoma of the frontal bone with a unique location: a clinical and pathological case illustration and review of the literature. Indian J Pathol Microbiol. 2014; 57:301-304.
8. Nguyen L, Zwagerman NT, Grandhi R, McFadden K, Richardson RM. Intraosseous Angiolipoma of the Cranium: Case report and review of the literature. Surg Neurol Int. 2014; 5:79.
9. Yu K, Van Dellen J, Idaewor P, Roncaroli F. Intraosseous angiolipoma of the cranium: case report. Neurosurgery. 2009; 64:E189-190; discussion E190.
10. Amirjamshidi A, Ghasemi B, Abbasioun K. Giant Intradiploic Angiolipoma of the skull. Report of the first case with MR and histopathological characteristics reported in the literature and a review. Surg Neurol Int. 2014; 5:50.

Received May 14, 2020; Revised July 14, 2020; Accepted July 17, 2020.

**Address correspondence to:*
Zhenggang Xiong, Neuropathology Division, Department of Pathology and Laboratory Medicine, Robert Wood Johnson Medical School and University Hospital, Rutgers University, 125 Paterson Street, MEB 231, New Brunswick, NJ 08903, USA.
E-mail: xz460@rwjms.rutgers.edu

Released online in J-STAGE as advance publication July 19, 2020.

Communication

DOI: 10.5582/irdr.2020.03039

Comprehensive Rare Disease Care model for screening and diagnosis of rare genetic diseases – an experience of private medical college and hospital, South India

Sathish Raju Nilakantam[1], Deepa Bhat[2,3,*], M.D. Ravi[4], (Col) M Dayananda[1], H. Basavanagowdappa[5], Jagadish Kumar K[4]

[1] Department of Hospital Administration, JSS Medical College & Hospital, JSS Academy of Higher Education and Research, Mysuru, Karnataka, India;
[2] Centre for Medical Genomics & Counseling, Department of Medical Genetics, JSS Medical College & Hospital, JSS Academy of Higher Education and Research, Mysuru, Karnataka, India;
[3] Department of Anatomy, JSS Medical College & Hospital, JSS Academy of Higher Education and Research, Mysuru, Karnataka, India;
[4] Department of Paediatrics, JSS Medical College & Hospital, JSS Academy of Higher Education and Research, Mysuru, Karnataka, India;
[5] Department of General Medicine, JSS Medical College & Hospital, JSS Academy of Higher Education and Research, Mysuru, Karnataka, India.

SUMMARY Rare diseases (RD) of genetic origin are raising public health concern contributing to a massive economic burden in India. Establishing Specialty Centers to bridge the RD community with apex centers is felt as a need in developing countries. Hence a Comprehensive Rare Disease Care (CRDC) model was set up at the department of pediatrics under Center for Human Genomics and Counseling at a medical college hospital in South India. The patients suspected to have genetic disease were evaluated as per the work flow of the designed model. The utilization statistics depict the outcome of this model. In the face of limited resources, it was possible to establish a functional RD unit with meticulous planning, supportive administration and trained interdisciplinary staff. A scalable prototype that could be replicated in other Medical colleges and Hospitals of India is described.

Keywords Rare/genetic diseases, medical genetics, model, planning, public health, genetic counseling, management, interdisciplinary team

1. Epidemiological scenario of rare diseases in India

Rare diseases (RD) are health conditions that affect a small percentage of the population. India contains a wide array of them due to cultural and genetic diversity (*1*). The majority of RD are genetic in origin. Besides the large population and high birth rate, consanguinity among many communities has contributed to increased occurrence (*2*).

There is no universal definition or prevalence data for RD and each country has adopted a definition based on its population, healthcare system and resources (*3*). Hence there is no figure on their burden and associated morbidity and mortality. If the international estimate of 6% to 8% prevalence is applied to India, we must have around 72 to 96 million people affected by RDs, which would be significant number (*4*). The "Rare Disease Terminology & Definitions Used in Outcomes Research Working Group" has concluded the average global prevalence of 40-50 cases per 100,000 people can be called a rare disease (*5*).

Almost all known reported genetic disorders are found in India. Diagnosis may be difficult, due to variable presentations and modest number of clinicians experienced in handling specific RD. They are often inherited, severe, chronic, untreatable and life-threatening. A vast majority of them overwhelmingly affect children, thus contributing to the disease burden of the country (*6*).

2. Current status of genetic outpatient and laboratory services for diagnosis and treatment of RD in India

Medical genetic services are presently available in 13 different premier cities as a separate department or unit under the pediatrics department. They cater to an average of 20-40 patients on a daily basis. In addition, most medical geneticists are also actively involved in diagnostic, counselling and research laboratory work due to lack of well-defined roles and sufficient manpower (*7*). The clinical evaluation, investigations, genetic counselling and referral to patient advocacy groups are

performed in isolation leading to compartmentalization of health care delivery. Hence, the patients from several strata of society are deprived of timely and adequate genetic facilities.

3. Need to establish a Comprehensive Rare Disease Care (CRDC) model for RD

Though clinical diagnosis has gained momentum, genetic outpatient and laboratory services are available only in first-tier cities across the country. Referral to these centers has led to overloading of the premier centers and depriving timely access to patients from farther regions. Patients from the rural and suburban areas of the country need to travel long distances to reach them (*6*). Public health policy or national program addressing these concerns is not available. The cost of treatment/ management is high and causes considerable financial burden to the individuals and their families, hindering their treatment.

To address this concern, Comprehensive Rare Disease Care (CRDC) model for handling RD attainable at tertiary care teaching hospitals was planned. This model was developed at Centre for Human Genomics and Counselling (CHGC) services for screening and diagnosis of rare diseases at JSS Medical College and Hospital, using a project management cycle framework. The experience of establishment and significant outcomes of this model are delineated in this manuscript.

4. Purpose and distinctiveness of CRDC model in comparison with established genetic services of apex centers in India

In 2015, around 40 Clinical geneticists were practicing all over India in 13 different premier cities like New Delhi, Lucknow, and Vellore etc. as a separate department or units under the pediatrics department. They are functioning as per Medical Council of India Regulations (*7*). Once genetic causation is suspected, most of the cases are refereed to these centers, which are obviously a strain on the meager resources. With the existing immense caseload across the nation, these centers and geneticists would be inadequate.

This CRDC model is expected to bridge this gap by attending the patients/families suspected or affected with genetic etiology in specialty departments and connect them with apex centers when necessary, cost cutting the burden associated with unnecessary visits. It was built in line with guidelines and recommendations of successful working models in other specialties (*8*).

5. Experience in establishing CRDC model

Since many of the genetic diseases present immediately after birth of children, Department of Pediatrics was chosen to be the work setting to initiate the CRDC model at tertiary care hospitals (*9*). The center utilized the existing expertise of the institute by obtaining necessary training at apex centers. Meticulous planning and designing with a clear vision of operation, interdisciplinary framework and utilization of available resources were key highlights of the model. Needs assessment aided obtaining baseline data on prevalence and pattern of suspected genetic disorders in this region. This helped to prioritize the investigations to be initiated. Visits to apex centers and discussions with expertise facilitated this stage. The multidisciplinary planning team included representation from the departments of Hospital Administration, Anatomy, Biochemistry, Pathology, Radiology, Pediatrics, Obstetrics and Gynecology. The workflow and standard operating procedure were defined by a team of experts.

Prerequisites for establishing CHGC under CRDC model:

i) Pre-Conception and Pre-Natal Diagnostic Techniques (PCPNDT) act registration: provides regulatory guidelines for genetic counseling centers, genetic laboratories, clinics, regulations for prenatal diagnostic procedures and registration guidelines. Permission decisions must be taken keeping futuristic goals in mind.

ii) Manpower: a) Essential minimum requirement: An inhouse Pediatrician trained in clinical geneticsa genetic counselor b) Ideal situation: Department of Medical genetics with clinical geneticist and genetic counselor.

iii) Consent forms: for genetic tests and procedures, usage of familial information in clinical diagnosis, permission for getting clinical photography and video recording, including for research and publication purposes (*10*).

iv) Documentation and Record Maintenance: The outcome of genetics consultations are not just applicable to individuals, but also families, and have potential significance for future generations as well. Preferably records should be maintained indefinitely except in certain circumstances where the information will be of minimal importance to future interaction with the patient or other members of the family (*11*).

Before inception, communication was sent to all clinical departments and announced through mass media to sensitize the nature and scope of work, to ensure prompt referrals. A biweekly clinic, dedicated to the detailed assessment of new cases and follow - up of the registered cases was planned. Staffing comprised of a multidisciplinary team including genetic counselor, trained pediatrician, hospital administrator, staff nurse, medico social worker. The team was reinforced with experts from laboratory and researchers working for projects in genetics. One faculty in each speciality department was assigned to address the patients requiring referrals (to narrow down the clinical diagnosis & correlation with investigations). The upgradation and

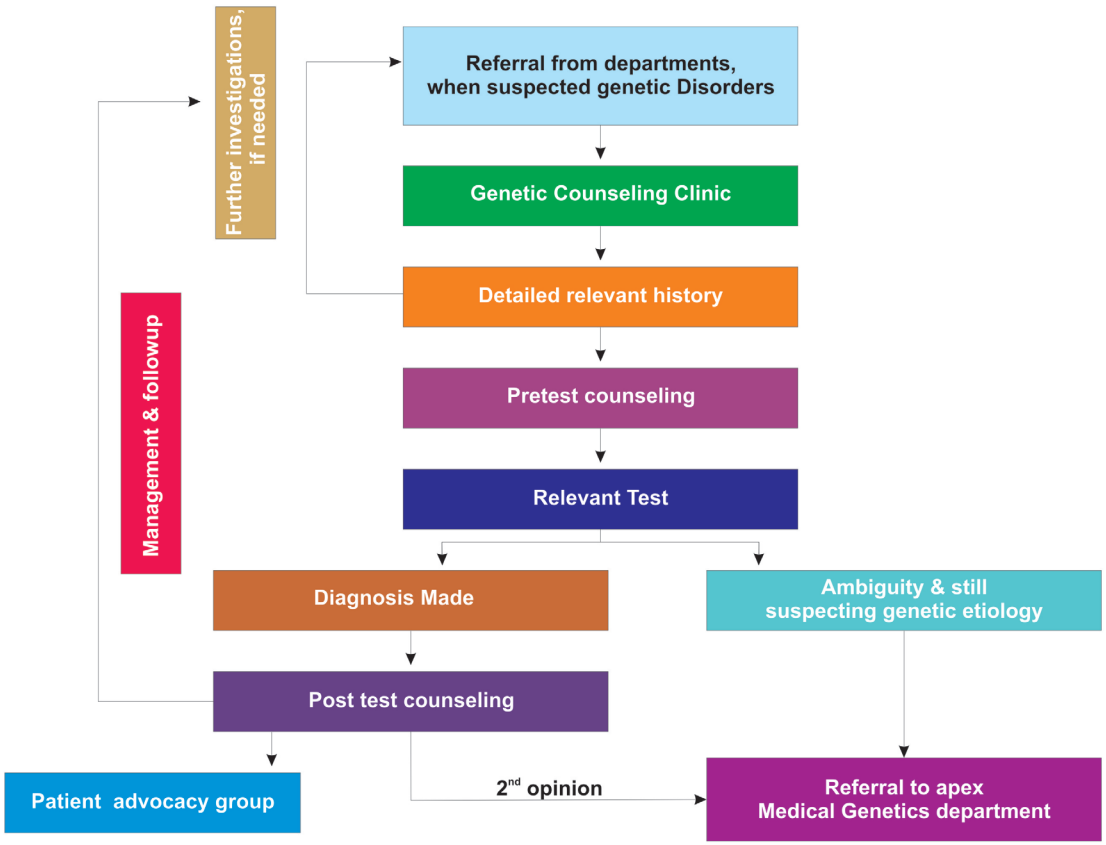

Figure 1. Process flow of the Center for Human Genomics and Counseling (CHGC) under Comprehensive Rare Disease Care (CRDC) model.

strengthening of existing lab facilities in biochemistry, pathology (fetal autopsy) microbiology, speech & hearing, occupational therapy, physiotherapy, physical & rehabilitation center were done.

The workflow of the CHGC under the CRDC model is depicted in Figure 1. The consultant/Proband with suspected or confirmed genetic etiology referred from specialty departments will be evaluated by a Genetic counselor. The clinical proforma records socio-demographic details, pedigree, occupational and exposure history. Detailed birth and clinical history, examination, primary investigations, and differential diagnosis are documented. The pathway of care also records the sequence of healthcare providers accessed prior to being evaluated in the clinic and source of referral to the center. The average assessment time for a single patient during pretest counseling was 45 min. After a detailed assessment, the case will be discussed with the consultant wherever necessary to verify the differential diagnosis, discuss if further investigation is required to obtain more phenotype details. Pretest counseling will be done explaining the probable diagnosis, need for testing and its details. The necessary genetic tests will be offered in accord with the clinician. The principles of genetic counseling *i.e.* autonomy, non-directiveness, and confidentiality are strictly adhered to at every level. The Turn Around Time (TAT) varies from 10 days to 8 weeks, depending on the type of investigation sent.

Once the reports are available, they are called for post-test counseling depending on the outcome. The number of sessions required varies from case to case. If the confirmatory diagnosis was established, a further management plan is drawn up and discussed. If the reports are inconclusive or ambiguous, further evaluation is suggested. Referrals are sent to apex centers wherever needed. The follow up and monitoring of confirmed cases are continued as required. The psychosocial interventions, support through advocacy groups, coping strategies, and quality of life were addressed. Extended family evaluation is done if necessary. Additionally they are directed to Patient Advocacy groups and Non-Government Organizations (ex: Organization for Rare Disease India) for assistance on moral support, research advances, clinical trials, and education with awareness.

The outcome of CHGC under the CRDC model is depicted by the case statistics in Figure 2. The patient inflow gradually picked up due to availability of accessible genetic services avoiding concerns associated with reaching apex centres.

6. Challenge and perspectives

The CRDC model, though in its infancy, provides

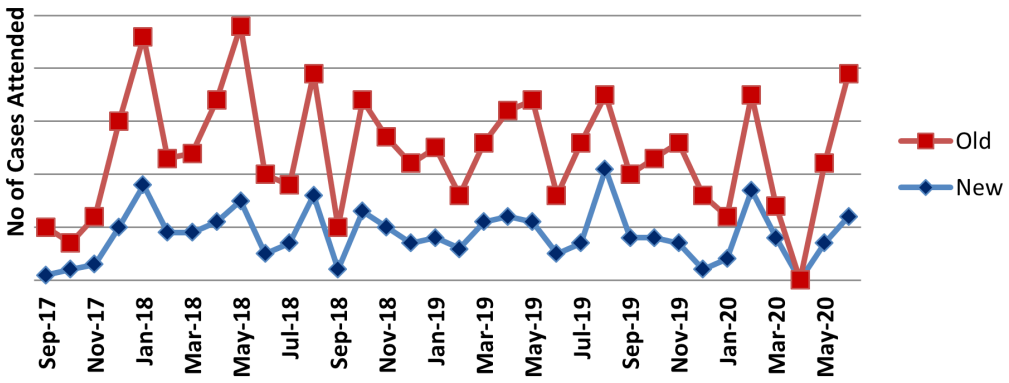

Figure 2. The outpatient statistics of New and Old cases at Human Genomics and Counseling (CHGC) since inception until date.

some opportunities and highlights key challenges. The center offers convenient one stop services to patients of surrounding districts with suspected or confirmed genetic causation. In the current Indian context of human resource supply constraints, it is scalable and can facilitate the development of locally acceptable and efficient models of care. Training the pediatricians to manage these patients in primary care and vertically integrate with such centers and first tier cities is advisable. This may pre-empt visits to specialists (especially lifelong follow-up and monitoring conditions) unless deemed necessary. The center provides opportunities for better training of healthcare personnel dealing with RD patients. The pediatric residents get extensive exposure to the varied clinical presentations, and management approaches. The training modules can be extended to other health professionals in the future. Last, such a dedicated establishment may yield better and diverse research opportunities focusing on medical genetics.

The challenges associated are a coordination of multiple stakeholders, space and infrastructure, cost-effective expansion, lack of national standardization, customization to local requirements, and shortage of manpower compared to case load. Finally, the education and training of health professionals to be medical geneticists/genetic counselors is a long way to accomplish adequate numbers.

Future Strategy is to establish a network and comprehensive system for coordination of referrals in the tiered healthcare system. Also a mechanism to raise awareness on RD among the medical fraternity and general public is to be planned.

To conclude, RDs are an essential public health concern and provide a challenge to healthcare worldwide. Provision of affordable services with preventive and palliative potential to several RDs should be a practical reality. This CRDC model could provide a cost-effective and geographically compatible model of care which vertically integrates apex centers and the primary health care system. This scalable prototype can be replicated in similar resource-constrained settings in a high prevalence geographical location.

Acknowledgements

To Departments of Paediatrics and Hospital Administration, JSS Medical College and Hospital, JSS Academy of Higher Education and Research for their exceptional support in this research.

Ethical approval: The study was approved by the institutional Ethical committee.

References

1. GUaRDIAN Consortium, Sivasubbu S, Scaria V. Genomics of rare genetic diseases-experiences from India. Hum Genomics. 2019; 14:52.
2. Verma IC. Burden of genetic disorders in India. Indian J Pediatr. 2000; 67:893-898.
3. Choudhury MC, Saberwal G. The role of patient organizations in the rare disease ecosystem in India: an interview based study. Orphanet J Rare Dis. 2019; 14:117.
4. Šimerka P. Council Recommendation of 8 June 2009 on an action in the field of rare diseases (2009/C 151/02). Official Journal of the European Union. 2009; 171:7-10.
5. Richter T, Nestler-Parr S, Babela R, Khan ZM, Tesoro T, Molsen E, Hughes DA; International Society for Pharmacoeconomics and Outcomes Research Rare Disease Special Interest Group. Rare disease terminology and definitions-a systematic global review: report of the ISPOR Rare Disease Special Interest Group. Value Health. 2015; 18:906-914.
6. Verma IC, Puri RD. Global burden of genetic disease and the role of genetic screening. Semin Fetal Neonatal Med. 2015; 20:354-363.
7. Aggarwal S, Phadke SR. Medical genetics and genomic medicine in India: current status and opportunities ahead. Mol Genet Genomic Med. 2015; 3:160-171.
8. Menon V, Sarkar S, Thomas S. Establishing a psychosomatic clinic in a low resource setting: Process, challenges, and opportunities. J Neurosci Rural Pract. 2016; 7:171-175.
9. Kumar P, Radhakrishnan J, Chowdhary MA, Giampietro PF. Prevalence and patterns of presentation of genetic disorders in a pediatric emergency department. Mayo Clin Proc. 2001; 76:777-783.

10. Mcguire A. Health Research Authority. 2010; 118. Available from: *https://www.hra.nhs.uk/planning-and-improving-research/application-summaries/research-summaries/comparing-breast-cervical-and-bowel-cancer-screening-participation* (Accessed 21 November 2018).
11. Shoenbill K, Fost N, Tachinardi U, Mendonca EA. Genetic data and electronic health records: A discussion of ethical, logistical and technological considerations. J Am Med Informatics Assoc. 2014; 21:171-180.

Received May 16, 2020; Revised July 14, 2020; Accepted July 27, 2020.

**Address correspondence to:*
Deepa Bhat, Department of Medical Genetics and Department of Anatomy, JSS Medical College & Hospital, JSS Academy of Higher Education and Research, Mysuru – 570004, Karnataka, India.
E-mail: deepabhat@jssuni.edu.in

Released online in J-STAGE as advance publication July 31, 2020.

Communication

DOI: 10.5582/irdr.2020.03025

An update on microRNAs as potential novel therapeutic targets in testicular germ cell tumors

Marco De Martino[1,2], Francesco Esposito[2], Paolo Chieffi[1,*]

[1] Dipartimento di Psicologia, Università della Campania "Luigi Vanvitelli", Caserta, Italy;
[2] Istituto di Endocrinologia ed Oncologia Sperimentale-CNR c/o Dipartimento di Medicina Molecolare e Biotecnologie Mediche, Università degli Studi di Napoli "Federico II", Napoli, Italy.

SUMMARY Testicular germ cell tumors (TGCTs) are the most frequent solid malignant tumors in men 20-40 years of age and the most frequent cause of death from solid tumors in this age group. Recent studies have underscored the fact that miRNA deregulation is a feature of carcinogenesis, including TGCT development and progression. MiRNAs are a group of small noncoding RNAs that bind to the 3′-untranslated region (UTR) of the targeted mRNAs, thus causing mRNA degradation or the inhibition of its translation, regulating gene expression in a temporal and tissue-specific manner. However, few miRNAs have been found to play key roles in TGCTs; recently, other miRNAs have been identified, representing novel potential therapeutic targets.

Keywords HMGA1, microRNA, testicular germ cell tumor (TGCT), seminoma

Among solid tumors, testicular germ cell tumors (TGCTs) have the highest incidence among young men (between 20 and 34 years of age), and their incidence has increased over the past few decades. TGCTs have their origin in a blocked maturation of primordial germ cells (PGCs) (*1-3*), and more evidence has reinforced the idea that an alteration of epigenetic status is able to initiate human malignant germ cell tumors and to do so in the place of somatic mutations. This clarifies the role of both genetic susceptibility and environmental factors, known as the 'geno-environment', in TGCTs (*4-9*). About 90% of TGCTs are successfully treated with cisplatin-based chemotherapy. However, this form of therapy can lead to secondary cancers and cardiovascular disease. TGCTs are classified into two principal groups: germ cell neoplasias *in situ* (GCNIS) that are seminomas or nonseminomas (NSE), and spermatocytic tumors that are not GCNIS. NSE tumors encompass embryonal carcinoma, choriocarcinoma, yolk sac tumors (YSTs), and teratoma. TGCTs may develop from a non-invasive type of tumor called carcinoma *in situ* (CIS): microscopy reveals abnormal cells even though they are still confined inside the membrane of the seminiferous tubules (*10-14*).

MicroRNAs (miRNAs) are short non-coding RNA fragments that, by binding to the 3′UTR, are able to negatively regulate gene transcripts (*15*). Thus, recent studies have underscored the fact that miRNA deregulation is a feature of carcinogenesis, including TGCT development and progression (*16-19*). Although different miRNA signatures are associated with histological subtypes of TGCTs, various miRNAs have been found to play a key role in TGCTs. Voorhoeve *et al*. reported that two miRNAs (miR-372 and miR-373) can escape the cell cycle arrest induced by p53 (*20*). Indeed, these two miRNAs were not expressed or only slightly expressed in TGCT-derived cell lines where p53 was mutated or downregulated, indicating that miR-372 and miR-373 induce TGCT growth to elude the p53 checkpoint of the cell cycle. In this context, several data suggest that miR-372 and miR-373 may act as oncogenes in TGCTs through the inhibition of LATS2, a tumor suppressor gene (*20*). Dieckmann *et al*. confirmed that serum levels of microRNA (miR)-371a-3p (a so-called M371 test) are better than the standard markers of GCT with the same level of sensitivity and a specificity of around 90% (*21*).

Moreover, Ozata *et al*. found that PEG3 mRNA can be strongly suppressed by the action of miR-514a-3p, inducing apoptosis. In particular, levels of PEG3 expression are elevated in TGCTs where the expression of miR-514a-3p is lacking (*22*).

Recent studies have reported that the deregulation of miRNA expression in cancer cells can modify the tumor microenvironment, inducing cancer progression. However, this mechanism has yet to be elucidated in TGCTs. Recent research has found that epigenetic modifications downregulate miR-125b in

TGCT samples. Indeed, xenograft models of TGCTs indicated that miR-125b plays a key role in tumor-stroma crosstalk, underscoring its tumor suppressor role and the possibility of using miR-125b as an miRNA therapeutic (*23*).

Intriguingly, both Let-7a and miR-26a were found to be downregulated in several human cancer types, acting as tumor suppressor miRNAs (*24,25*). Moreover, these miRNAs inhibited cell proliferation and invasiveness of malignant melanoma derived-cell lines, suggesting that miR-26a and Let-7a may represent novel therapies for melanoma (*26)*. Indeed, Let-7 is able to repress several oncogenes such as MYCN, AURKB, CCNF, RRM2, MKI67, and C12orf5 in TGCTs (*27*). A previous study determined that mitotic cells (spermatogonia and primary spermatocytes) express HMGA1, while HMGA2 is highly expressed in meiotic and postmeiotic cells (secondary spermatocytes and spermatids) (*28,29*). In addition, other studies have demonstrated that the expression of HMGA1 and HMGA2 plays a key role in TGCT tumorigenesis and that the two can serve as a helpful diagnostic tool when the histological differential diagnosis is in question (*30-36*). In particular, HMGA1 protein is overexpressed in human seminomas.

Recently, De Martino and colleagues found that Let-7a and miR-26a are downregulated in human seminoma, with levels negatively correlating with *HMGA1*. In addition, they found that *HMGA1* is a target of Let-7a and miR-26a in seminomas and that Let-7a and miR-26a are able to inhibit seminoma cell growth and motility. Intriguingly, since miRNAs may act on several target transcripts that share the same microRNA responsive element (MRE) inhibitory action, a topic of great interest would be to study the transcriptomic effects of Let-7a and miR-26a overexpression in seminoma-derived cell lines using RNA-seq analysis in order to obtain a broader portrait of overall changes in levels of gene expression (*37*).

The study of the deregulated molecular pathways in TGCTs has now led to the development of successful clinical approaches. Indeed, most patients with TGCTs respond well to cisplatin-based chemotherapy. However, several patients have developed chemoresistance to first-line treatments for TGCTs. Therefore, new therapies based on novel strategies could increase the potential to treat cisplatin-resistant patients and limit adverse drug reactions. Interestingly, the ability of Let-7a and miR-26a to prevent seminoma cell growth could lead to new insights in therapeutic perspectives. In fact, modern forms of therapy may originate from the restoration of normal Let-7a and miR-26a levels in seminomas *via* the administration of synthetic miRNA oligonucleotides.

References

1. Chieffi P. Molecular targets for the treatment of testicular germ cell tumors. Mini Rev Med Chem. 2007; 7:755-759.
2. Lobo J, Gillis AJM, Jerónimo C, Henrique R, Looijenga LHJ. Human germ cell tumors are developmental cancers: Impact of epigenetics on pathobiology and clinic. Int J Mol Sci. 2019; 20: 258.
3. Franco R. Boscia F, Gigantino V, Marra L, Esposito F, Ferrara D, Pariante P, Botti G, Caraglia M, Minucci S, Chieffi P. GPR30 is overexpressed in post-puberal testicular germ cell tumors. Cancer Biol Ther. 2011; 11: 609-613.
4. Chieffi P, Chieffi S, Franco R, Sinisi AA. Recent advances in the biology of germ cell tumors: Implications for the diagnosis and treatment. J Endocrinol Invest. 2012; 35:1015-1020.
5. Chieffi P, Chieffi S. Molecular biomarkers as potential targets for therapeutic strategies in human testicular germ cell tumours: an overview. J Cell Physiol. 2013; 22:1641-1646.
6. Chieffi P, Chieffi S. An up-date on newly discovered immunohistochemical biomarkers for the diagnosis of human testicular germ cell tumors. Histol Histopathol. 2014; 29:999-1006.
7. Chieffi P. An overview on predictive biomarkers of testicular germ cell tumors. J Cell Physiol. 2017; 232:276-280.
8. Boscia F, Passaro C, Gigantino V, Perdonà S, Franco R, Portella G, Chieffi S, Chieffi P. High levels of GPR30 protein in human testicular carcinoma *in situ* and seminomas correlate with low levels of estrogen receptor-beta and indicate a switch in estrogen responsiveness. J Cell Physiol. 2015; 230:1290-1297.
9. Chieffi P, De Martino M, Esposito F. Further insights into testicular germ cell tumor oncogenesis: Potential therapeutic targets. Expert Rev Anticancer Ther. 2020; 20:189-195.
10. Vicini E, Loiarro M, Di Agostino S, Corallini S, Capolunghi F, Carsetti R, Chieffi P, Geremia R, Stefanini M, Sette C. 17-β-estradiol elicits genomic and non-genomic responses in mouse male germ cells. J Cell Physiol. 2006; 206:238-245.
11. Pero R, Lembo F, Chieffi P, Del Pozzo G, Fedele M, Fusco A, Bruni CB, Chiariotti L. Translational regulation of a novel testis-specific RNF4 transcript. Mol Reprod Dev. 2003; 66:1-7.
12. Picascia A, Stanzione R, Chieffi P, Kisslinger A, Dikic I, Tramontano D. Proline-rich tyrosine kinase 2 regulates proliferation and differentiation of prostate cells. Mol Cell Endocrinol. 2002; 186:81-87.
13. Sinisi AA, Chieffi P, Pasquali D, Kisslinger A, Staibano S, Bellastella A, Tramontano D. EPN: a novel epithelial cell line derived from human prostate tissue. *In Vitro* Cell Dev Biol Anim. 2002; 38:165–172.
14. Marra L, Cantile M, Scognamiglio G, Perdonà S, La Mantia E, Cerrone M, Gigantino V, Cillo C, Caraglia M, Pignata S, Facchini G, Botti G, Chieffi S, Chieffi P, Franco R. Deregulation of HOX B13 expression in urinary bladder cancer progression. Curr Med Chem. 2013; 20:833-839.
15. Forzati F, De Martino M, Esposito F, Sepe R, Pellecchia S, Malapelle U, Pellino G, Arra C, Fusco A. miR-155 is positively regulated by CBX7 in mouse embryonic fibroblasts and colon carcinomas, and targets the KRAS oncogene. BMC Cancer. 2017; 17:170.
16. Wang L, Xu C. Role of microRNAs in mammalian spermatogenesis and testicular germ cell tumours. Reproduction. 2015; 149:R127- R137.

17. Lu J, Getz G, Miska EA, Alvarez-Saavedra E, Lamb J, Peck D, Sweet-Cordero A, Ebert BL, Mak RH, Ferrando AA, Downing JR, Jacks T, Horvitz HR, Golub TR. MicroRNA expression profiles classify human cancers. Nature. 2005; 435:834–838.
18. Calin GA, Ferracin M, Cimmino A, Di Leva G, Shimizu M, Wojcik SE, Iorio MV, Visone R, Sever NI, Fabbri M, Iuliano R, Palumbo T, Pichiorri F, Roldo C, Garzon R, Sevignani C, Rassenti L, Alder H, Volinia S, Liu CG, Kipps TJ, Negrini M, Croce CM. A MicroRNA signature associated with prognosis and progression in chronic lymphocytic leukemia. N Engl J Med. 2005; 353:1793-1801.
19. Rounge TB, Furu K, Skotheim RI, Haugen TB, Grotmol T, Enerly E. Profiling of the small RNA populations in human testicular germ cell tumours shows global loss of piRNAs. Mol Cancer. 2015; 14:153.
20. Voorhoeve PM. le Sage C, Schrier M, Gillis AJ, Stoop H, Nagel R, Liu YP, van Duijse J, Drost J, Griekspoor A, Zlotorynski E, Yabuta N, De Vita G, Nojima H, Looijenga LH, Agami R. A genetic screen implicates miRNA-372 and miRNA-373 as oncogenes in testicular germ cell tumors. Cell. 2006; 124:1169-1181.
21. Dieckmann KP, Radtke A, Geczi L, Matthies C, Anheuser P, Eckardt U, Sommer J, Zengerling F, Trenti E, Pichler R, Belz H, Zastrow S, Winter A, Melchior S, Hammel J, Kranz J, Bolten M, Krege S, Haben B, Loidl W, Ruf CG, Heinzelbecker J, Heidenreich A, Cremers JF, Oing C, Hermanns T, Fankhauser CD, Gillessen S, Reichegger H, Cathomas R, Pichler M, Hentrich M, Eredics K, Lorch A, Wülfing C, Peine S, Wosniok W, Bokemeyer C, Belge G. Serum levels of MicroRNA-371a-3p (M371 test) as a new biomarker of testicular germ cell tumours: Results of a prospective multicentric study. J Clin Oncol. 2019; 37:1412-1423.
22. Ozata DM, Li X, Lee L, Liu J, Warsito D, Hajeri P, Hultman I, Fotouhi O, Marklund S, Ahrlund-Richter L, Juhlin CC, Larsson C, Lui WO. Loss of miR-514a-3p regulation of PEG3 activates the NF-kappa B pathway in human testicular germ cell tumors. Cell Death Dis. 2017; 8:e2759.
23. Batool A, Wang YQ, Hao XX, Chen SR, Liu YX. A miR-125b/CSF1-CX3CL1/tumor-associated macrophage recruitment axis controls testicular germ cell tumor growth. Cell Death Dis. 2018; 9:962.
24. Yang X, Zhang XF, Lu X, Jia HL, Liang L, Dong QZ, Ye QH, Qin LX. MicroRNA-26a suppresses angiogenesis in human hepatocellular carcinoma by targeting hepatocyte growth factor-cMet pathway. Hepatology. 2014; 59: 1874-1885.
25. Mi Y, Liu F, Liang X, Liu S, Huang X, Sang M, Geng C. Tumor suppressor let-7a inhibits breast cancer cell proliferation, migration and invasion by targeting MAGE-A1. Neoplasma. 2019; 66:54-62.
26. Qian H, Yang C, Yang Y. MicroRNA-26a inhibits the growth and invasiveness of malignant melanoma and directly targets on MITF gene. Cell Death Discov. 2017; 3:17028.
27. Murray MJ, Saini HK, Siegler CA, Hanning JE, Barker EM, van Dongen S, Ward DM, Raby KL, Groves IJ Scarpini CG, Pett MR, Thornton CM, Enright AJ, Nicholson JC, Coleman N CCLG. LIN28 Expression in malignant germ cell tumors downregulates let-7 and increases oncogene levels. Cancer Res. 2013; 73:4872-4884.
28. Chieffi P, Battista S, Barchi M, Di Agostino S, Pierantoni G, Fedele M, Chiariotti L, Tramontano D, Fusco A. HMGA1 and HMGA2 protein expression in mouse spermatogenesis. Oncogene. 2002; 21:3644-3650.
29. Di Agostino S, Fedele M, Chieffi P, Fusco A, Rossi P, Geremia R, Sette C. Phosphorylation of high mobility group protein A2 by Nek2 kinase during the first meiotic division in mouse spermatocytes. Mol Biol Cell. 2004; 15:1224-1232.
30. Franco R, Esposito F, Fedele M, Liguori G, Pierantoni G, Botti G, Tramontano D, Fusco A, Chieffi P. Detection of high mobility group proteins A1 and A2 represents a valid diagnostic marker in post-puberal testicular germ cell tumours. J Pathol. 2008; 214:58-64.
31. Esposito F, Boscia F, Gigantino V, Tornincasa M, Fusco A, Franco R, Chieffi P. The high mobility group A1-oestrogen receptor β nuclear interaction is impaired in human testicular seminomas. J Cell Physiol. 2012; 227:3749-3755.
32. Chieffi P, De Martino M, Esposito F. New anti-cancer strategies in testicular germ cell tumors. Recent Pat Anticancer Drug Discov. 2019; 14:53-59.
33. Chieffi P. Recent advances in molecular and cell biology of testicular germ-cell tumors. Int Rev Cell Mol Biol. 2014; 312:79-100.
34. De Martino M, Fusco A, Esposito F. HMGA and cancer: A review on patent literatures. Recent Pat Anticancer Drug Discov. 2019; 14:258-267.
35. Chieffi P. An up-date on epigenetic and molecular markers in testicular germ cell tumors. Intractable Rare Dis Res. 2017; 6:319-321.
36. Chieffi P. An up-date on novel molecular targets in testicular germ cell tumors subtypes. Intractable Rare Dis Res. 2019; 8:161-164.
37. De Martino M, Esposito F, Pellecchia S, Cardoso Penha RC, Botti G, Fusco A, Chieffi P. HMGA1-Regulating microRNAs Let-7a and miR-26a are downregulated in human seminomas. Int J Mol Sci. 2020; 21:3014. doi: 10.3390/ijms21083014.

Received April 27, 2020; Accepted May 30, 2020.

*Address correspondence to:
Paolo Chieffi, Dipartimento di Psicologia, Università della Campania "Luigi Vanvitelli", Caserta, 31 81100 Caserta, Italy.
E-mail: paolo.chieffi@unicampania.it

Released online in J-STAGE as advance publication June 4, 2020.

IRDR
Intractable & Rare Diseases Research

Guide for Authors

1. Scope of Articles

Intractable & Rare Diseases Research (Print ISSN 2186-3644, Online ISSN 2186-361X) is an international peer-reviewed journal. Intractable & Rare Diseases Research devotes to publishing the latest and most significant research in intractable and rare diseases. Articles cover all aspects of intractable and rare diseases research such as molecular biology, genetics, clinical diagnosis, prevention and treatment, epidemiology, health economics, health management, medical care system, and social science in order to encourage cooperation and exchange among scientists and clinical researchers.

2. Submission Types

Original Articles should be well-documented, novel, and significant to the field as a whole. An Original Article should be arranged into the following sections: Title page, Abstract, Introduction, Materials and Methods, Results, Discussion, Acknowledgments, and References. Original articles should not exceed 5,000 words in length (excluding references) and should be limited to a maximum of 50 references. Articles may contain a maximum of 10 figures and/or tables. Supplementary Data are permitted but should be limited to information that is not essential to the general understanding of the research presented in the main text, such as unaltered blots and source data as well as other file types.

Brief Reports definitively documenting either experimental results or informative clinical observations will be considered for publication in this category. Brief Reports are not intended for publication of incomplete or preliminary findings. Brief Reports should not exceed 3,000 words in length (excluding references) and should be limited to a maximum of 4 figures and/or tables and 30 references. A Brief Report contains the same sections as an Original Article, but the Results and Discussion sections should be combined.

Reviews should present a full and up-to-date account of recent developments within an area of research. Normally, reviews should not exceed 8,000 words in length (excluding references) and should be limited to a maximum of a maximum of 10 figures and/or tables and 100 references. Mini reviews are also accepted, which should not exceed 4,000 words in length (excluding references) and should be limited to a maximum of 5 figures and/or tables and 50 references.

Policy Forum articles discuss research and policy issues in areas related to life science such as public health, the medical care system, and social science and may address governmental issues at district, national, and international levels of discourse. Policy Forum articles should not exceed 3,000 words in length (excluding references) and should be limited to a maximum of 5 figures and/or tables and 30 references.

Case Reports should be detailed reports of the symptoms, signs, diagnosis, treatment, and follow-up of an individual patient. Case reports may contain a demographic profile of the patient but usually describe an unusual or novel occurrence. Unreported or unusual side effects or adverse interactions involving medications will also be considered. Case Reports should not exceed 3,000 words in length (excluding references) and should be limited to a maximum of 5 figures and/or tables and 30 references.

Communications are short, timely pieces that spotlight new research findings or policy issues of interest to the field of global health and medical practice that are of immediate importance. Depending on their content, Communications will be published as "Comments" or "Correspondence". Communications should not exceed 1,500 words in length (excluding references) and should be limited to a maximum of 2 figures and/or tables and 20 references.

Editorials are short, invited opinion pieces that discuss an issue of immediate importance to the fields of global health, medical practice, and basic science oriented for clinical application. Editorials should not exceed 1,000 words in length (excluding references) and should be limited to a maximum of 10 references. Editorials may contain one figure or table.

News articles should report the latest events in health sciences and medical research from around the world. News should not exceed 500 words in length.

Letters should present considered opinions in response to articles published in *Intractable & Rare Diseases Research* in the last 6 months or issues of general interest. Letters should not exceed 800 words in length and may contain a maximum of 10 references. Letters may contain one figure or table.

3. Editorial Policies

For publishing and ethical standards, *Intractable & Rare Diseases Research* follows the Recommendations for the Conduct, Reporting, Editing, and Publication of Scholarly Work in Medical Journals (*http://www.icmje.org/recommendations*) issued by the International Committee of Medical Journal Editors (ICMJE), and the Principles of Transparency and Best Practice in Scholarly Publishing (*https://doaj.org/bestpractice*) jointly issued by the Committee on Publication Ethics (COPE), the Directory of Open Access Journals (DOAJ), the Open Access Scholarly Publishers Association (OASPA), and the World Association of Medical Editors (WAME).

Intractable & Rare Diseases Research will perform an especially prompt review to encourage innovative work. All original research will be subjected to a rigorous standard of peer review and will be edited by experienced copy editors to the highest standards.

Ethics: *Intractable & Rare Diseases Research* requires that authors of reports of investigations in humans or animals indicate that those studies were formally approved by a relevant ethics committee or review board. For research involving human experiments, a statement that the participants gave informed consent before taking part (or a statement that it was not required and why) should be indicated. Authors should also state that the study conformed to the provisions of the Declaration of Helsinki (as revised in 2013). When reporting experiments on animals, authors should indicate whether

the institutional and national guide for the care and use of laboratory animals was followed.

Conflict of Interest: All authors are required to disclose any actual or potential conflict of interest including financial interests or relationships with other people or organizations that might raise questions of bias in the work reported. If no conflict of interest exists for each author, please state "There is no conflict of interest to disclose".

Submission Declaration: When a manuscript is considered for submission to *Intractable & Rare Diseases Research*, the authors should confirm that 1) no part of this manuscript is currently under consideration for publication elsewhere; 2) this manuscript does not contain the same information in whole or in part as manuscripts that have been published, accepted, or are under review elsewhere, except in the form of an abstract, a letter to the editor, or part of a published lecture or academic thesis; 3) authorization for publication has been obtained from the authors' employer or institution; and 4) all contributing authors have agreed to submit this manuscript.

Cover Letter: The manuscript must be accompanied by a cover letter prepared by the corresponding author on behalf of all authors. The letter should indicate the basic findings of the work and their significance. The letter should also include a statement affirming that all authors concur with the submission and that the material submitted for publication has not been published previously or is not under consideration for publication elsewhere. The cover letter should be submitted in PDF format. For example of Cover Letter, please visit: Download Centre (*https://www.irdrjournal.com/downcentre*).

Copyright: When a manuscript is accepted for publication in *Intractable & Rare Diseases Research*, the transfer of copyright is necessary. A JOURNAL PUBLISHING AGREEMENT (JPA) form will be e-mailed to the authors by the Editorial Office and must be returned by the authors as a scan. Only forms with a hand-written signature are accepted. This copyright will ensure the widest possible dissemination of information. Please note that your manuscript will not proceed to the next step in publication until the JPA Form is received. In addition, if excerpts from other copyrighted works are included, the author(s) must obtain written permission from the copyright owners and credit the source(s) in the article.

Peer Review: *Intractable & Rare Diseases Research* uses single-blind peer review, which means that reviewers know the names of the authors, but the authors do not know who reviewed their manuscript. The external peer review is performed for research articles by at least two reviewers, and sometimes the opinions of more reviewers are sought. Peer reviewers are selected based on their expertise and ability to provide high quality, constructive, and fair reviews. For research manuscripts, the editors may, in addition, seek the opinion of a statistical reviewer. Consideration for publication is based on the article's originality, novelty, and scientific soundness, and the appropriateness of its analysis.

Suggested Reviewers: A list of up to 3 reviewers who are qualified to assess the scientific merit of the study is welcomed. Reviewer information including names, affiliations, addresses, and e-mail should be provided at the same time the manuscript is submitted online. Please do not suggest reviewers with known conflicts of interest, including participants or anyone with a stake in the proposed research; anyone from the same institution; former students, advisors, or research collaborators (within the last three years); or close personal contacts. Please note that the Editor-in-Chief may accept one or more of the proposed reviewers or may request a review by other qualified persons.

Language Editing: Manuscripts prepared by authors whose native language is not English should have their work proofread by a native English speaker before submission. If not, this might delay the publication of your manuscript in *Intractable & Rare Diseases Research*.

The Editing Support Organization can provide English proofreading, Japanese-English translation, and Chinese-English translation services to authors who want to publish in *Intractable & Rare Diseases Research* and need assistance before submitting a manuscript. Authors can visit this organization directly at *http://www.iacmhr.com/iac-eso/support.php?lang=en*. IAC-ESO was established to facilitate manuscript preparation by researchers whose native language is not English and to help edit works intended for international academic journals.

4. Manuscript Preparation

Manuscripts are suggested to be prepared in accordance with the "Recommendations for the Conduct, Reporting, Editing, and Publication of Scholarly Work in Medical Journals", as presented at *http://www.ICMJE.org.*

Manuscripts should be written in clear, grammatically correct English and submitted as a Microsoft Word file in a single-column format. Manuscripts must be paginated and typed in 12-point Times New Roman font with 24-point line spacing. Please do not embed figures in the text. Abbreviations should be used as little as possible and should be explained at first mention unless the term is a well-known abbreviation (*e.g.* DNA). Single words should not be abbreviated.

Title page: The title page must include 1) the title of the paper (Please note the title should be short, informative, and contain the major key words); 2) full name(s) and affiliation(s) of the author(s), 3) abbreviated names of the author(s), 4) full name, mailing address, telephone/fax numbers, and e-mail address of the corresponding author; and 5) conflicts of interest (if you have an actual or potential conflict of interest to disclose, it must be included as a footnote on the title page of the manuscript; if no conflict of interest exists for each author, please state "There is no conflict of interest to disclose"). Please visit Download Centre and refer to the title page of the manuscript sample.

Abstract: The abstract should briefly state the purpose of the study, methods, main findings, and conclusions. For articles that are Original Articles, Brief Reports, Reviews, Policy Forum articles, or Case Report, a one-paragraph abstract consisting of no more than 250 words must be included in the manuscript. For Communications, Editorials, News, or Letters, a brief summary of main content in 150 words or fewer should be included in the manuscript. Abbreviations must be kept to a minimum and non-standard abbreviations explained in brackets at first mention. References should be avoided in the abstract. Three to six key words or phrases that do not occur in the title should be included in the Abstract page.

Introduction: The introduction should be a concise statement of the basis for the study and its scientific context.

Materials and Methods: The description should be brief but with sufficient detail to enable others to reproduce the experiments. Procedures that have been published previously should not be described in detail but appropriate references should simply be cited. Only new and significant modifications of previously published procedures require complete description. Names of products and manufacturers with their locations (city and state/country) should be given and sources of animals and cell lines should always be indicated. All clinical investigations must have been conducted in accordance with Declaration of Helsinki principles. All human and animal studies must have been approved by the appropriate institutional review board(s) and a specific declaration of approval must be made within this section.

Results: The description of the experimental results should be succinct but in sufficient detail to allow the experiments to be analyzed and interpreted by an independent reader. If necessary, subheadings may be used for an orderly presentation. All figures and tables must be referred to in the text.

Discussion: The data should be interpreted concisely without repeating material already presented in the Results section. Speculation is permissible, but it must be well-founded, and discussion of the wider implications of the findings is encouraged. Conclusions derived from the study should be included in this section.

Acknowledgments: All funding sources should be credited in the Acknowledgments section. In addition, people who contributed to the work but who do not meet the criteria for authors should be listed along with their contributions.

References: References should be numbered in the order in which they appear in the text. Citing of unpublished results, personal communications, conference abstracts, and theses in the reference list is not recommended but these sources may be mentioned in the text. In the reference list, cite the names of all authors when there are fifteen or fewer authors; if there are sixteen or more authors, list the first three followed by *et al*. Names of journals should be abbreviated in the style used in PubMed. Authors are responsible for the accuracy of the references. The EndNote Style of *Intractable & Rare Diseases Research* could be downloaded at **EndNote** (*https://www.irdrjournal.com/examples/Intractable_Rare_Diseases_Research.ens*).

Examples are given below:

Example 1 (Sample journal reference):

Inagaki Y, Tang W, Zhang L, Du GH, Xu WF, Kokudo N. Novel aminopeptidase N (APN/CD13) inhibitor 24F can suppress invasion of hepatocellular carcinoma cells as well as angiogenesis. Biosci Trends. 2010; 4:56-60.

Example 2 (Sample journal reference with more than 15 authors):

Darby S, Hill D, Auvinen A, *et al*. Radon in homes and risk of lung cancer: Collaborative analysis of individual data from 13 European case-control studies. BMJ. 2005; 330:223.

Example 3 (Sample book reference):
Shalev AY. Post-traumatic stress disorder: Diagnosis, history and life course. In: Post-traumatic Stress Disorder, Diagnosis, Management and Treatment (Nutt DJ, Davidson JR, Zohar J, eds.). Martin Dunitz, London, UK, 2000; pp. 1-15.

Example 4 (Sample web page reference):

World Health Organization. The World Health Report 2008 – primary health care: Now more than ever. *http://www.who.int/whr/2008/whr08_en.pdf* (accessed September 23, 2010).

Tables: All tables should be prepared in Microsoft Word or Excel and should be arranged at the end of the manuscript after the References section. Please note that tables should not in image format. All tables should have a concise title and should be numbered consecutively with Arabic numerals. If necessary, additional information should be given below the table.

Figure Legend: The figure legend should be typed on a separate page of the main manuscript and should include a short title and explanation. The legend should be concise but comprehensive and should be understood without referring to the text. Symbols used in figures must be explained. Any individually labeled figure parts or panels (A, B, *etc*.) should be specifically described by part name within the legend.

Figure Preparation: All figures should be clear and cited in numerical order in the text. Figures must fit a one- or two-column format on the journal page: 8.3 cm (3.3 in.) wide for a single column, 17.3 cm (6.8 in.) wide for a double column; maximum height: 24.0 cm (9.5 in.). Please make sure that the symbols and numbers appeared in the figures should be clear. Please make sure that artwork files are in an acceptable format (TIFF or JPEG) at minimum resolution (600 dpi for illustrations, graphs, and annotated artwork, and 300 dpi for micrographs and photographs). Please provide all figures as separate files. Please note that low-resolution images are one of the leading causes of article resubmission and schedule delays.

Units and Symbols: Units and symbols conforming to the International System of Units (SI) should be used for physicochemical quantities. Solidus notation (*e.g*. mg/kg, mg/mL, mol/mm^2/min) should be used. Please refer to the SI Guide *www.bipm.org/en/si/* for standard units.

Supplemental data: Supplemental data might be useful for supporting and enhancing your scientific research and *Intractable & Rare Diseases Research* accepts the submission of these materials which will be only published online alongside the electronic version of your article. Supplemental files (figures, tables, and other text materials) should be prepared according to the above guidelines, numbered in Arabic numerals (*e.g*., Figure S1, Figure S2, and Table S1, Table S2) and referred to in the text. All figures and tables should have titles and legends. All figure legends, tables and supplemental text materials should be placed at the end of the paper. Please note all of these supplemental data should be provided at the time of initial submission and note that the editors reserve the right to limit the size and length of Supplemental Data.

5. Submission Checklist

The Submission Checklist will be useful during the final checking of a manuscript prior to sending it to *Intractable & Rare Diseases Research* for review. Please visit Download Centre and download the Submission Checklist file.

6. Online Submission

Manuscripts should be submitted to *Intractable & Rare Diseases Research* online at *https://www.irdrjournal.com*. The manuscript file should be smaller than 5 MB in size. If for any reason you are unable to submit a file online, please contact the Editorial Office by e-mail at *office@irdrjournal.com*

7. Accepted Manuscripts

Proofs: Galley proofs in PDF format will be sent to the corresponding author *via* e-mail. Corrections must be returned to the editor (*office@irdrjournal.com*) within 3 working days.

Offprints: Authors will be provided with electronic offprints of their article. Paper offprints can be ordered at prices quoted on the order form that accompanies the proofs.

Page Charge: No page charges will be levied to authors for the publication of their article except for reprints.

Misconduct: *Intractable & Rare Diseases Research* takes seriously all allegations of potential misconduct and adhere to the ICMJE Guideline (*http://www.icmje.org/recommendations*) and COPE Guideline (*http://publicationethics.org/files/Code_of_conduct_for_journal_editors.pdf*). In cases of suspected research or publication misconduct, it may be necessary for the Editor or Publisher to contact and share submission details with third parties including authors' institutions and ethics committees. The corrections, retractions, or editorial expressions of concern will be performed in line with above guidelines.

(As of June 2020)

Intractable & Rare Diseases Research
Editorial and Head Office
Pearl City Koishikawa 603,
2-4-5 Kasuga, Bunkyo-ku,
Tokyo 112-0003, Japan.
E-mail: office@irdrjournal.com